



Consiglio Nazionale
delle Ricerche



UNIVERSITÀ
DI SIENA
1240



UNIVERSITÀ DI PISA

GIOVANI *si*



Regione Toscana

DIPARTIMENTO SCIENZE DELLA VITA

DOTTORATO DI RICERCA IN SCIENZE DELLA VITA

CICLO XXXIII

COORDINATORE Prof. Massimo Valoti

Physiological, biochemical and metabolomic changes in two
Italian cultivars of *Olea europaea* in response to UV-B
radiations

SETTORE SCIENTIFICO-DISCIPLINARE: BIO/01

TUTOR: Dr. Claudio Cantini

DOTTORANDA: Dr.ssa Chiara Piccini

CO-RELATORE: Prof. Giampiero Cai

A.A. 2020-2021

Abstract

The stratospheric ozone layer is undergoing a deterioration due to factors of natural and anthropogenic origin that decrease the amount of UV-B radiation filtered and consequently increase the damage to living organisms. Although many countries have signed the Montreal Protocol with the goal of reducing the release of ozone-depleting substances, many researchers are uncertain about the recovery of the ozone layer, whose status is therefore constantly monitored. This scenario includes studies on the effects that excessive UV-B exposure can have on organisms. Being sessile, plants are particularly at risk because they are more exposed to this stress factor. In this PhD thesis the effects of prolonged UV-B stress (14 hours per day for 8 weeks) have been analyzed and compared on two cultivars of olive tree (*Olea europaea* L.), Olivastra Seggianese (Tuscan cultivar) and Giarraffa (Sicilian cultivar). The choice of the olive tree is based on its economic importance and its large-scale cultivation in almost all the Italian territory. The analyses carried out in this study show that UV-B radiation is a dangerous source of stress for the olive tree. Both cultivars, while proving resistant to the treatment, showed prominent effects although in different ways and times. It was possible to determine the critical points at which the most evident effects occur, i.e., after the first two weeks of stress (T2) and during the last two weeks (T6-T8). The data obtained suggest possible mechanisms by which Giarraffa responds and resists to UV-B stress more effectively than the Olivastra Seggianese, including the ability to maintain photosynthetic efficiency, a more effective and rapid activation of the antioxidant response, higher availability of flavonoids, increased hydroxycinnamic acids derivatives, optimization of GPox use as well as a relatively high content of mannitol and Hsp70. Moreover, Giarraffa opted for a targeted choice of RubisCO isoforms and managed SuSy content, saving energy during the critical stress point. In addition, the Giarraffa cultivar is better adapted to prolonged UV-B stress due to a higher presence of palmitic acid, α -linolenic acid, and stearic acid, as well as some terpenes and long-chain alkanes. In conclusion, emerging data indicate that the Giarraffa cultivar has developed better adaptive capacities than the Seggianese cultivar, probably due to the area of origin where the incident solar radiation is higher than in the native area of the Tuscan cultivar.

Table of contents

Chapter 1: General introduction	5
UV-B radiation	5
Atmospheric pollution and reduction of ozone layer.....	7
Effects of UV-B on plants.....	11
Mechanism of plant defenses	14
Study model: <i>Olea europaea</i> L.	15
Structure of PhD work.....	18
Chapter 2: effects of UV-B radiations on photosynthesis-related processes.....	21
Introduction	21
Materials and methods	22
Plant growth conditions.....	22
Application of UV-B stress	22
Determination of photosynthetic efficiency	23
Analysis of photosynthetic pigments	24
Analysis of sugars.....	25
Determination of the antioxidant capacity, polyphenols and flavonoids	26
Statistical analysis.....	27
Results	28
Photosynthetic efficiency.....	28
Photosynthetic pigments.....	30
Sugars	33
Antioxidant capacity, polyphenols and flavonoids.....	35
Discussion.....	38
Conclusions.....	43
Chapter 3: biochemical responses of olive to UV-B radiations	45
Introduction	45
Materials and Methods	46
Plant growth conditions and application of UV-B Treatment.....	46
Antioxidant enzymes extraction and quantification	46
Lipid peroxidation.....	47
Ribulose-1,5-Bisphosphate Carboxylase/Oxygenase (RubisCO) Activity.....	47
Protein Extraction.....	48
1-D Electrophoresis, Western Blotting and Image Analysis	48
2-D Electrophoresis, Western Blotting and Image Analysis	49

Microscopy analysis.....	50
Statistical analysis.....	51
Results	51
Microscopy analysis.....	51
Antioxidant enzymes analysis	53
Lipid peroxidation analysis (Malondialdehyde)	56
Ribulose-1,5-Bisphosphate Carboxylase/Oxygenase (RubisCO) Activity	57
Proteomic analysis.....	58
1-D Analysis.....	58
2-D analysis of Ribulose-1,5-Bisphosphate Carboxylase/Oxygenase (RubisCO).....	63
Discussion.....	66
Conclusions.....	72
Chapter 4: Metabolomics of UV-B responses.....	74
Introduction	74
Material and Methods.....	75
Plant growth conditions and application of UV-B treatment	75
Preparation of leaf extracts	75
Gas chromatography–mass spectrometry.....	75
Ultra-high performance liquid chromatography–mass spectrometry	76
Statistical analysis.....	76
Results	77
Phenolic profile	77
Lipophilic profile	78
Discussion.....	86
Olive plant UHPLC–MS metabolite profile.....	86
Olive plant GC–MS metabolite profile	88
Conclusions.....	91
Chapter 5: Conclusions and perspectives	92
References	96
Sitography:	118

Chapter 1: General introduction

UV-B radiation

The Sun emits energy in the form of solar radiation in a broad spectrum of electromagnetic waves. According to their different wavelengths and the different characteristics they exhibit (frequency and speed of propagation), it is possible to divide the spectrum into sections (figure 1):

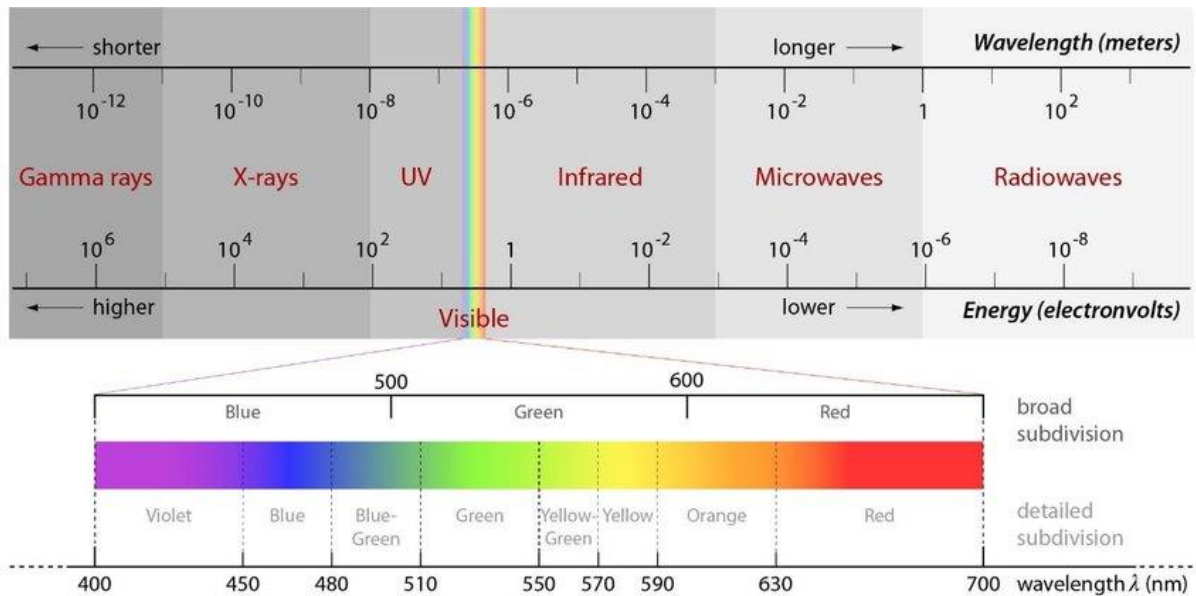


Figure 1. The electromagnetic spectrum (Verhoeven and Archaeology 2017)

Specifically, ultraviolet (UV) radiation is the fraction of the electromagnetic spectrum with wavelengths between 100 and 400 nanometers (nm), as shown in figure 2.

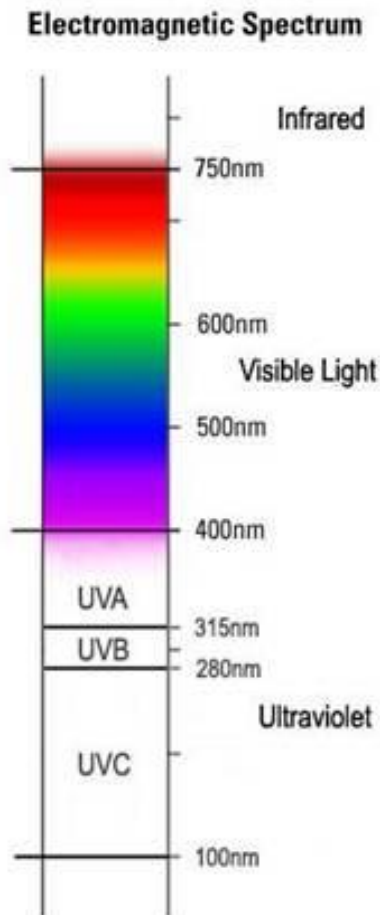


Figure 2. Portion of the electromagnetic spectrum in which the wavelengths of the three regions that are part of the ultraviolet radiation are highlighted: UV-C (100-280 nm), UV-B (280-315 nm), UV-A (315- 400 nm) (GreenFacts).

Ultraviolet radiation is divided into three spectral bands:

- UV-C (wavelength $\lambda=100-280$ nm): they do not reach the earth's surface, exposure can accidentally occur from anthropogenic sources, such as germicidal lamps (Matsumura and Ananthaswamy 2004).
- UV-B (wavelength $\lambda=280-315$ nm): they are responsible for various health effects of organisms and ecosystems (Solomon 2008).
- UV-A (wavelength $\lambda=315-400$ nm): corresponds to 95% of the total radiation capable of reaching the earth's surface (Maverakis et al. 2010).

The energy content of UV radiation confers the property of ionizing molecules and inducing chemical reactions. As the wavelength decreases, the energy content increases, as described by Planck's law. In fact, UV-B radiation, which has a shorter wavelength than UV-A radiation, has a higher energy content and an erythemal action 1000 times greater than that of

UV-A (Maverakis et al. 2010). After the first observations and studies by Cornu in 1879 (Cornu 1879) and Hartley in 1881 (Hartley 1881), research focused on the study of solar radiation and how much it could actually reach the Earth's surface. The impact of UV radiation appeared to be limited to specific wavelengths and this necessarily had to be caused by an absorbing substance in the atmosphere, which was later identified as ozone (Hartley 1881). Molecular oxygen (O₂) and molecular nitrogen (N₂) are among the major components of the atmosphere that can absorb UV radiation with a wavelength less than 220 nm and UV in the range 220-240 nm (Baird and Cann 2012). In contrast, radiation with wavelengths in the range 220-320 nm is mainly absorbed by ozone (O₃), which naturally occurs in the lower region of the stratosphere. However, this molecule, while absorbing UV-C radiation (100-280 nm), cannot fully absorb the incident UV-B radiation that, to a lesser extent, reaches the Earth's surface. Most of the UV-A ultraviolet radiation, in the 320-400 nm range, is partially filtered in the atmosphere and reaches the Earth's surface. This component is the least dangerous from the biological point of view (Baird and Cann 2012).

UV radiation is believed to be both a vital force in the formation of biological macromolecules and a serious constraint in the evolution of life exposed to sunlight in the absence of an atmosphere capable of filtering UV (Caldwell 1979). Solar radiation is the basis of photosynthesis (Verdaguer et al. 2012) and chemical processes necessary for animal and plant life. However, excess radiation in the ultraviolet spectrum is dangerous and very harmful to organisms. At the organismal level, adverse effects include increased skin cancer, cataracts, and immunodeficiency disorders (Solomon 2008; Maverakis et al. 2010). UV also affects terrestrial and aquatic ecosystems by altering growth, food chains, and biochemical cycles. UV also negatively affects plant growth, reducing agricultural productivity (Wang et al. 2003; Zlatev et al. 2012). Ultimately, ozone acts as a natural filter that protects living organisms on earth (Hegglin et al. 2014).

Atmospheric pollution and reduction of ozone layer

The ozone layer is a region of the stratosphere of particular importance as it filters out the ultraviolet component from solar radiation incident on the earth; if not, it would cause harm to humans and other life (plant and animal) (Kumar and Häder 1999; Baird and Cann 2012). O₃ is contained in all layers of the atmosphere, both upper (stratosphere) and lower (troposphere). Most O₃ is found between 15-50 km from the Earth's surface (most often between about 20 and

40 km) (Kumar and Häder 1999) as a layer commonly referred to as the ozonosphere (figure 3).

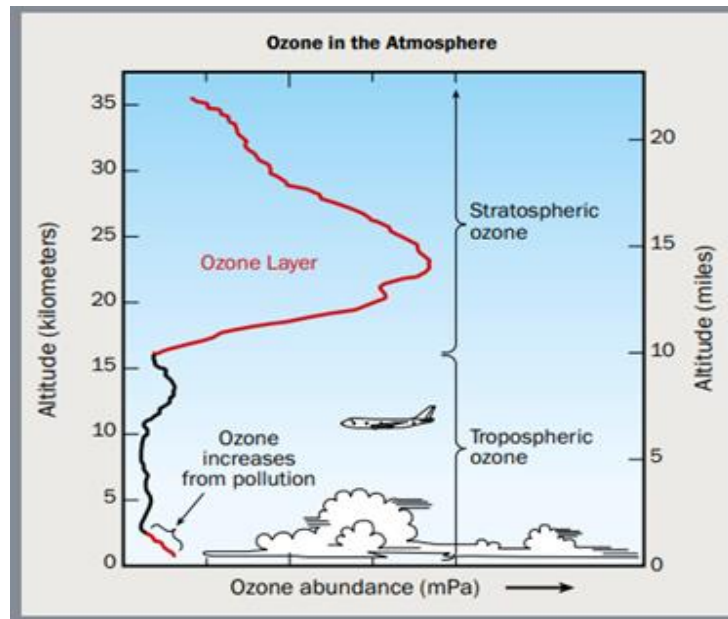
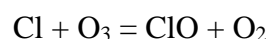


Figure 3. Variation in the concentration of ozone in the atmosphere as the altitude varies (Hegglin et al. 2014).

Stratospheric ozone is formed naturally by chemical reactions involving ultraviolet solar radiation (sunlight) and oxygen molecules, which make up 21% of the atmosphere. In the first step, ultraviolet solar radiation breaks down an oxygen (O_2) molecule to produce two oxygen ($2 O$) atoms in a process called photolysis (Molina and Rowland 1974); in the second step, each of these highly reactive atoms combines with an oxygen (O_2) molecule to produce an ozone (O_3) molecule. The O_3 molecules can in turn absorb UV radiation and dissociate into an oxygen molecule (O_2) and atomic oxygen (O); usually this free oxygen atom quickly recombines with an oxygen molecule to form another ozone molecule (NASA Ozone Watch, 2021).

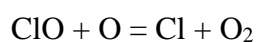
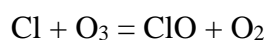
In addition to this "ozone-oxygen cycle," other reactions affect the concentration of ozone in the stratosphere. The depletion of the ozone layer is enhanced by the interaction of ozone molecules with other molecules in the atmosphere containing nitrogen, hydrogen, chlorine, and bromine (NASA Ozone Watch, 2021). These constitute the catalysts for O_3 to O_2 conversion reactions and have a very important effect on the balance of the ozone amount in the atmosphere; for example, chlorine activates the following catalytic chain of reactions (Molina and Rowland 1974):





These substances can have both a natural origin (such as volcanic eruptions, salt spray, and emissions of volatile organic compounds from plants) and an anthropogenic origin, such as fossil fuels used in electricity production, transportation, industrial processes, and solvents used in chemical industries, mining, agricultural activities, and waste treatment (Environmental European Agency, 2021). These substances are responsible for the phenomenon of air pollution (Kampa and Castanas 2008). Since the 19th century, the widespread use of pesticides, solvents, plastics, and cooling fluids has significantly increased the amount of chemical compounds released into the atmosphere. Since the second industrial revolution and especially after World War II, the problem has dramatically increased (Mosley 2014), causing a dangerous thinning of the ozone layer and a consequent increase in the amount of solar radiation reaching the Earth's surface. This has raised the risk of harmful effects on all organisms (Pessoa 2012). There are numerous substances known as "Ozone Depleting Substances" (ODS) that contain at least one atom of chlorine, fluorine, or bromine; they have the ability to destroy ozone molecules by turning them into oxygen and undermining the stability of the ozone layer (Newman et al. 2009). Among these substances, the most important are chlorofluorocarbons (CFCs) (Parson and Greene 1995).

CFCs are extremely stable and inert molecules that do not readily react with other chemicals in the troposphere. As a result, they have been widely produced for half a century; initially they were used as refrigerants and later found widespread use in industry as propellants in aerosol sprays, refrigerant gases in air conditioners, solvents for cleaning electronic circuits and foams. CFC molecules introduced into the troposphere migrate intact into the stratosphere where, no longer protected by the ozone layer, dissociate through the action of UV light, releasing chlorine atoms (Kumar and Häder 1999; Newman et al. 2009). The free chlorine atoms react with the ozone molecules, subtracting an oxygen atom to form chlorine monoxide (ClO) and an oxygen molecule. When a chlorine monoxide molecule comes across a free oxygen atom, the oxygen atom breaks up the chlorine monoxide, binding to the oxygen atom and releasing the free chlorine atom into the stratosphere.



This process can repeat itself an innumerable number of times, increasing the rate of ozone depletion, which is significantly higher than the rate of regeneration (Molina and Rowland

1974; Newman et al. 2009). Some CFCs have very long lifetimes, are persistent, and thus can damage the ozone layer for over 100 years (Newman et al. 2009). Molina and Rowland (1974), as well as other researchers, had shown that human activities altered the balance of stratospheric ozone and that this phenomenon was primarily due to the production of chlorine-containing chemicals such as chlorofluorocarbons (CFCs). In spite of this, and in spite of the enormous amount of chlorine recorded in the atmosphere, the suggestion to stop the production of CFCs worldwide was met with skepticism. Only in 1985, with great surprise, huge losses of ozone were detected at Antarctic level; it was hypothesized that the ozone depletion was related to the increase of CFC concentrations in the atmosphere (Farman et al. 1985) and later this hypothesis was confirmed by further scientific expeditions (de Zafra et al. 1987).

In 1987, to address ozone depletion, a global treaty (the Montreal Protocol) was signed to protect the ozone layer. The Montreal Protocol came into force in 1989 and aims to phase out the production and use of ozone-depleting chemicals. The compounds regulated by the Montreal Protocol are grouped under the term ODS (ozone-depleting substances); most of these accumulate in the lower atmosphere because they are relatively unreactive gases that do not readily dissolve in rain or snow and are transported by natural air motions into the stratosphere. Once accumulated, they are converted to more reactive gases that participate in catalytic reactions destroying ozone molecules (Velders et al. 2007). Global consumption of ozone-depleting substances has been reduced by about 98% since countries began following the Montreal Protocol. As a result, the ozone layer is showing the first signs of recovery (Barnes et al. 2019). However, the ozone layer is not expected to fully recover before the second half of this century. This is because substances that deplete the ozone layer remain in the atmosphere for many years. Most of these substances are also powerful greenhouse gases. Some of them have a global warming effect up to 14,000 times stronger than carbon dioxide (CO₂), the main greenhouse gas. Therefore, the elimination of ozone-depleting substances, such as hydrochlorofluorocarbons (HCFCs) and chlorofluorocarbons (CFCs), has also contributed to the fight against climate change (Velders et al. 2007; Newman et al. 2009). On the other hand, global phasing out has led to a sharp increase in the use of other types of gases in various applications. These fluorinated gases ("F-gases") do not damage the ozone layer but have a significant global warming effect. Therefore, in 2016, member states that are signatories to the Montreal Protocol agreed to add the most common type of fluorinated gas, hydrofluorocarbons (HFCs), to the list of substances to be controlled (Hegglin et al. 2014). Despite efforts to date, scientists are still uncertain about the timeframe needed to reach the ozone levels of the first

half of the last century (Barnes et al. 2019); thus, much remains to be done to fully recover the ozone layer.

Effects of UV-B on plants

Although measures have been implemented to reduce the amount of chemicals released into the atmosphere and damaging the ozone layer, the intensity of ultraviolet (UV-B) radiation reaching the Earth's surface is estimated to increase until the mid-21st century (McKenzie et al. 2006). Excessive exposure to UV-B radiation has diverse negative impacts that include a wide range of morphological, physiological, and reproductive aspects on plants and animals, as well as humans. In addition, it can alter biogeochemical cycles, can act synergistically with other environmental problems (such as global warming, ocean acidification, and pollution) thereby deeply impacting ecosystems (Abbasi and Abbasi 2017). With respect to plants, although UV-B radiation represents only a small fraction of the solar radiation that reaches the Earth's surface, it induces a photobiological effect relevant to the anatomy, morphology, physiology, and biochemistry of plants (Searles et al. 2001; Kakani et al. 2003).

Sunlight provides the energy needed for plant growth, but intense light radiation (particularly in the UV-B spectrum) can induce stress responses that potentially lead to severe damage to DNA, proteins, membrane lipids, and other cellular components (Müller-Xing et al. 2014). DNA is one of the macromolecules most at risk because of UV radiation; in particular, UV-B radiation can cause genetic mutations through two lesions: the production of cyclobutane-pyrimidine dimers (CPDs) and, to a lesser extent, the production of pyrimidine (6-4)-pyrimidinone (6-4 PP) dimers (Britt 1996). Their relative proportion and non-random distribution within the eukaryotic genome depends on sequence composition and chromatin structure (Pfeifer 1997; Kwon and Smerdon 2005; Law et al. 2013). In plants, CPDs can account for up to 90% of all pyrimidine dimers induced by UV-B exposure (Dany et al. 2001). In addition to being mutagenic, DNA modifications interrupt cellular metabolism. Both RNA and DNA polymerase are unable to read the unrepaired dimers, leading to a blockage of gene transcription and DNA replication (Britt 1996). Furthermore, UV-induced oxidative DNA injury in plants (Watanabe et al. 2006) occurs (although not exclusively) due to endogenous photosensitizers generating free radicals upon their activation (Manova and Gruszka 2015). Indeed, exposure of plant tissues to UV-B radiation increases the production of reactive oxygen species (ROS), such as O_2^- , H_2O_2 , and $-OH$, causing damage to nucleic acids as well as to proteins and lipids (Soheila et al. 2001).

The photosynthetic mechanism is particularly sensitive to UV-B exposure. Direct damage to the photosynthetic apparatus mainly includes inactivation of photosystem II (PSII); indeed, the two proteins D1 and D2 (which form the core of PSII) can be degraded (Jansen et al. 1998). In addition, UV-B radiation causes a decrease in photosynthetic efficiency, resulting in reduced growth rate and alterations in carbon and nitrogen metabolism (Dotto and Casati 2017; Piccini et al. 2020). UV-B radiation can also affect stomatal conductance, thereby altering the rate of net CO₂ assimilation, and the rate of water loss through transpiration (Kataria et al. 2013; Koubouris et al. 2015). In addition, excess UV-B radiation results in decreased levels of photosynthetic pigments (Lidon and Ramalho 2011; Machado et al. 2017; Piccini et al. 2020), alteration of thylakoid integrity, and changes in chloroplast ultrastructure (Kataria et al. 2013). In addition, reduced RubisCO activity and content, a different composition of Rubisco isoforms (Dias et al. 2018; Piccini et al. 2021), and down-regulation of photosynthetic gene transcription have been described (Strid et al. 1994).

In plants, the effects of UV-B radiation are of great importance in photomorphogenesis, namely the process by which light regulates plant development (Kendrick et al. 1997). Plant processes regulated by light signals include leaf expansion, stem elongation, flowering induction, and seed germination (Higuchi and Hisamatsu 2016). UV-B radiation can also cause photomorphogenic changes and damage, especially in leaves. Their curling, for example, aims to reduce the surface exposed to radiation (Jansen et al. 1998); Bornman and Vogelmann (1991) reported a 45% increase in leaf thickness in *Brassica campestris* and a similar result was described in *Brassica napu* (Cen and Bornman 1993). Increased UV-B radiation has been found to reduce the height of *Abies faxoniana* plants, as well as total biomass production and roots (Yao and Liu 2009). In a greenhouse experiment by (Zuk-Golaszewska et al. 2003), different UV-B radiation treatments on two species (*Avena fatua* and *Setaria viridis*) induced changes in the morphology of leaves and plants such as decrease in plant height and in the fresh mass of leaves, shoots and roots, as well as reduction of leaf area and curling of leaves.

An example of how UV-B radiation treatments induced changes in the morphology of olive leaves and plants (figure 4; figure5).



Figure 4. curlig olive leaves cause by exposure to UV-B radiation.

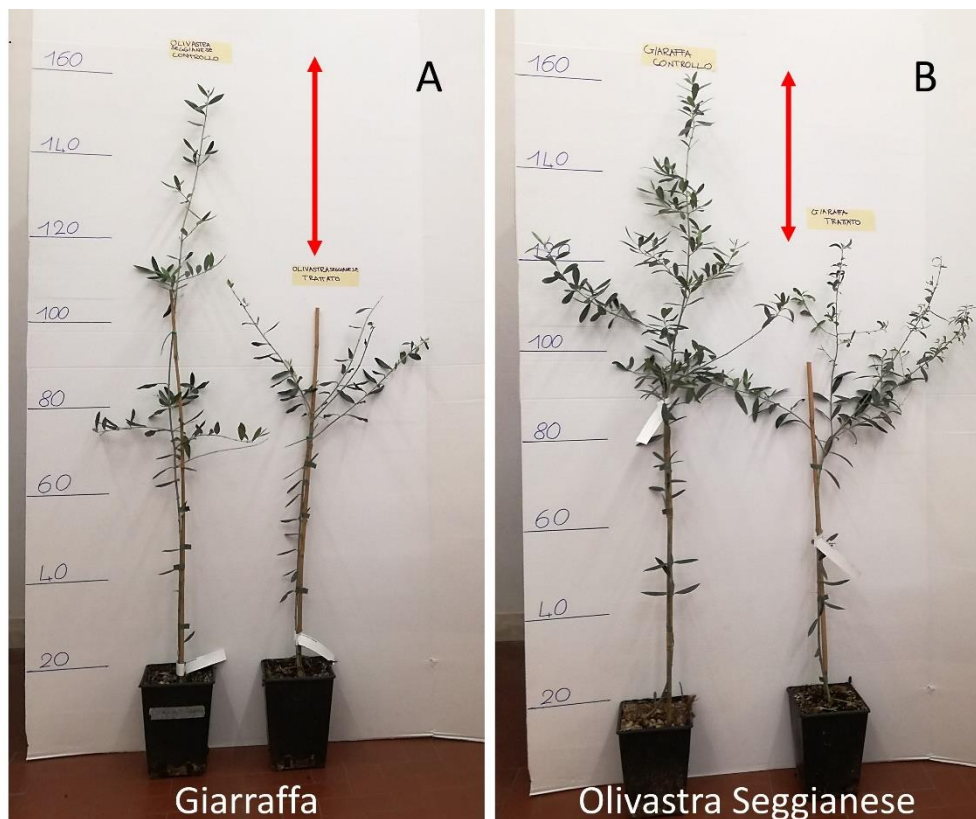


Figure 5. Comparison between olive trees (cultivar Giarraffa (A) and cultivar Seggianese (B)) control and treated with UV-B radiation for eight weeks. At the end of the experiment a decrease in stressed plant height can be observed.

High intensities of UV-B radiation also induce increased production in plant cells of reactive oxygen species (ROS), a class of extremely reactive compounds that have a mismatched electron and are able to snatch an electron from other molecules, thereby oxidizing them. Among the most deleterious radicals that commonly form in the cell are the "superoxide" anion (O_2^-), the "hydrogen peroxide" (H_2O_2), the "singlet" oxygen (1O_2) and the "hydroxyl radical" (OH^\cdot) which are responsible for oxidative damage to DNA, proteins, lipids and other cellular compounds (Panagopoulos et al. 1990; Foyer et al. 1994; Smirnoff 1998; Mahdavian et al. 2008).

In addition, exposure of plants to UV-B radiation leads to an increasing content of several secondary metabolites, such as flavonoids (Beggs and Wellmann 1985; Tevini et al. 1991). Secondary metabolites play a key role in plant interactions with other organisms, including herbivores, parasites, and microbial pathogens (Paul et al. 2012; Ballaré 2014). Alterations in the reproductive system, such as decreased pollen germination, have also been observed (Feng et al. 2000); Koubouris et al., (2015) showed that excessive UV-B irradiation in olive trees causes a reduction in pollen germination, reduced pollen tube length and therefore a decreased fruit yield.

Mechanism of plant defenses

Although plants have developed several repair mechanisms over time, the damage caused by UV radiation is still considerable (Pang and Hays 1991). The defense mechanisms that plants activate in response to this stress include, first and foremost, a network of processes aimed at repairing DNA lesions and maintaining genome stability through error removal and reconstruction of the original genetic information (Manova and Gruszka 2015). Repair of UV-B damaged DNA occurs primarily through light-dependent photoreactivation (Britt 1996). A study by Pang and Hays (1991) in *Arabidopsis* showed that photoreactivation is the predominant way by which cyclobutane-pyrimidine dimers are repaired as opposed to the much slower removal in the dark, presumably by excision repair. In the end, if DNA lesions are not removed, cells may still be able to cope with them by replicating the damaged DNA because many polymerases allow cells to tolerate DNA damage (Schuch et al. 2017).

The endogenous defense system includes a number of compounds that act in different ways to counteract ROS production and their reactions. Cellular antioxidants include enzymes, non-enzymatic substances, and other metabolites such as chelating agents and phenolic and

aromatic molecules (Hideg et al. 2013; Schuch et al. 2017). Enzymes with antioxidant function are superoxide dismutase (SOD), catalase (CAT), glutathione peroxidase (GPox), and ascorbate peroxidase (APX) (Zlatev et al. 2012; Hideg et al. 2013; Rácz et al. 2018). There are also non-enzymatic antioxidant mechanisms, such as tocopherol, ascorbate, phenols, alkaloids, flavonoids, and proline (Reddy et al. 2004; Chen and Dickman 2005; Gong et al. 2005; Jaleel et al. 2009; Ahmad et al. 2010; Gill and Tuteja 2010; Yin et al. 2010; Impa et al. 2012). Relief from UV-B stress is mainly attributed to flavonoids and related phenolic compounds that effectively absorb UV-B radiation during PAR (photosynthetically active radiation) transmission to chloroplasts (Caldwell et al. 1983; Li et al. 1993; Reuber et al. 1996). Indeed, exposure to UV-B radiation can increase the concentration of UV-B-absorbing metabolites in epidermal cell layers thereby attenuating UV-B transmission in the mesophyll layer and protecting the photosynthetic apparatus (Burchard et al. 2000). Tolerance and responses to UV-B radiation primarily involve leaves, which are the first protective barrier to UV-B penetration; in fact, UV-B promotes leaf thickening, changes in cuticle composition, and increases in phenolic compounds (Liakoura et al. 1999; Liakopoulos et al. 2006). The epicuticular wax layer also represents a line of defense against adverse environmental conditions (Le Provost et al. 2013) and particularly against UV-B (Ni et al. 2014). Epicuticular wax consists of a heterogeneous mixture of lipophilic substances (such as terpenes, alkanes, esters, aldehydes, and fatty acids) forming a hydrophobic layer that limits water loss (Ni et al. 2014); this layer is capable of reflecting 10% to 30% of the incident UV-B radiation (Kakani et al. 2003). However, exposure to increased ultraviolet radiation causes changes in the chemical composition of wax (Gil et al. 2012) as well as changes in metabolic pathways leading to the accumulation of secondary metabolites that protect plant cells from ROS (Kaling et al. 2015). The effects of UV-B radiation are species-specific and depend on interactions with other environmental parameters (Sullivan and Teramura 1990; Gwynn-Jones 2001; Kyparissis et al. 2001). However, most plant species are assumed to have adequate tolerance and repair capacity to cope with increased UV-B radiation (Taulavuori et al. 1998; Müller-Xing et al. 2014).

Study model: *Olea europaea* L.

The olive tree (*Olea europaea* L.) is an evergreen fruit tree; it belongs to the Oleaceae family and comprises more than 30 genera including *Olea*. The species *Olea europaea* L. belongs to the genus *Olea*, which includes both cultivated and wild types of the olive tree (Green 2002). The species can be considered a complex of 6 subspecies that differ in some morphological features and in a specific geographical distribution (Besnard et al. 2002). In the subspecies

europaea two botanical varieties are distinguished: *O. e.* subsp. *Europaea* var. *sylvestris* (wild olive or oleaster) and *O. e.* subsp. *europaea* var. *europaea* (sativa), i.e. the cultivated olive. The wild form is a shrub of small stature (1-5 meters), has young hardened branches, thorny and quadrangular, narrow and short leaves (1-2 cm), sometimes truncated or heart-shaped at the base and small fruits with bitter taste and low oil content (Pignatti 1982). The cultivated olive tree can be as high as 15-20 meters, has young unarmed branches, round and flexible, oblong and lanceolate leaves, with cedar green color on the upper page and silvery gray on the lower one, large flowers and large fleshy drupes (Pignatti 1982; Amouretti and Comet 1985). The wild form of *Olea europaea* was formerly widespread in various regions of the Mediterranean and, most likely, the cultivated form has differentiated from ancestral populations (Ciferri 1950; Zohary and Hopf 1994). The olive tree is a thermophilic species characteristic of the Mediterranean basin; since ancient times, the Mediterranean has been the hub for both the plant's diffusion and its cultivation development (Brun and Amouretti 1993). The origin of the olive tree is still uncertain even if the most accepted hypothesis is that it originates in some area of the eastern Mediterranean (Ciferri 1950; Morettini 1972; Breton et al. 2009); from this area the plant has been propagated, with the development of new forms, in the Aegean area, in North Africa and then in the southern area of Spain and Italy.

The olive genetic heritage of the Mediterranean basin is very rich and is characterized by a multitude of varieties. According to estimates by the Olive Germplasm Production and Protection Division of the FAO (FAO, 2021), the world olive germplasm contains more than 2,629 different varieties, with many local varieties and ecotypes contributing to this diversity (Muzzalupo 2012). The plant has adapted and diversified in different pedoclimatic conditions becoming one of the most widespread species (FAO, 2021). Italy is the country with the highest biodiversity of the olive tree counting about 800 varieties with strong potential for development; the number is probably underestimated due to lack of information on minor local cultivars widespread in the various olive-growing areas (Muzzalupo 2012).

In this study, two Italian cultivars were analyzed: Olivastra Seggianese (figure 6) and Giarraffa (figure 7). I selected the two cultivars based on historical information about their long-term presence and thus acclimation to two very different environments in Italy. Olivastra Seggianese is a cultivar only widespread in its area of origin; it is found mainly around Seggiano, Tuscany, in central Italy, located 490 m above sea level, with an average annual temperature around 12 °C and an annual solar radiation of 170 MJ per square meter. Plants of this cultivar reach

considerable size. The fruits are small with a spherical shape and ripen early and simultaneously. The quantity of oil in the olives is high and of good quality. It is a hardy plant which resists low temperatures. Giarraffa, on the other hand, is cultivated in many areas of Sicily, but it is also found in Calabria and Puglia; it is one of the most ancient cultivars of Sicily, in the extreme south of Italy and partly south of the African coast, with an average annual temperature higher than 20 °C and a solar radiation ≥ 200 MJ per square meter (Meteo Aeronautica Militare 2021). The trees are of medium height. The fruits are quite large, ovoid, ripen early and is suitable for both fruit consumption -table olive- and oil. This cultivar shows low hardiness and high susceptibility to attacks by common animal pests. It has an average tolerance to low temperatures.



Figure 6. Olives and leaves of the Giarraffa cultivar (<http://www.monnaoliva.it/>)



Figure 7. Olives and leaves of the Olivastra Seggianese cultivar (<http://www.consorziolioseggiano.it/>)

Structure of PhD work

The concepts outlined above concerning the UV-B pollution and their effects on olive trees led me and my tutor to organize the thesis work in order to identify the physio-molecular parameters that differentiate the response of the two selected cultivars. The experimental phase was preceded by a careful selection of the two cultivars (and of the plant's age) as well as by the implementation of the appropriate technical conditions, such as the choice of UV lamps and the most suitable incubation chamber. The evaluation of current scientific literature on the effect of UV-B radiation on plants has been an integral part of the initial work. The PhD project therefore aimed to assess the effects of prolonged UV-B stress (14 hours per day) over time (8 weeks) on the two cultivars of olive trees examined. It was compared the responsiveness of the two cultivars by determining the most critical phases as well as the different adaptation (figure 8).

According to studies in the literature, the photosynthetic apparatus is one of the first targets of UV-B radiation stress; therefore, it was initially monitored the photosynthetic efficiency of plants for 8 weeks in order to determine the susceptibility of the two olive cultivars to stress and obtain a screening of the most critical phases. Subsequently, the study focused on 5 time points (T0, T2, T4, T6 and T8) on which analyses were performed to detect changes in photosynthetic pigments such as lutein, chlorophyll a, chlorophyll b and β -carotene in response to UV-B stress. In addition, on the same 5 time points, analyses were performed in the leaves of both cultivars to assess the concentration of photosynthetic sugars (sucrose, fructose, glucose, glucose 6-phosphate) and an alcohol-sugar with a protective function (mannitol). Subsequently, analyses were performed on the same 5 time points to assess the antioxidant capacity of plants in response to ROS accumulation following UV-B exposure. In particular, I analyzed changes in the content of secondary metabolites with antioxidant function such as polyphenols and flavonoids. This part of the work is described in chapter 2 (“Effects of UV-B radiations on photosynthesis-related processes”).

Afterwards, to obtain a complete picture of the antioxidant system in olive plants subjected to UV-B stress, on the same 5 time points I also analyzed changes in the activity of antioxidant enzymes such as superoxide dismutase (SOD), catalase (CAT), and glutathione peroxidase (GPox). In addition, I analyzed malondialdehyde (MDA) as a parameter of ROS-induced oxidation in macromolecules such as lipids. Three time points (T0, T4, and T8) were selected to perform protein analyses on leaf samples to assess changes in specific proteins such as

Hsp70, sucrose synthase, and RubisCO (the latter being the key enzyme in the Calvin cycle for carbon fixation). Specifically, I focused on the effects of UV-B radiation on RubisCO in terms of quantity (1-D analysis), isoform variation (2-D analysis), and enzyme activity. Subsequently, on the same 3 time points, transmission electron microscopy (TEM) observations were made on leaf samples to find correlations between changes in photosynthetic parameters and ultrastructural changes. This part of the work is described in chapter 3 (“Biochemical responses of olive to UV-B radiations”)

Finally, because few works in the literature have focused on the metabolic study of olive in response to UV-B stress, gas chromatography-mass spectrometry (GC-MS) and high-performance liquid chromatography-mass spectrometry (UHPLC-MS) analyses were performed on leaf samples collected at four time points (T2, T4, T6, T8). The objective was to gain insight into variation in metabolic pathways, particularly lipophilic and phenolic profiles, and thus identify metabolites involved in defense mechanisms in response to UV-B stress. This part of the work is described in chapter 4 (“Metabolomics of UV-B responses”).

Chapter 5 (“Conclusions and Perspectives”) closes the thesis work and summarizes the main findings obtained.

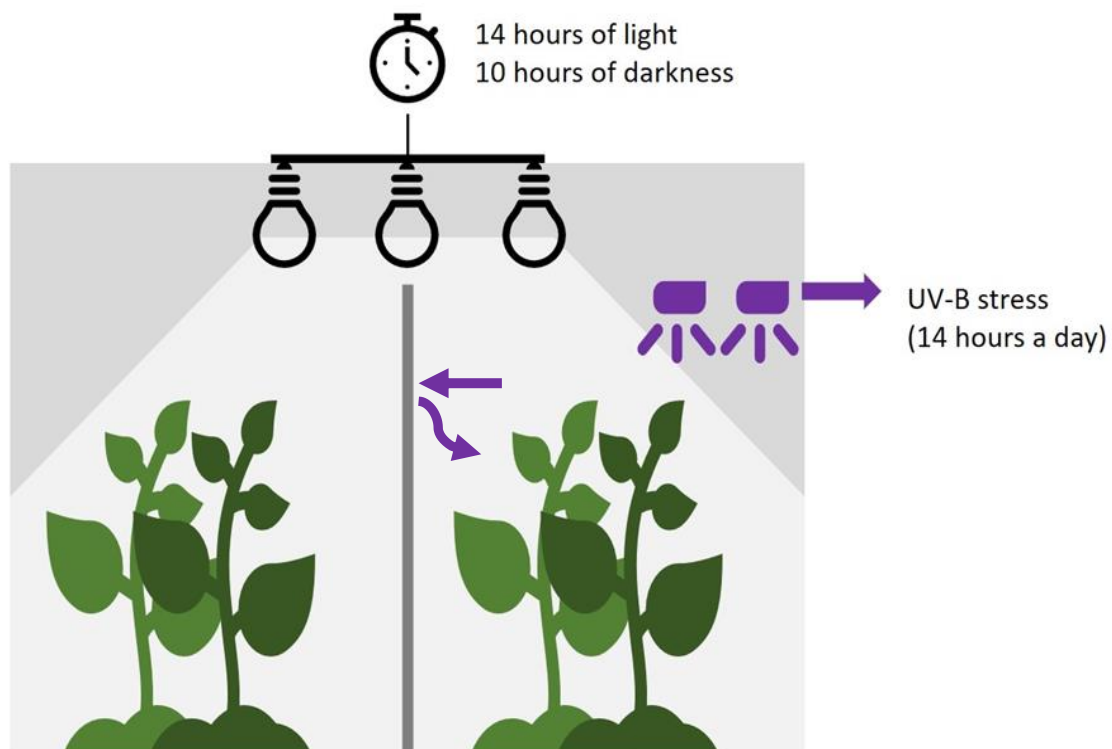


Figure 8. Schematic illustration of the experimental design. Olive trees of two cultivars Giarraffa and Olivastra Seggianese were subjected to UV-B radiation for 8 weeks, 14 hours a day.

Figure 9 outlines the various experimental steps and the analyses performed for each.

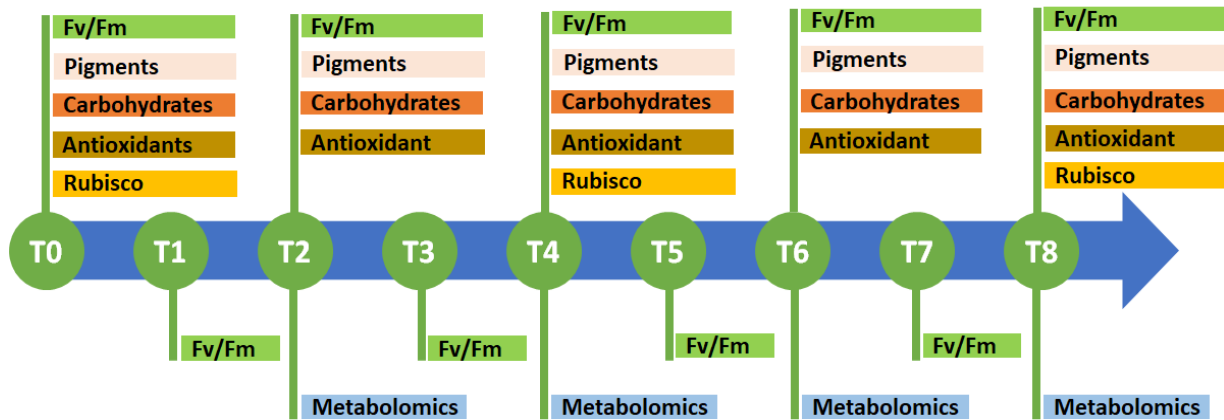


Figure 9. Timeline of analyses performed. Photosynthetic efficiency was measured weekly; concentrations of pigments, sugars, and antioxidant capacity (antioxidants, polyphenols, flavonoids, and antioxidant enzymes SOD, CAT, and GPox) were measured every two weeks. At times T2, T4, T6 and T8, changes in metabolic pathways (lipid and phenolic profile) were measured. At times T0, T4 and T8, the amount, change in isoforms and enzymatic activity of RubisCO was analyzed.

Chapter 2: effects of UV-B radiations on photosynthesis-related processes

Introduction

A major target of UV-B radiation is the photosynthetic apparatus, which is particularly sensitive to UV-B exposure (Kataria et al. 2013). As a consequence, high UV-B radiation results in decreased photosynthetic efficiency, reduced growth rate, and alterations in carbon and nitrogen metabolism (Kataria et al. 2013; Dotto and Casati 2017). UV-B radiation can also affect stomatal conductance, altering the rate of water loss through transpiration and the net rate of CO₂ assimilation (Kataria et al. 2013; Koubouris et al. 2015). Studies of injury to the photosynthetic apparatus by UV-B radiation have shown inactivation of photosystem II (PSII) (Zlatev et al. 2012; Kataria et al. 2013), decreased levels of photosynthetic pigments (Sebastian et al. 2018), altered integrity of thylakoids and chloroplast ultrastructure (Kataria et al. 2013), reduced Rubisco activity (Yu et al. 2013; Dias et al. 2018), and down-regulation of photosynthetic gene transcription (Strid et al. 1994). UV-B can also cause morphological changes, especially in leaves. The curling of leaves sometimes observed is both a damage and a way to reduce the surface area exposed to radiation (Fonini et al. 2017). Increased UV-B radiation has also been observed to impact plant height, leaf mass and area, total biomass production, and leaf morphology (Zuk-Golaszewska et al. 2003; Yao and Liu 2009). Although plants have developed numerous repair and protection mechanisms over time, the damage caused by UV-B radiation is still significant (Rácz et al. 2018). Among the defense mechanisms that plants activate in response to UV-B stress, enzymatic and nonenzymatic mechanisms counteracting ROS production are of extreme importance. Antioxidants include enzymes such as superoxide dismutase, catalase, and enzymes of the Halliwell/Asada pathway, as well as non enzymatic substances such as glutathione, ascorbate, tocopherols, carotenoids, albumin, bilirubin, chelating agents, and phenols (Zlatev et al. 2012; Hideg et al. 2013; Rácz et al. 2018). Among phenolic compounds, flavonoids are capable of effectively absorbing UV-B radiation and neutralizing reactive oxygen species (ROS) (Agati et al. 2012). In addition, UV-B exposure can increase the concentration of other phenolic compounds such as hydrocinnamic acids and secoiridoids that can effectively protect plants from the deleterious effects of UV-B stress (Dias et al. 2020).

The Mediterranean region is highly susceptible to climate change and the negative effects of high levels of UV-B radiation on typical regional species have already been highlighted (Nogues and Baker 2000; Martínez-Lüscher et al. 2015; Dias et al. 2018). Olive (*Olea*

europaea L.) is one of the most important and oldest crops in the Mediterranean basin. Despite the high adaptation of this species to the environmental conditions of the Mediterranean, the high levels of UV-B radiation expected in the near future (Sanchez-Lorenzo et al. 2017; Díaz-Guerra et al. 2018) together with other environmental factors in this region (such as cloudiness of the sky and high air pollutants) pose a risk to olive cultivation and productivity (Dias et al. 2018, 2020; Brito et al. 2019). Therefore, it is urgent to understand how high UV-B radiation affects the physiology of olive plants; at the same time, it is necessary to identify the most suitable cultivars for the new conditions, allowing farmers to grow selected cultivars more suitable for future environmental conditions. In this chapter I aimed to complement the contribution of previous investigations (Silva et al. 2018; Dias et al. 2018, 2019, 2020) by studying the physiological response to high levels of UV-B radiation; in particular, I focused on photosynthesis, pigments, carbohydrates and antioxidant compounds of the two Italian cultivars of *Olea europaea* (Olivastra Seggianese and Giarraffa) under investigation. In the present study I examined the two cultivars of olive trees in order to assess the effects of chronic UV-B stress (14 hours per day for 8 weeks) by comparing the susceptibility/tolerance of the two cultivars and identifying the most critical time points and adaptive response of olive plants.

Materials and methods

Plant growth conditions

Olive trees (*Olea europaea* L.) of 18 months of two cultivars (Olivastra Seggianese and Giarraffa) were taken from the nursery of the “Società Pesciatina di Orticoltura” (Pescia, PT, Italy) where the plants were grown in a greenhouse. Subsequently, plants were transferred to climatic cells with the following environmental conditions: temperature: 21 °C; relative humidity (RH): 60%; photoperiod: 14 light h, 10 dark h (Allen et al. 1997); light intensity: 500 $\mu\text{mol m}^{-2} \text{s}^{-1}$; watering: 400 mL water for each plant once a week; commercial substrate type: “Vigor Plant soil” (Vigor plant Italia srl Fombio), same composition for all plants.

Application of UV-B stress

Ultraviolet radiation was provided by two TL20W / 12 lamps (Philips) that emit in the wavelength of UV-B rays and that have already been widely used and described in the literature; lamps were prepared and used exactly according to the protocol of Allen et al. (1997). Plants ($n = 16$ for each cultivar) were positioned under UV-B lamps in the climatic cell. Every day, the homogeneity of the UV-B radiation emitted by the lamps was verified using a

Power Meter 840 with Sensor 818-UV (Newport Optical, California, USA). The UV-B biologically effective dose (BED), $25 \text{ kJm}^{-2} \text{ d}^{-1}$, was calculated according to Correia et al., (2012). Control plants ($n = 16$ for each cultivar), present in the same climatic cell, have been carefully separated from those treated by means of a plasterboard panel that shielded most of the UV radiation (BED of $1 \text{ kJm}^{-2} \text{ d}^{-1}$). The UV-B treatment corresponds to a high UV-B dose, but within the natural values already reported in some parts of the earth surface (Forster et al. 2011). The UV-B treatment was carried out for a period of 8 weeks for 14 h a day. The treatment scheme was performed according to Nogues and Baker (2000). During the treatment eight time points were established: the first one before the onset of UV-B treatment (T0), after 1, 2, 3, 4, 5, 6, 7 and 8 weeks of UV-B treatment (indicated respectively as T1, T2, T3, T4, T5, T6, T7 and T8). Photosynthetic efficiency was measured in fresh material in all time points (in control and UV-B treated plants), since it is an indicator of the plant photosynthetic performance and it is a non-destructive parameter. Additionally, leaf samples were collected in five representative sampling times (T0, T2, T4, T6 and T8), immediately frozen in liquid nitrogen and stored at $-80 \text{ }^\circ\text{C}$.

Determination of photosynthetic efficiency

Photosynthetic efficiency has been estimated by induction of chlorophyll fluorescence using a Handy PEA 2000 fluorimeter (Hansatech Instruments, King's Lynn, Norfolk, UK). Fluorometric analysis of leaf chlorophyll was performed *in vivo* at ambient temperature, and the changes of the level of fluorescence emission were measured in order to obtain the effectiveness of light use in the photosynthetic process. After 30 min of dark adaptation, the leaf was illuminated for about one second (peak at 650 nm, $3000 \mu\text{mol m}^{-2} \text{ s}^{-1}$, an intensity of excitation sufficient to ensure the closure of all PSII reaction centers) and the fluorescence signal was recorded. For each plant (both control and stressed), the values of Fv/Fm and PI were collected weekly for 8 weeks in order to identify the time when plants begin to perceive UV-B stress. The following equations were used to calculate Fv/Fm and PI parameters (Sriastava et al. 1999):

$$F_v/F_m = (F_m - F_0)/F_m$$

$$PI_{ABS} = \frac{1 - (F_0/F_m)}{M_0/V_j} \times \frac{F_m - F_0}{F_0} \times \frac{1 - V_j}{V_j}$$

where F_m is the maximum fluorescence value, F_0 is fluorescence value at zero instant, F_v is a difference between F_m and F_0 , V_J is relative F_v , and M_0 is the initial slope of fluorescence kinetics. F_v/F_m , therefore, represents an index from the maximum value of 1.00, equivalent to 100% of the maximum photochemical efficiency of photosystem II. The performance Index (Pi), a more sensitive parameter indicating the possible variations of the entire photosynthetic apparatus, including photosystems I (PSI) and II (PSII). Pi is a multiparametric expression that considers all the main photochemical processes, such as absorption and capture of excitation energy, transport of electrons over the primary plastoquinone (QA) and dissipation of excess excitation energy.

Analysis of photosynthetic pigments

Analysis of the photosynthetic pigments was carried out on frozen leaf samples using high performance liquid chromatography technique (HPLC—Waters LC Module One, Waters S.p.A., Milano, Italy) following the method of Suzuki et al. (1993). Olive leaves were powdered with liquid nitrogen, approximately 20 mg of each leaf sample was mixed in Eppendorf tubes with 1 mL of ethanol. Subsequently, samples were homogenized by Ultraturrax (IKA[®]-Werke GmbH & Co. KG, Staufen im Breisgau, Germany IKA) for about 2 min until complete rupture of cells. The homogenate was centrifuged at 13,000 g for 5 min at 4 °C. After that, supernatants containing pigments were transferred to a glass test tube. Then 20 μ L aliquots of sample were injected into the HPLC column. The column used was a C18 (25 cm \times 4.6 mm, grain size 5 μ). The mobile phase is a ternary mobile phase with the following gradient conditions (Table 1):

Table 1. Gradient values used in HPLC analyses for pigment separation. Solvent A: methanol; Solvent B: water; Solvent C: acetone.

TIME (min.)	% A	% B	% C
INITIAL	75	25	0
4	75	25	0
5	100	0	0
11	80	0	20
20	65	0	35
30	75	25	0

The chromatographic run was carried out at a flow of 1 mL min^{-1} , room temperature; the eluate was monitored at the wavelength of 440 nm and the separation time was 30 min. The following reference pigments have been used: xanthophyll (lutein) $10 \mu\text{g mL}^{-1}$ (elution time 17.59 min); trans β -carotene $50 \mu\text{g mL}^{-1}$ (elution time 37.49 min); chlorophyll a $10 \mu\text{g mL}^{-1}$ (elution time 25.23 min); chlorophyll b $10 \mu\text{g mL}^{-1}$ (elution time 21.7 min). Identification of the various components was obtained by programming the integrated UV detector with specific excitation wavelengths (440 nm) by comparing the retention times with those of reference standards and by comparing the characteristics of the absorption spectra of individual chromatographic fractions with those found in the literature. Subsequently, the concentrations of the 4 pigments were determined through the CSW-32 analysis software (Clarity—Data APEX, Prague, The Czech Republic) calculating each peak area. The protocol was repeated three times for each sample.

Analysis of sugars

Analysis of sugars (sucrose, fructose, glucose, glucose 6-phosphate and mannitol) was conducted by HPLC. Approximately 100 mg of leaf samples were first powdered with liquid nitrogen and then supplemented with 1 mL of water in 2 mL Eppendorf tubes. Subsequently, samples were homogenized using the Ultra-turrax homogenizer for about 2 min until complete

rupture of cells. The homogenate was subjected to centrifugation at 3000 g for 5 min, the supernatants transferred to 2 mL Eppendorf tubes and then centrifuged again at 12,000 g for 5 min. Samples were filtered (0.45 μm) and about 20 μL of each extract was injected and examined using a Waters Sugar-Pak I ion exchange column (6.5 \times 300 mm) at a temperature of 90 °C. The mobile phase consists of MilliQ water (pH 7) with a flow of 0.3 mL min⁻¹. The overall duration of the separation was 30 min. The elution times of sugars are as follows: glucose 6-P, 5 min; sucrose, 8 min; glucose, 10 min; fructose, 11 min; mannitol, 13 min. Identification of the components was obtained using a Waters 2410 refractive index detector, by comparing the retention times with those of reference standards. For each peak, the retention factor allows to identify the type of eluted molecule, while the curve area is proportional to the quantity. The protocol was repeated three times for each sample.

Determination of the antioxidant capacity, polyphenols and flavonoids

Frozen leaves (1 g) were macerated with 3 mL of 70% acetone. Subsequently, samples were homogenized with a Micra rt homogenizer (IKA[®]-Werke GmbH & Co. KG, Staufen im Breisgau, Germany) for about 2 min, and then inserted in a sonicator for 20 min for the complete breakage of cellular components. The homogenate was centrifuged at 4000 g for 5 min at 4 °C. Then, the supernatants were taken and used for analysis.

- *Ferric Ion Reducing Antioxidant Power—FRAP*

The FRAP test, acronym for "Ferric Ion Reducing Antioxidant Power", was originally developed to evaluate the antioxidant capacity of blood plasma at clinical level but was later adapted to analysis of food and botanical samples (Benzie and Strain 1996). It is based on the ability of antioxidants to reduce the Fe (III) 2,4,6-tripyridyl-s-triazine complex to Fe (II) at pH 3.6. Changes in the color reaction allows to determine the reducing power at 593 nm. The FRAP test is a test aimed at evaluating the maintenance of the redox state of the cells and it is therefore possible to arbitrarily define the FRAP unit as the number of moles of Fe (III) reduced to Fe (II) by a mole of tested antioxidant. For determination of total antioxidants, each reaction tube contained 2040 μL of acetate buffer, 200 μL of 2,4,6-Tri(2-pyridyl)-s-triazine (TPTZ), 200 μL of ferric chloride and 20 μL of leaf extract. Subsequently, samples were placed at 37 °C for 60 min. After incubation, samples were read at a wavelength of 593 nm. The antioxidant content was calculated based on a calibration curve of standard solutions of ferrous sulphate. The experiment was conducted in triplicate for each sample.

- *Folin-Ciocalteu method for the determination of total polyphenols*

The colorimetric assay for determination of total polyphenols was initially proposed by Folin and Denis and then modified by Folin and Ciocalteu (Ainsworth and Gillespie 2007). It is based on the addition of a particular oxidizing reagent, the Folin-Ciocalteu (FC) reagent, consisting of a mixture of phosphotungstic acid ($H_3PW_{12}O_{40}$) and phosphomolybdic acid ($H_3PMO_{12}O_{40}$) capable of oxidizing polyphenolic substrates and other antioxidant molecules by providing changes to color reaction. The oxidation reaction of phenolic substrates was carried out at pH 10 to accelerate the reaction kinetics. The mixture of W_8O_{23} and Mo_8O_{23} oxides has its maximum absorption at 765 nm (Ainsworth and Gillespie 2007). Each reaction tube contained 500 μ L of leaf extract, 3000 μ L of distilled water, 250 μ L of FC reagent, 750 μ L of sodium carbonate (Na_2CO_3) and 950 μ L of distilled water. Subsequently, samples were placed at 37 °C for 30 min. After the incubation, samples were read at 765 nm. Polyphenols content was calculated based on a calibration curve of standard solutions of gallic acid. The experiment was conducted in triplicate for each sample.

- *Aluminum Chloride method for the determination of total flavonoids*

The aluminum chloride method (Abozed et al. 2014) allows to determine the content of total flavonoids by separating their contribution from that of polyphenols. The assay is based on the ability of aluminum chloride to form complexes with flavonoids. Formation of these complexes is accompanied by a change in the color reaction. Each reaction tube contained 500 μ L of leaf extract, 1.5 mL of 95% ethanol, 100 μ L of aluminum chloride, 100 μ L of potassium acetate and 2.8 mL of distilled water. Samples were maintained at room temperature for 30 min, and then were read at 415 nm. Total flavonoids were determined based on a calibration curve of standard solutions of quercetin. The experiment was conducted in triplicate for each sample.

Statistical analysis

In order to verify the significance of the data obtained, the ANOVA test of the two-factor variance with replication and the *t*-test (* $p < 0.05$, ** $p < 0.01$) were carried out. To verify the correlation between the performance index and the flavonoid content and between Fv/Fm and the flavonoid content, the Pearson correlation coefficient was carried out. ANOVA and the Pearson correlation coefficient were performed by the Systat 11 statistical package (Systat Software Inc., Richmond, CA, USA).

Results

Photosynthetic efficiency

The Fv/Fm in the control plants of both cultivars did not differ significantly (confirmed by ANOVA test) as the response trend of both cultivars overlap over time (figure 10).

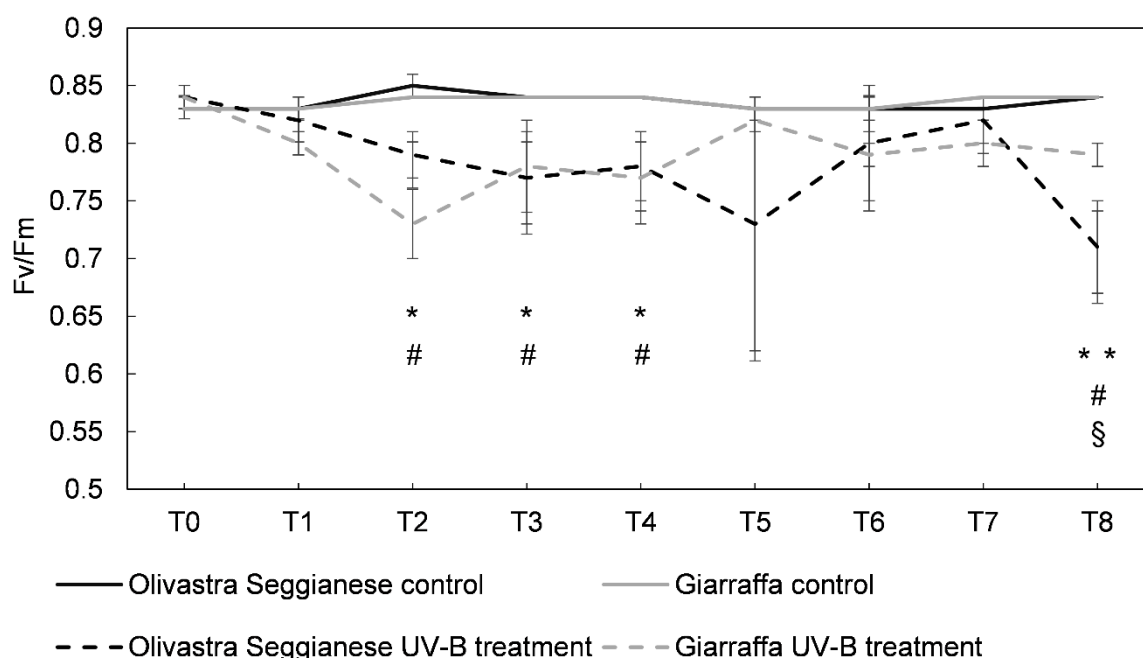


Figure 10. On the x-axes the time points, on the y-axes the Fv/Fm value. Maximum photochemical efficiency (Fv/Fm) in the two olive cultivars, Olivastra Seggianese and Giarraffa, under control and UV-B treatment in the different sampling times. In each line, values are given as mean \pm standard deviation. Asterisk (*) represent significant differences between control and treated plants of Olivastra Seggianese ($p \leq 0.05$; ** $p \leq 0.01$). Hashtag (#) represent significant differences between control and treated plants of Giarraffa ($p \leq 0.05$). The § symbol represent significant differences between Olivastra Seggianese treated plants and Giarraffa treated plants ($p \leq 0.05$).

The Fv/Fm values in control plants ranged from 0.83 to 0.84 all over the experiment. However, more discrepancies were evident when comparing the trend of plants subjected to UV-B with those of control. As expected, before the onset of stress (T0), all plants (control and those undergoing UV-B stress) have similar Fv/Fm values. After the first week of stress (T1), control plants and UV-B plants from the cultivar Olivastra Seggianese showed similar ($p > 0.05$) Fv/Fm averages. However, comparing both cultivars under UV-B conditions, the Fv/Fm in Olivastra Seggianese was significantly higher than the one of Giarraffa (0.82 ± 0.01 and 0.80

± 0.01 , respectively). At T2, it is possible to observe a remarkable decrease ($p \leq 0.05$) in the Fv/Fm ratio in UV-B treated plants when compared with the controls, for both cultivars. At this point the Fv/Fm was around 0.79 in UV-B Olivastra Seggianese plants and 0.73 in UV-B Giarrappa plants. From T3 to T4, UV-B treated plants of both cultivars showed a lower value of Fv/Fm ($p \leq 0.05$) than control, but no significant differences were found in both cultivars treated with UV-B. At T5, the UV-B Olivastra Seggianese reported slightly higher fluctuations with a sharp decrease, but this was not statistically significant (compared to UV-B Giarrappa and control plants). In the next sampling points (T6 and T7), control and UV-B plants showed similar ($p > 0.05$) Fv/Fm values. At T8, UV-B-stressed Olivastra Seggianese showed a decrease ($p \leq 0.01$) in the Fv/Fm to values around 0.71, while controls remain stable. UV-B Giarrappa plants were still in a plateau phase, but with an Fv/Fm significantly lower ($p \leq 0.05$) than the control. At this time UV-B plants of the two cultivars showed a statistically significant difference ($p \leq 0.05$).

As specified in the method section, the performance Index (Pi) is a more sensitive parameter indicating the possible variations of the entire photosynthetic apparatus, including photosystems I (PSI) and II (PSII). Concerning the performance index (Pi), the controls of both cultivars have a similar trend of response (figure 11), and do not differ significantly as confirmed by the ANOVA test. Contrarily, the Pi of UV-B plants, which present similar values for all the plants at time point 0 decreased ($p \leq 0.05$) after one week (T1) of UV stress. At time point 1, controls of Olivastra Seggianese had a Pi around 13.18, while UV-B plants had 9.14. For the control plant of Giarrappa the Pi was around 11.16, while in UV-B plants it was 6.15. After the T2, the Pi decreased significantly ($p \leq 0.05$) in UV-B plants. While the average Pi in control plants of Olivastra Seggianese is 14.1, in UV-B plants was approximately 5 and in UV-B Giarrappa was approximately 3.73 at T2 (against a value of 11.46 in control plants). Subsequently, from T3 onward, UV-B plants of both cultivars enter a plateau phase which persisted up to T7. After a further week of stress (T8), the Pi of the UV-B Olivastra Seggianese plants were affected by a significant drop (1.79 against 12.43 of control plants). The Pi in UV-B Giarrappa plants persist in the plateau phase, with an average Pi value lower than that of controls. At this time point, differences between the mean value of stressed plants of both cultivars were statistically significant ($p \leq 0.01$).

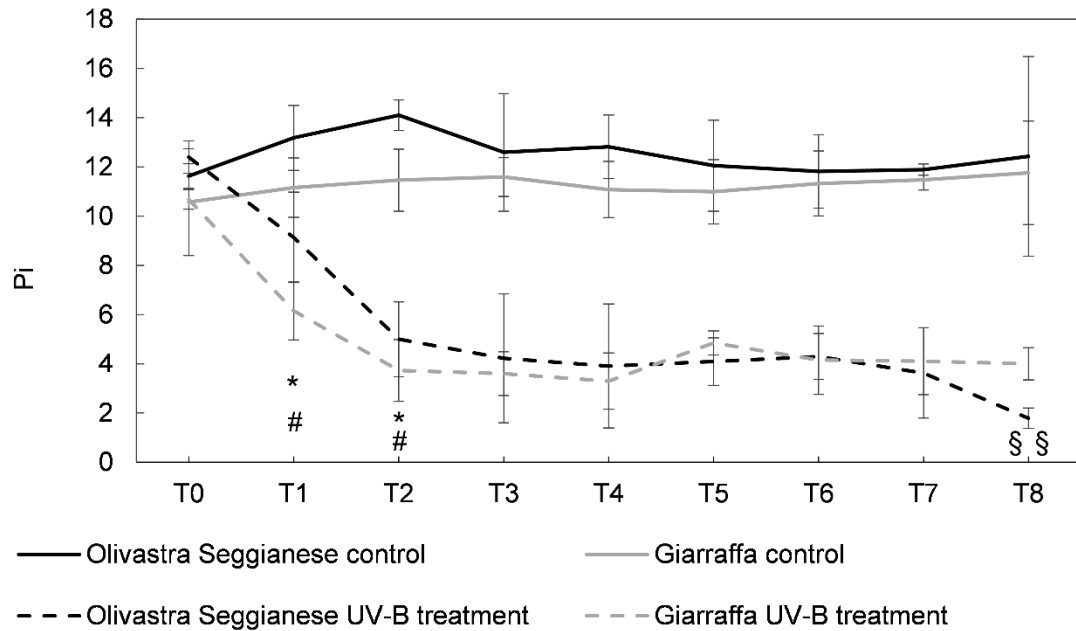


Figure 11. On the x-axes the time points, on the y-axes the Pi value. Performance index (Pi) in the two olive cultivars, Olivastra Seggianese and Giarraffa, under control and UV-B treatment in the different sampling times. In each line, values are given as mean \pm standard deviation. Asterisk (*) represent significant differences between control and treated plants of Olivastra Seggianese ($p \leq 0.05$). Hashtag (#) represent significant differences between control and treated plants of Giarraffa ($p \leq 0.05$). Double §§ represent significant differences between Olivastra Seggianese treated plants and Giarraffa treated plants ($p \leq 0.01$).

Photosynthetic pigments

Figures 12 and 13 show the content of pigments in olive leaves of both cultivars (control and UV-B treated plants). The content of chlorophyll a, chlorophyll b, β -carotene and lutein during the sampling times was similar ($p > 0.05$) in control and UV-B Olivastra Seggianese plants. Although the absolute quantity is slightly lower in treated plants than in control ones, the observed difference is inherent in the experimental variation. Therefore, I assumed no statistically significant differences in Olivastra Seggianese between controls and treated plants (also confirmed by ANOVA test).

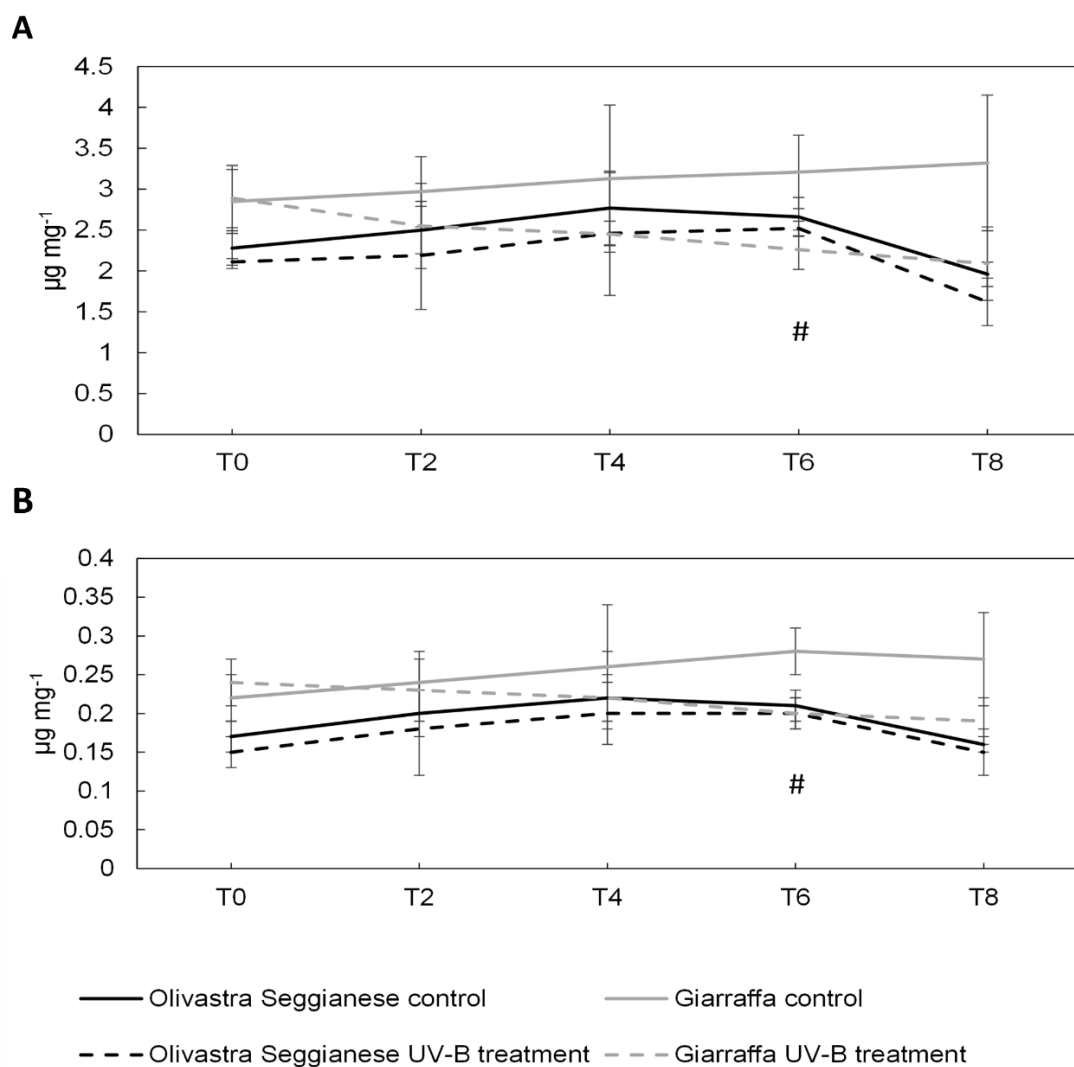


Figure 12. On the x-axes the time points, on the y-axes the concentration of pigments expressed in $\mu\text{g mg}^{-1}$. **(A)** Chlorophyll a content in the two olive cultivars, Olivastra Seggianese and Giarraffa, under control and UV-B treatment in the different sampling times. For each column, values are given as mean \pm standard deviation. Hashtag (#) represent significant differences between control and treated plants of Giarraffa ($p \leq 0.05$). **(B)** Chlorophyll b content in the two olive cultivars, Olivastra Seggianese and Giarraffa, under control and UV-B treatment in the different sampling times. For each column, values are given as mean \pm standard deviation. Hashtag (#) represent significant differences between control and treated plants of Giarraffa ($p \leq 0.05$).

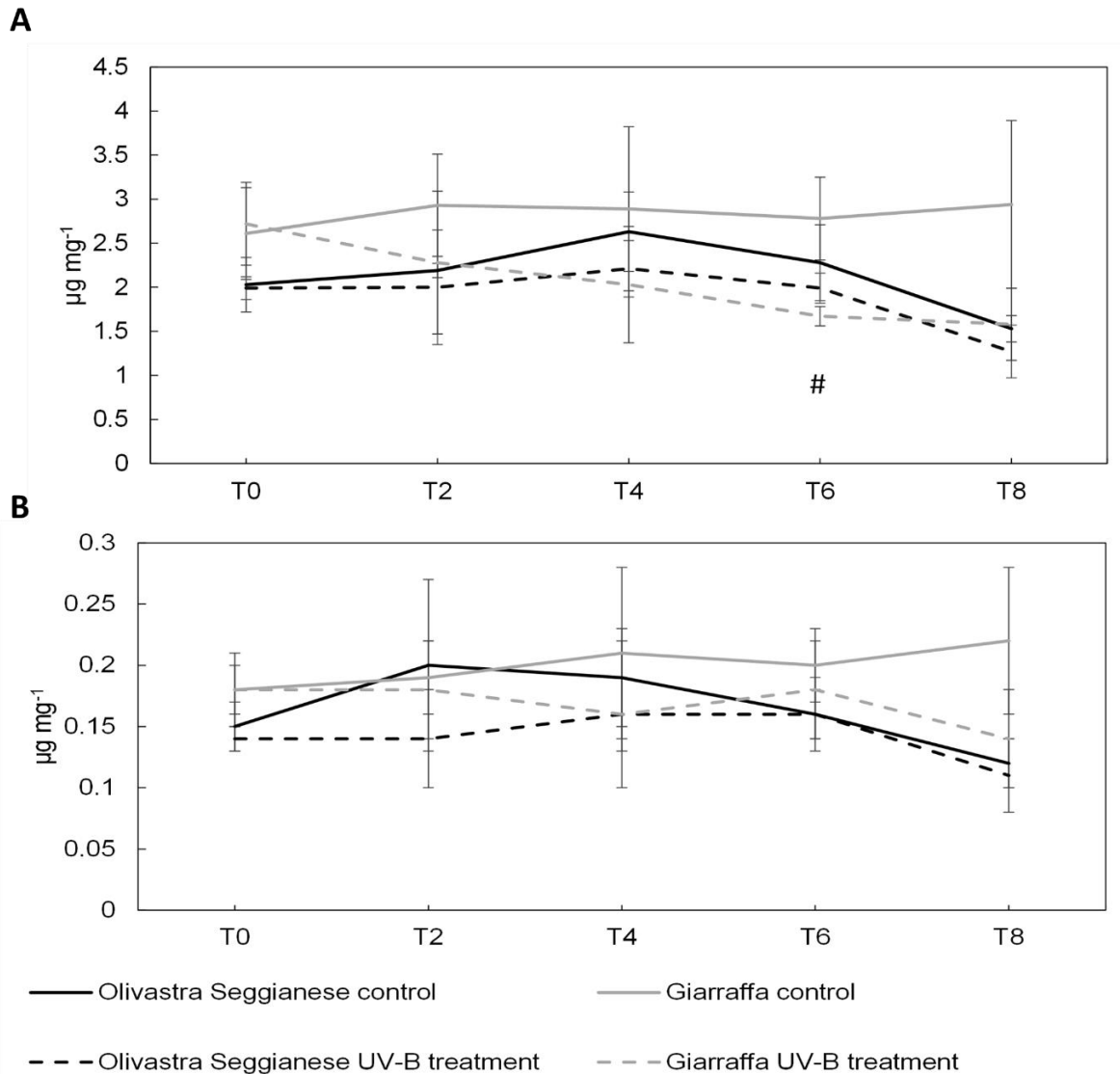


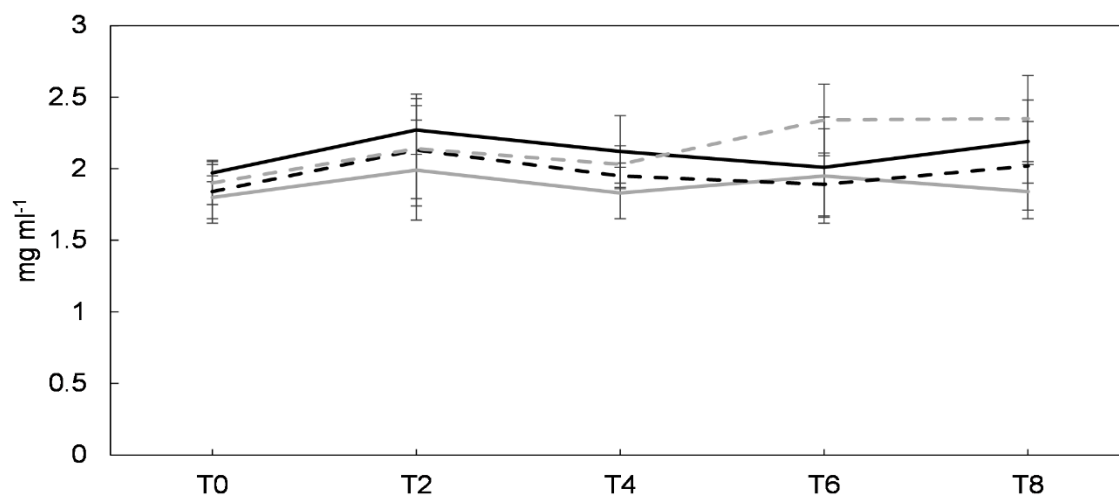
Figure 13. On the x-axes the time points, on the y-axes the concentration of pigments expressed in $\mu\text{g mg}^{-1}$. **(A)** β -carotene content in the two olive cultivars, Olivastra Seggianese and Giarraffa, under control and UV-B treatment in the different sampling times. For each column, values are given as mean \pm standard deviation. Hashtag (#) represent significant differences between control and treated plants of Giarraffa ($p \leq 0.05$). **(B)** Lutein content in the two olive cultivars, Olivastra Seggianese and Giarraffa, under control and UV-B treatment in the different sampling times. For each column, values are given as mean \pm standard deviation.

Also, the content of these pigments in control and UV-B Giarraffa plants was similar ($p > 0.05$), except at time point 6 where the levels of chlorophyll a, chlorophyll b and β -carotene were higher ($p \leq 0.05$) in control plants. Even in this case, the ANOVA test did not show significant differences between control and treated plants.

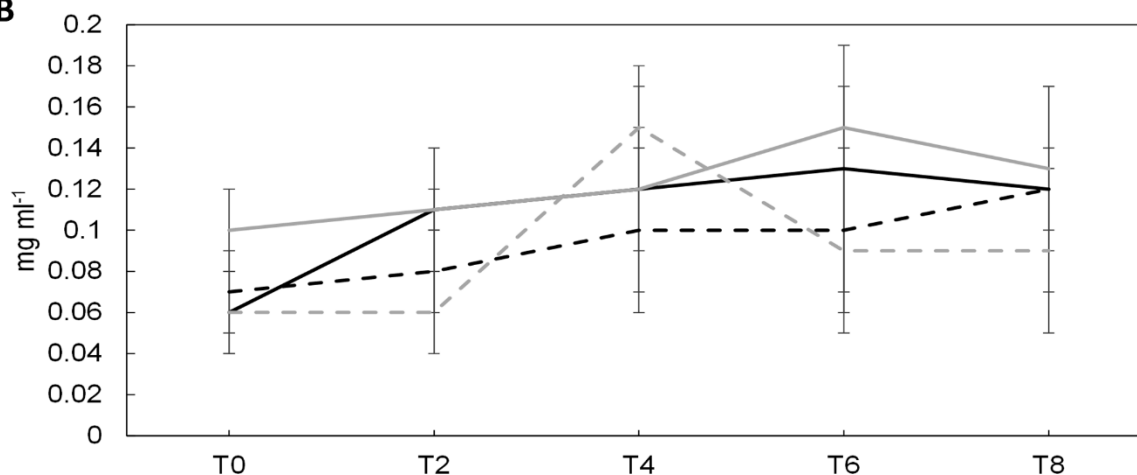
Sugars

At T0 the content of sucrose, glucose 6-P, glucose, fructose and mannitol was similar ($p > 0.05$) in both cultivars. As regards glucose 6-P and sucrose, no statistically significant differences were found between control and UV-B plants of both cultivars (figures 14 A,B, also confirmed by the ANOVA test). Although the average values fluctuated in the various cases analyzed, they were all part of a physiological fluctuation.

A



B



— Olivastra Seggianese control — Giarrafra control
 - - - Olivastra Seggianese UV-B treatment - - - Giarrafra UV-B treatment

Figure 14. On the x-axes the time points, on the y-axes the concentration of sugars expressed in mg ml^{-1} . **(A)** 6-P glucose content in the two olive cultivars, Olivastra Seggianese and Giarrafra, under control and UV-B treatment in the different sampling times. For each column, values are given as mean \pm standard deviation. **(B)** Sucrose content in the two olive cultivars, Olivastra Seggianese and Giarrafra, under control and UV-B treatment in the different sampling times. For each column, values are given as mean \pm standard deviation.

The levels of glucose (figure 15A) in the control and UV-B Giarraffa plants were similar ($p > 0.05$). In fact, the ANOVA test did not give significant results. On the contrary, in the case of Olivastra Seggianese there were significant differences between control and UV-B plants, as confirmed by the ANOVA test. In fact, at the T2, T4 and T8, UV-B plants showed levels of glucose lower than control plants. At time point 6, UV-B plants showed a glucose level higher ($p \leq 0.05$) than the control. Concerning the content of fructose, I found that fluctuations for the Olivastra Seggianese cultivar were statistically significant while those for the Giarraffa cultivar were not (data confirmed by the ANOVA test); at time point 2 the levels of this sugar in UV-B plants of both cultivars were higher than in control plants (figure 15B). Moreover, at time point 6, the UV-B Olivastra Seggianese plants showed a content of fructose significantly lower than the control ones ($p \leq 0.01$).

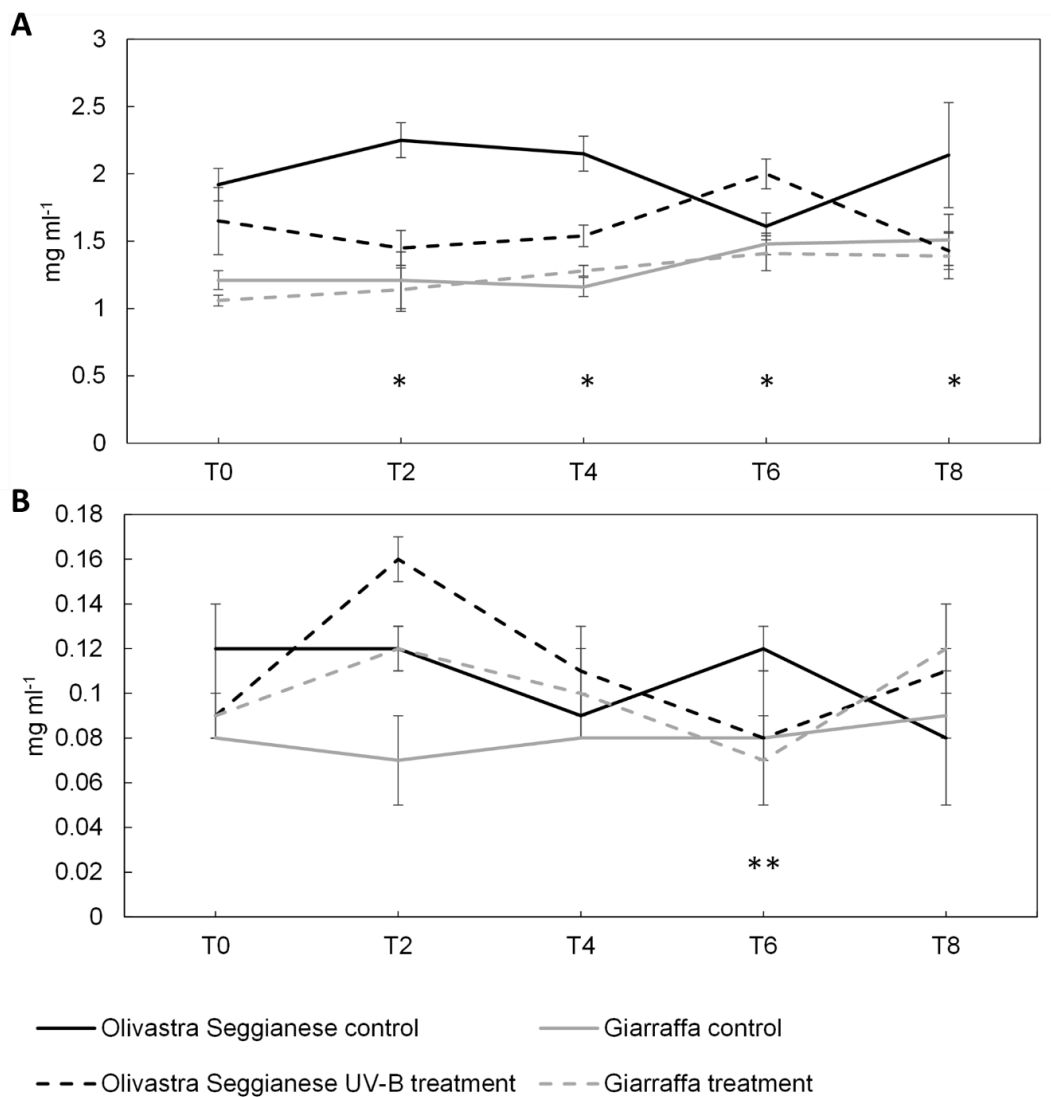


Figure 15. On the x-axes the time points, on the y-axes the concentration of sugars expressed in mg ml⁻¹. (A) Glucose content in the two olive cultivars, Olivastra Seggianese and Giarraffa, under control and UV-B treatment

in the different sampling times. For each column, values are given as mean \pm standard deviation. Asterisk (*) represent significant differences between control and treated plants of Olivastra Seggianese ($p \leq 0.05$). (B) Fructose content in the two olive cultivars, Olivastra Seggianese and Giarraffa, under control and UV-B treatment in the different sampling times. For each column, values are given as mean \pm standard deviation. Double asterisk (***) represent significant differences between control and treated plants of Olivastra Seggianese ($p \leq 0.01$).

Results of mannitol (figure 16) showed that the concentration of this alcohol-sugar increases in treated plants of both cultivars significantly compared to the controls (as confirmed by the ANOVA). The content of mannitol in the Giarraffa cultivar at the T2 point was significantly different between control and treated plants. In fact, mannitol in UV-B plants was 0.85 mg ml^{-1} while in control was 0.64 mg mL^{-1} ($p \leq 0.05$) (figure 16). Furthermore, UV-B Giarraffa plants maintained high mannitol concentrations throughout the treatment, unlike UV-B Seggianese plants which resumed the control values after the peak at T2.

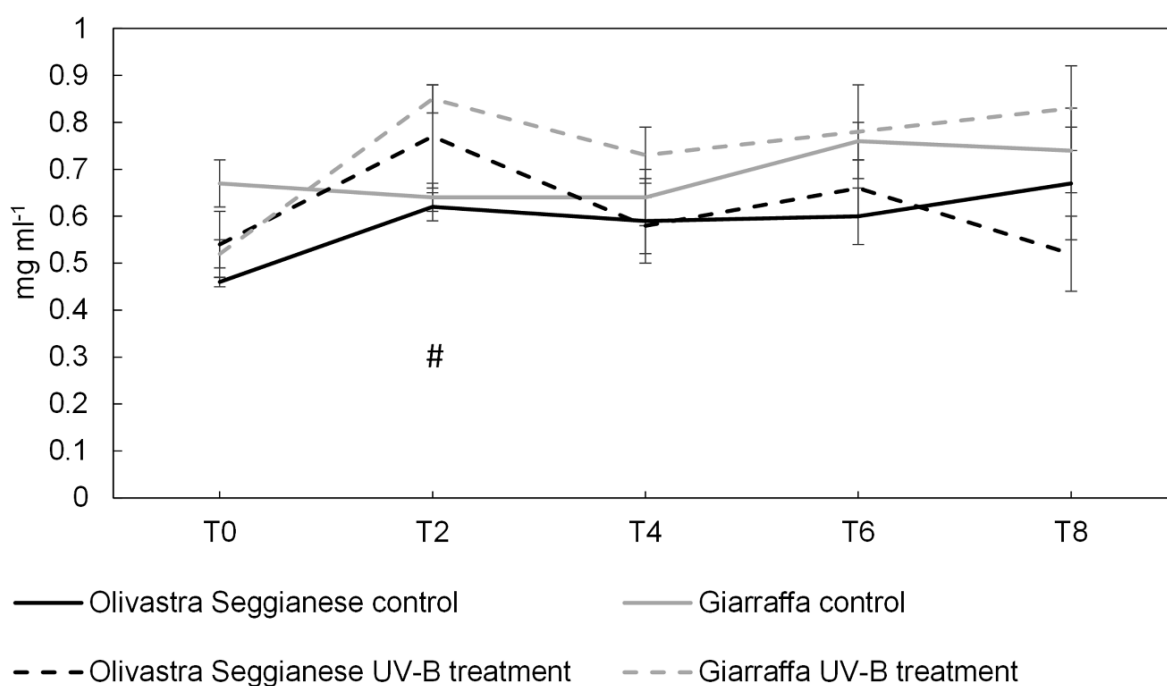


Figure 16. On the x-axes the time points, on the y-axes the concentration of mannitol expressed in mg ml^{-1} . Mannitol content in the two olive cultivars, Olivastra Seggianese and Giarraffa, under control and UV-B treatment in the different sampling times. For each column, values are given as mean \pm standard deviation. Hashtag (#) represent significant differences between control and treated plants of Giarraffa ($p \leq 0.05$).

Antioxidant capacity, polyphenols and flavonoids

Figure 17 shows the antioxidant capacity of olive leaves of both cultivars (control and UV-B treated plants). No significant differences were found in the content of antioxidants between

Olivastra Seggianese and Giarraffa control and UV-B plants throughout the experiment duration.

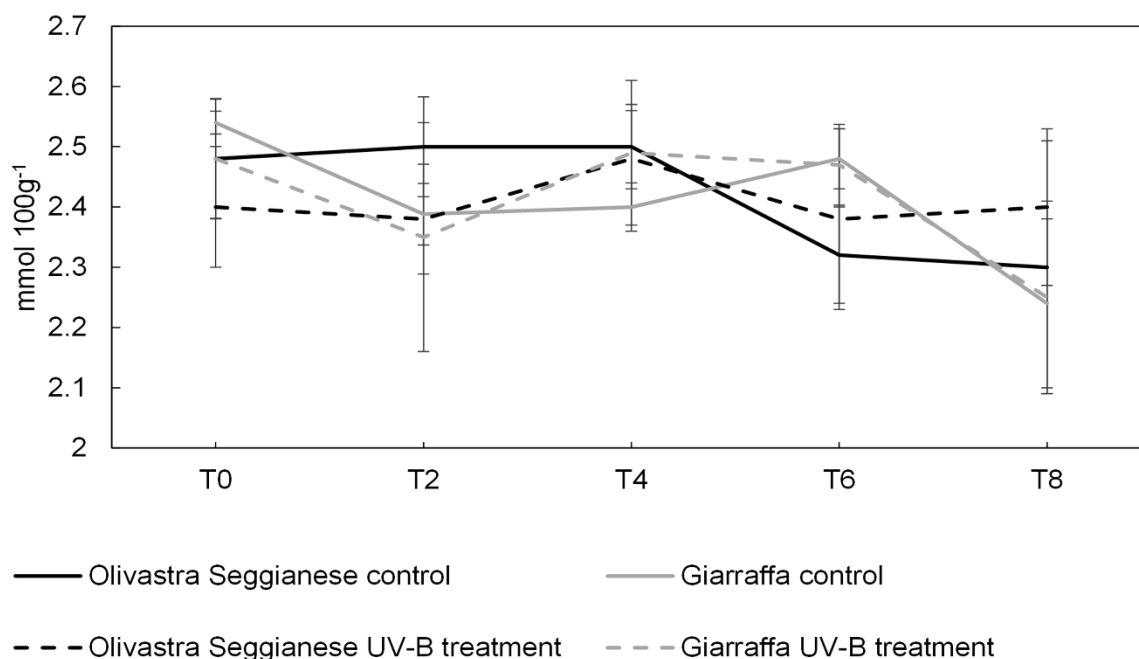


Figure 17. On the x-axis the time points, on the y-axis the concentration of antioxidants expressed in mmol 100 g⁻¹. Antioxidant capacity in the two olive cultivars, Olivastra Seggianese and Giarraffa, under control and UV-B treatment in the different sampling times. For each line, values are given as mean \pm standard deviation.

Concerning polyphenols, a clear difference ($p \leq 0.05$) in the total content between the two cultivars was observed (figure 18). In fact, at T0 all plants of Olivastra Seggianese showed an average value of polyphenols of about 13 mg g⁻¹ FW, while plants of Giarraffa had a value of about 9 mg g⁻¹ FW. Despite this difference, controls of both cultivars show a similar trend, particularly after T4. On the contrary, UV-B plants of both cultivars show a different trend of response. In fact, UV-B Olivastra Seggianese plants, when compared to control, exhibited a slight increase ($p > 0.05$) in total polyphenols at T4, with an average content of 15.42 mg g⁻¹ FW that was followed by a plateau phase until T8. Increase of polyphenols in UV-B Giarraffa plants, as compared to controls, is much more evident from T0 to T2, reaching an average content of 10.33 mg g⁻¹ FW, subsequently plants decreased slightly until T8 with polyphenols content values similar ($p > 0.05$) to those of controls.

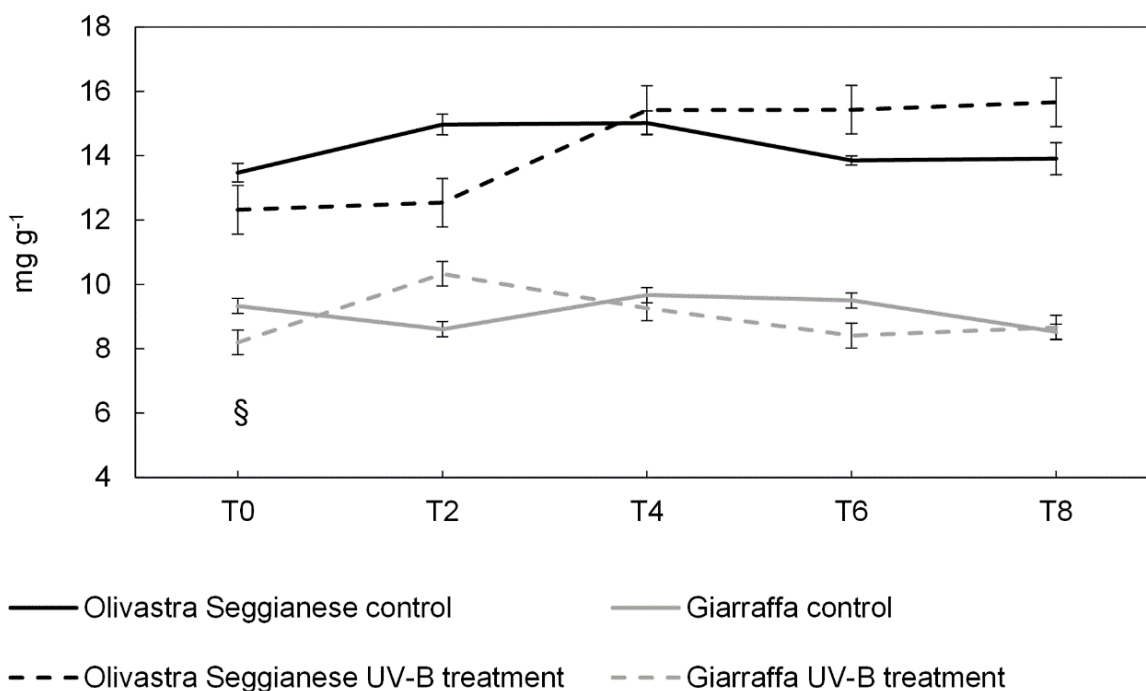


Figure 18. On the x-axes the time points, on the y-axes the concentration of polyphenols expressed in mg g^{-1} . Polyphenols content in the two olive cultivars, Olivastra Seggianese and Giarraffa, under control and UV-B treatment in the different sampling times. For each line, values are given as mean \pm standard deviation. The symbol § represents significant differences between Olivastra Seggianese plants and Giarraffa plants ($p \leq 0.05$).

Figure 19 shows the total flavonoids present in the leaves of both cultivars (control and UV-B treated plants). The data obtained showed that at T0 the content of flavonoids in plants of the two cultivars was very similar ($p > 0.05$) as all plants have an average value of about $70 \text{ mg } 100 \text{ g}^{-1} \text{ FW}$. The controls of both cultivars showed a similar and linear trend, albeit with some oscillations. On the contrary, UV-B plants of both cultivars showed a different trend. In fact, UV-B Olivastra Seggianese plants, compared to the control, showed an increase ($p \leq 0.05$) in total flavonoids at T4 with an average content of $83.62 \text{ mg } 100 \text{ g}^{-1} \text{ FW}$. This increase was followed by a plateau phase lasting until T8, with flavonoid content values similar ($p > 0.05$) to those of controls. Increase of flavonoids in UV-B Giarraffa plants, as compared to controls, is much more evident at T2 ($p \leq 0.05$), whose average content is $85.11 \text{ mg } 100 \text{ g}^{-1} \text{ FW}$. Subsequently Giarraffa plants enter a plateau phase until T6, while maintaining a flavonoid content always higher ($p \leq 0.05$) than the control. From T6 a decrease in flavonoid content was observed until T8 where the content of flavonoids returned to values similar ($p > 0.05$) to the controls.

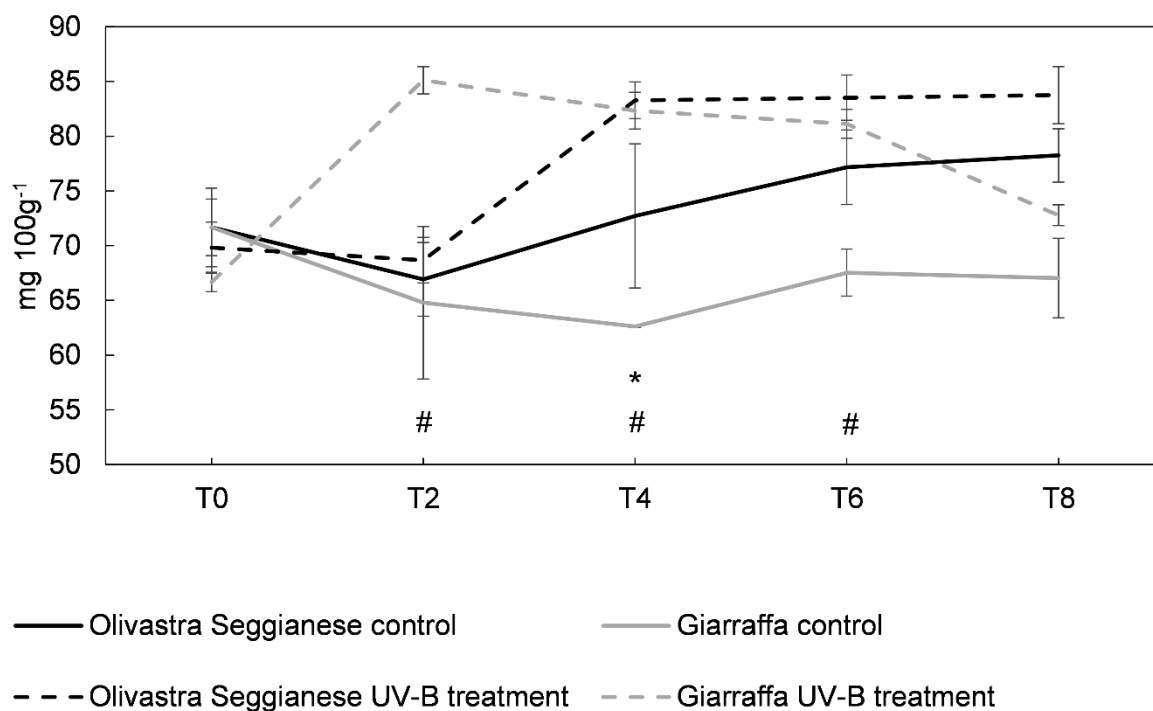


Figure 19. Content of flavonoids in the two olive cultivars, On the x-axis the time points, on the y-axis the concentration of flavonoids expressed in mg 100 g⁻¹. Olivastra Seggianese and Giarraffa, under control and UV-B treatment in the different sampling times. For each line, values are given as mean \pm standard deviation. Asterisk (*) represent significant differences between control and treated plants of Olivastra Seggianese ($p \leq 0.05$). Hashtag (#) represent significant differences between control and treated plants of Giarraffa ($p \leq 0.05$).

Discussion

Among all physiological processes, photosynthesis is one of the most sensitive to the various stresses that a plant can undergo, especially to the stress induced by high UV-B radiation (Sullivan et al. 2003). In this study, I found that the photosynthetic apparatus of both olive cultivars was affected by UV-B. Indeed, photosynthetic efficiency varies over time as stress progresses, comparably with data in the literature (Demmig and Björkman 1987; Johnson et al. 1993). More differences are evident when comparing stressed plants with control plants. Before stress (T0), control plants and those to be stressed have Fv/Fm values in the optimal range.

The first symptoms of stress were found already after the second week (T2) of UV-B exposure, particularly in the Giarraffa cultivar, where the Fv/Fm reach values (<0.75) that are typical of stressed plants (Murchie and Lawson 2013). However, after this critical point UV-B Giarraffa plants were able to recover and maintain the levels of photosynthetic efficiency within the optimal range (around 0.8). Contrarily, the Olivastra Seggianese plants were capable of

maintaining an Fv/Fm value within the optimal range (despite the high variability in the T5), but over the time (T8) showed symptoms of stress. These data suggests that the Giarraffa cultivar is not able to respond immediately in order to preserve the photosynthetic efficiency, but after an adaptive stage triggers a stress protective mechanism allowing the UV-B plants to reestablish the performance and continue to photosynthesize. The Olivastra Seggianese responds earlier but is not able to maintain this capacity over time following the accumulation of the negative effects of UV-B exposure. The pattern of response of the Olivastra Seggianese cultivar is in line with the one reported by Noguès and Backer (2000) in olive plants. These authors reported a decrease of the Fv/Fm to values lower than 0.75 after 14 days of an UV-B BED of $24 \text{ KJ m}^{-2} \text{ d}^{-1}$ (8 h per day). On the contrary, Dias et al. (2018) in a Portuguese olive cultivar exposed to a lower UV-B BED ($12.4 \text{ KJ m}^{-2} \text{ d}^{-1}$ for 5 days) found only a small decrease of the Fv/Fm (0.84), unable to compromise the photosynthetic efficiency. In another Mediterranean species, grapevine plants exposed during 60 days to a UV-B BED of $9.6 \text{ KJ m}^{-2} \text{ d}^{-1}$ were able to maintain the Fv/Fm above 0.75 (Martínez-Lüscher et al. 2015). The degree of damage of UV-B radiation on the PSII functionality seems also to depend on the intensity and duration of exposure as well as the plant species. For instance, according to Albert et al. (2011) in some arctic plants the UV-B radiation can be considered a source of high stress since it causes a decrease in Fv/Fm and a progressively increasing damage on the photosystem II.

The pattern of response of Pi suggests that UV-B conditions reduce the absorption, capture and conversion of excitation energy in electron transport (Stirbet et al. 2018), as the UV-B Olivastra Seggianese is more affected at the end of experiment. As observed for the Fv/Fm, after the first week of UV-B exposure (T2), the Pi was more affected. As also demonstrated in other studies, Pi seems to be more sensitive to environmental stresses than Fv/Fm (Brestic and Zivcak 2013). The decrease of Pi, as found here for both cultivars, is in line with what reported in the literature for other species (maize, sorghum, amaranth and cotton) exposed to high UV-B radiation (Shine and Guruprasad 2012; Kataria et al. 2013).

Taking into account the profiles of Fv/Fm and Pi, I hypothesize that Giarraffa can trigger defense mechanisms suitable for long-lasting UV-B stress unlike Olivastra Seggianese. Comparing the maps of UV index in the various Italian regions (2020) and in the area of origin of the two cultivars, Giarraffa is widely cultivated throughout southern Italy, where the UV index is higher than in Tuscany, the region of origin of Olivastra Seggianese. Possibly the

Sicilian cultivar would adapt over time to growth and survive in environments with higher UV radiation, so that Giarraffa is better equipped to respond to a prolonged UV-B stress.

There are few studies on the photosynthetic pigments of *O. europaea* and on their change following UV-B stress. UV-B radiation can cause variations in the levels of chlorophyll between 10-70% in plants of agricultural interest (Tevini et al. 1981; Mirecki and Teramura 1984; He et al. 1993; Pal et al. 1999; Kakani et al. 2003) depending on the species and the intensity of applied stress agent. Chlorophylls are one of most abundant pigments in plant chloroplasts and they are vital to absorb sunlight for photosynthesis. Carotenoids, besides their function as accessory light-harvesting pigments, also act as antioxidants protecting chlorophylls from photooxidation (Kataria et al. 2013). Within carotenoids, lutein is found mainly in antenna complexes and β -carotene can be found mostly in the reaction centers (Siefermann-Harms 1985, 1990). In the Olivastra Seggianese cultivar, UV-B treatment seems not to affect the response profile of chlorophyll a, chlorophyll b, β -carotene and lutein for all the various time points analyzed. However, in the Giarraffa cultivar UV-B seems to reduce accumulation of pigments (chlorophylls and β -carotene), particularly after a prolonged period of UV-B exposure (T6). This suggests an adaptation mechanism triggered in Giarraffa that aims to reduce energy absorption and therefore defend against excessive UV-B radiation (Vasques et al. 2016). Moreover, a reduction of pigment content can also represent a degradation by UV-B radiation as suggested for *Oryza sativa*, *Prunus dulcis* and *Bryum argenteum* (Ranjbarfordoei et al. 2011; Lidon and Ramalho 2011; Hui et al. 2013). In *Eucalyptus globulus* (Machado et al. 2017) and in olive plants (Dias et al. 2018) exposed to a UV-B BED of around 6 and 12 KJ m⁻² d⁻¹, respectively, the increase of ROS was associated with a pigment decrease in UV-B treated plants.

Abiotic stresses can induce fluctuations in carbohydrates levels due to changes in CO₂ assimilation, in source-sink carbon partitioning and in the activity of enzymes related to sugars synthesis (Rosa et al. 2009). In the present study, the soluble sugars glucose and fructose were the most responsive to UV-B treatment. UV-B Olivastra Seggianese plants tend to accumulate less glucose, particularly after the second week, possible due to a reduction of the photosynthetic processes and to a higher use of this sugar to maintain cellular respiration, to counteract the stress conditions or even to restore/increase the levels of other reserve sugars (e.g., starch) or polyols (e.g., mannitol, that tend to increase at T2) (Stoop et al. 1996; Rosa et al. 2009; Vanlerberghe 2013). In turn, UV-B conditions seem to promote fructose accumulation

(except at T6), more markedly in the Olivastra Seggianese cultivar. Fructose increase can result from sucrose degradation as a response to stress or it can provide the substrate to secondary metabolites synthesis (e.g., lignin and phenolic compounds) (Rosa et al. 2009). Dias et al. (2018) reported that olive plants treated with a lower UV-B dose ($12 \text{ kJm}^{-2} \text{ d}^{-1}$) produced less sucrose and starch but maintained glucose and sorbitol contents. Also, in eucalyptus plants, UV-B treatment (BED of $6 \text{ kJm}^{-2} \text{ d}^{-1}$) decreased the pool of starch and soluble sugars (Machado et al. 2017). These authors argued that UV-B can induce starch degradation to provide more soluble sugars necessary to continue plant metabolic activities and to counteract the stress condition. Contrarily, moringa plants treated with a total UV-B dose of 26 kJm^{-2} showed high functional plasticity increasing soluble sugars, but not changing starch levels (Araújo et al. 2016). Given the key role of sucrose (Farrar et al. 2000; Salerno 2003; Roitsch and González 2004), I assume that plants under UV-B stress implement mechanisms to maintain constant sucrose levels and related metabolic processes. However, this is not always the case because sucrose content in leaves of *Eriophorum russeolum* decreased as a result of UV-B stress (Rinnan et al. 2008) while fructose and glucose concentration showed no significant decreases.

Mannitol is produced in large quantities and accumulated in the leaves of olive trees (Flora and Madore 1993) as well as in many other plants (Loescher et al. 1995; Everard et al. 1997). Like sucrose, it is transported in non-photosynthesizing tissues of plants (Pharr et al. 1995; Gupta and Kaur 2000; Loescher and Everard 2000); together with glucose, mannitol contributes to the osmotic potential and thus to cell turgor (Dichio et al. 2003) and plays an important role in the response to salt and drought stress (Conde et al. 2006; Ennajeh et al. 2009). In addition to osmotic regulation, mannitol increases scavenging of OH-radicals by stabilizing the structure of macromolecules (Abebe et al. 2003). The concentration of mannitol increases significantly in both olive cultivars analyzed. In Giarraffa at T2 the concentration of mannitol increases in plants subjected to UV-B compared to control and this cultivar maintains high concentrations of mannitol throughout the treatment compared to Seggianese; the latter does not show significant differences between control and stressed plants. Mannitol concentration may increase in response to UV-B stress for an osmoprotective and antagonistic function against free radicals (Shen et al. 1997). Since Giarraffa responds better than Seggianese to UV-B stress and has a higher concentration of mannitol, it probably developed this response mechanism to adapt to the more intense radiation in its area of origin.

High UV-B radiation can trigger an increase of reactive oxygen species (ROS) at cell level, which cause oxidation of proteins, lipids and other biomolecules, thus compromising the entire cellular functioning (Robson et al. 2015). To deal with the damage caused by ROS, living organisms have developed a complex defense system consisting of enzymatic and non-enzymatic antioxidants (Antolovich et al. 2002). The antioxidant capacity gives a general information about the antioxidant levels (Rubio et al. 2016) and in the Olivastra Seggiane and Giarruffa both control and UV-B plants respond similarly. Polyphenols play an important role in *O. europaea* oxidative stress control and antioxidant responses against abiotic stress, such as UV-B radiation, drought and heat (Dias et al. 2019, 2020). Olive leaves contain a large cultivar of phenolic compounds, such as flavonoids (e.g., luteolin-7-*O*-glucoside, luteolin-5-*O*-glucoside, luteolin-4-*O*-glucoside, quercetin-7-*O*-rutinoside, quercetin-3-*O*-glucoside, apigenin-7-*O*-glucoside and chrysoeriol-7-*O*-glucoside), secoiridoids (e.g., oleuropein), hydroxycinnamic acid derivatives (e.g., verbascoside), phenolic alcohols (e.g., hydroxytyrosol and tyrosol) and phenolic acids (e.g., chlorogenic and caffeic acids) (Talhouai et al. 2015; Nicoli et al. 2019; Dias et al. 2020). The profile of response of total polyphenols showed considerable difference already at T0, which can be attributed to varietal differences. Giarruffa respond promptly (after the first week) to UV-B radiation increasing polyphenols pools. On the other hand, Olivastra Seggiane plants respond slowly to UV-B triggering only an increase of polyphenols up to T2. This response can generally be assumed as an augment of the availability of antioxidant defense compounds (Sharma et al. 2019). Within the class of polyphenols, the flavonoids are one of the most abundant compounds with antioxidant properties (Agati et al. 2012). They are produced in the epidermal layers of leaves and they likely absorb a large portion of incident UV-B radiation reducing the penetration of UV in the lower tissues of leaves (Bilger et al. 1997; Agati et al. 2012). Moreover, these secondary metabolites also play an important role as ROS scavengers (Luengo Escobar et al. 2017). Flavonoids, especially the ortho-dihydroxy B-ring substituted flavonoids (e.g., quercetin 3-*O*-glucoside and luteolin 7-*O*-glucosides, commonly found in olive leaves), have an important role in ROS-scavenging. Flavonoids quench the ROS by reducing the singlet oxygen, hindering of enzymes involved in ROS generation (lipoxygenase, cyclooxygenase xanthine oxidase, monooxygenase), by chelating transition metal ions which trigger the ROS production, and quenching lipid peroxidation by number of free radical reactions, and help in the recycling of other antioxidants (Agati et al. 2012; Dias et al. 2020). Pearson's correlation analysis (Pearson 1896) between flavonoid content and Pi and between flavonoid content and Fv/Fm, shows us in both cases high coefficients with values of r equal to -0.712 and -0.749 respectively. A

negative relationship indicates that low scores on one variable correspond to high scores on the other variable (Pearson 1896). The worsening of the health of the plants showed by a decrease in the photosynthetic efficiency values (Fv/Fm and Pi) correlated to an increase in the flavonoid content. This increase, therefore, could be interpreted as a defense mechanism that plants put in place to cope with the stress from UV-B radiation. As observed for the total polyphenols, Giarraffa respond quickly to UV-B stress (during the first weeks), and over time total flavonoids levels tend to decrease. In turn, the Olivastra Seggianese responds later (after the second week) and maintains high levels of these compounds until the end of the experiment. These distinct profiles of antioxidant response and also photosynthetic efficiencies to UV-B treatment triggered in the two cultivars may be related and may support the hypothesis that Giarraffa is able to activate defense mechanisms already after the first weeks of UV-B stress thereby performing, in a long term, better than Olivastra Seggianese. This higher defense capacity of Giarraffa is also supported by the slight decrease of antioxidants over the second week, which may result from its efficient use to neutralize ROS and therefore protect olive plants from oxidative damage, as already reported in olive trees under UV-B conditions (Dias et al. 2020). The importance of polyphenols, particularly the flavonoids, in olive protection against UV-B stress was also highlighted by Noguès and Backer (2000). UV stress as other environmental factors including oxygen shortage or pathogen invasion induces oxidative stress by generation of ROS and the plants defend themselves by the activation of an antioxidants system. Flavonoids may work as ROS scavenging compounds in a cooperative or compensative activity within this complex antioxidant system. All this considered, a trait as a higher production of flavonoids, which this study demonstrated to vary within the cultivars, could be helpful in explaining olive fitness in hostile environments. Breeding of this species will take advantage of any information relative to parental lines to be used for crossing with superior metabolic performances.

Conclusions

Given the high and multiple importance of the olive tree, it is essential to study its responses to stressful agents, such as excessive UV-B radiation, in order to understand the defense mechanisms and identify the most resistant cultivars. This study confirms that UV-B radiation is a dangerous source of stress for olive trees, especially in today's increasingly changing environmental conditions. Although the two cultivars showed symptoms of UV-B stress and activated antioxidant defense mechanisms, they exhibited evident different response patterns and timescales. The T2 could be the critical stage, since around this time point started to be

more notorious the stress symptoms (e.g., reduction of Fv/Fm) and antioxidant defenses are activated. Giarrappa cultivar seems better suited to prolonged UV-B stress, possible due to a more efficient and quick activation of the antioxidant response (e.g., flavonoids use to counteract ROS) and due to its capacity to maintain the photosynthetic efficiency as well as a relatively higher content of mannitol. Moreover, pigments reduction after a long period of UV-B exposure can also be an adaptation mechanism triggered by Giarrappa to reduce energy absorption under UV-B stress. Olivastra Seggianese seems less suited to overcome UV-B stress for a long period (e.g., higher reduction of Fv/Fm) and has a higher necessity to use sugars (e.g., glucose) possible to counteract stress and to restore energy.

List of contributors to this chapter:

- **Claudio Cantini** (Institute for BioEconomy, National Research Council of Italy, 58022 Follonica, Italy)
- **Giampiero Cai** (Department of Life Sciences, University of Siena, via Mattioli 4, 53100 Siena, Italy)
- **Maria Celeste Dias** (Department of Life Sciences, Centre for Functional Ecology, University of Coimbra, Calçada Martim de Freitas, 3000-456 Coimbra, Portugal)
- **Marco Romi** (Department of Life Sciences, University of Siena, via Mattioli 4, 53100 Siena, Italy)

Chapter 3: biochemical responses of olive to UV-B radiations

Introduction

As described in the previous chapter, one of the main targets of UV-B radiation is the photosynthetic apparatus of plants (Kataria et al. 2013). High UV-B radiation causes decreased photosynthetic efficiency, reduced growth rate, and alterations in carbon and nitrogen metabolism (Dotto and Casati 2017; Piccini et al. 2020). UV-B radiation can also affect stomatal conductance, thereby altering both the rate of CO₂ assimilation and water loss through transpiration (Kataria et al. 2013; Koubouris et al. 2015). In addition, excess UV-B radiation affects photosystem II (PSII) (Zlatev et al. 2012; Kataria et al. 2013), photosynthetic pigment levels (Lidon and Ramalho 2011; Machado et al. 2017; Piccini et al. 2020), thylakoid and chloroplast integrity (Kataria et al. 2013), as well as RubisCO activity (Dias et al. 2018) and photosynthetic gene transcription (Strid et al. 1994). In particular, RubisCO (the enzyme that catalyzes the carboxylation step in the Calvin cycle) appears to be a target protein for various stresses, such as drought and heat (Crafts-Brandner and Salvucci 2000; Carmo-Silva et al. 2012). Like other proteins, RubisCO can be damaged by reactive oxygen species (ROS), the latter produced upon plant exposure to UV-B. In rice, Fedina et al., (2010) showed that UV-B radiation treatment of three different cultivars increases the activity of antioxidant enzymes while reducing RubisCO subunits. Other studies show that UV-B stress decreases both enzyme activity and the amount of RubisCO in various plant species (Allen et al. 1997; Bischof et al. 2000; Savitch et al. 2001; Dias et al. 2018). RubisCO is also characterized by many posttranslational modification sites (Houtz et al. 2008); therefore, I hypothesize that stressful treatment may generate RubisCO isoforms that are better adapted to cope with stressful conditions.

High levels of UV-B radiation are known to induce abundant ROS production in plants (Panagopoulos et al. 1990; Foyer et al. 1994; Smirnoff 1998; Mahdavian et al. 2008). Therefore, plants have developed protective mechanisms against ROS, such as batteries of antioxidant enzymes and accumulation of UV-absorbing compounds (Frohnmeier and Staiger 2003; Fedina et al. 2010). Antioxidant enzymes include superoxide dismutase (SOD), catalase (CAT), and glutathione peroxidase (GPox), while non-enzymatic substances include glutathione, ascorbate, tocopherols, carotenoids, albumin, bilirubin, chelating agents, and phenols (Zlatev et al. 2012; Hideg et al. 2013; Rácz et al. 2018). Among the latter, flavonoids can effectively absorb UV-B and neutralize ROS (Agati et al. 2012). In addition, UV-B

exposure increases the concentration of other protective phenolic compounds (Dias et al. 2020). In the previous chapter, it was shown that phenolic compounds are involved in the response of olive trees to excessive UV-B radiation (Piccini et al. 2020).

While RubisCO fuels the Calvin cycle by producing substrates for sucrose synthesis, sucrose degradation in sink tissues is carried out by enzymes such as invertase and sucrose synthase. In particular, sucrose synthase catalyzes the reversible conversion of sucrose and UDP to fructose and UDP-glucose (Baroja-Fernandez et al. 2012). Several experimental evidence indicate that UV-B stress can affect the activity of enzymes that metabolize sucrose, including sucrose synthase (Interdonato et al. 2011; Wang et al. 2018). In combination with RubisCO damage, altered enzyme activity of sucrose synthase may result in incorrect sucrose metabolization, leading to a decrease in available sugars.

This chapter complements the results obtained in chapter 2 by focusing on the biochemical and enzymatic analysis of both Italian cultivars of *Olea europaea* (Olivastra Seggianese and Giarraffa) subjected to chronic UV-B stress (14 h per day for eight weeks). In particular, I focused on the effects of UV-B radiation on RubisCO, in terms of quantity, enzymatic activity, and isoform variation. In addition, transmission electron microscope (TEM) observations were made on leaf samples to find correlations between changes in photosynthetic parameters and ultrastructural modifications. Additionally, I analyzed the activity of antioxidant enzymes (SOD, CAT, GPox) to obtain a complete picture of the antioxidant system in olive plants subjected to UV-B stress. I also analyzed malondialdehyde (MDA) as a parameter of ROS-induced oxidation in macromolecules such as lipids. Given the importance of sucrose, I also evaluated the effects of UV-B on the enzyme sucrose synthase. Overall damage at the biochemical level was assessed by analyzing changes in Hsp70, a chaperone protein whose content increases under stress conditions (Bierkens 2000).

Materials and Methods

Plant growth conditions and application of UV-B Treatment

Olive plants were grown and stressed by UV-B radiation exactly as described in the materials and methods of chapter 2.

Antioxidant enzymes extraction and quantification

Olive leaves were collected at selected time points (T2, two weeks; T4, four weeks; T6, six weeks and T8, eight weeks of treatment), immediately frozen in liquid nitrogen and stored at -80°C . Upon use, leaves were ground (0.5 g) with 5 mL of extraction buffer containing 0.1 M potassium phosphate buffer (pH 7.5), 0.5 mM Na_2EDTA , 2 mM DTT, 1 mM PMSF, 1% PVP (*m/v*) and 0.2% Triton X-100 (*v/v*) (Dias et al. 2020). The lysates were centrifuged at 10,000 g for 15 min at 4°C and used to determine the activities of SOD (EC1.15.1.1), CAT (EC 1.11.1.6) and GPox (EC 1.11.1.7). For SOD activity, 50 mM potassium phosphate buffer (pH 7.8), 13 mM methionine, 50 mM Na_2CO_3 , 0.1 M Na_2EDTA , 25 mM NBT, and the leaf extracts were mixed. Riboflavin (2 mM) was added, and the reaction was started by illuminating (fluorescent lamp of 15 W) the samples for 15 min. The absorbance was read at 560 nm, and one unit of enzyme activity was defined as the amount of SOD necessary to induce 50% inhibition on the rate of NBT reduction (Agarwal et al. 2005). CAT activity was determined at 25°C according to Beers and Sizer (1952). The reaction mixture contained 0.1 M potassium phosphate buffer (pH 7.0) and the leaf extract. To start the reaction, 20 mM H_2O_2 was added and after 5 min the reaction was stopped by addition of 150 μL of H_2SO_4 + 1 g of TiO_2 + 10 g of K_2SO_4 . The mixture was centrifuged at 10,000 g for 10 min at 4°C and the absorbance of supernatant was read at 415 nm. The activity of catalase was determined from a standard curve. GPox activity was determined in a mixture of 96 mM guaiacol, 12 mM H_2O_2 , 10 mM potassium phosphate buffer (pH 6) and the leaf extract (Dias et al. 2020). GPox activity was calculated measuring the increase of absorbance at 470 nm.

Lipid peroxidation

Lipid peroxidation was determined by measuring the formation of malondialdehyde (MDA) (Hodges et al. 1999). Frozen leaves, collected at the selected time points (T2, T4, T6 and T8), were ground (100 mg) with 1.5 mL of 0.1% trichloroacetic acid (TCA, *w/v*) and centrifuged at 10,000 g for 5 min at 4°C . Then, 1 mL of the supernatant was homogenized with 1 mL of 20% TCA (*w/v*) + 0.5% of thiobarbituric acid (*w/v*) as a positive control; in parallel, 1 mL of sample was homogenized with 1 mL of 20% TCA (*w/v*) as a negative control. Both groups were incubated at 95°C for 30 min, cooled on ice and centrifuged (10,000 g for 10 min at 4°C). The absorbance of the supernatant was read at 600, 532 and 440 nm in a spectrophotometer. MDA equivalents were determined according to Hodges et al. (1999).

Ribulose-1,5-Bisphosphate Carboxylase/Oxygenase (RubisCO) Activity.

Olive leaf samples of both cultivars were taken at 3 selected time points: before the onset of stress (T0), and after 4 weeks (T4) and 8 weeks of stress (T8). Subsequently, leaves were homogenized at 0 °C with 1 mL homogenization buffer consisting of 50 mM TRIS/HCl pH 7.8, 1 mM EDTA, 20 mM MgCl₂, 10 mM NaHCO₃, 5 mM DTT, 0.3 % BSA (w/v) and 10 mg/mL Polyclar AT (SERVA). After centrifugation (9000 g × 5min), samples were incubated for 20 min at room temperature prior to analysis according to Lilley and Walker (1974). The supernatant was mixed with the reaction medium consisting of 50 mM HEPES/KOH (pH 8.0), 10 mM KCl, 1 mM EDTA, 20 mM MgCl₂, 5 mM DTT, 2.5 mM ATP, 0.2 mM NADH, 10 mM NaHCO₃, 5 mM creatine phosphate, 20 U/mL creatine phosphokinase, 6 U/mL phosphoglycerate kinase, 6 U/mL glyceraldehyde phosphate dehydrogenase and 10 µL of the extract. After establishing a steady base rate, the reaction was started with the addition of 0.6 mM ribulose-1,5 biphosphate. The reaction was measured via the decrease in absorbance at 340 nm due to NADH oxidation.

Protein Extraction

Olive leaf samples of both cultivars were taken at 3 selected time points (T0, T4, and T8). Samples were extracted according to Wu et al. (2014), with a protocol effective in the extraction of proteins from recalcitrant plants such as olive and grapevine. Reagents were purchased from Sigma Aldrich. All samples were processed simultaneously to minimize experimental variability. Protein concentration of samples was determined using the 2-D Quant kit (GE HealthCare). The protocol was carried out exactly as described in the instruction manual using BSA as a reference. Each sample was analyzed in three replicates using a Shimadzu UV-160 spectrophotometer set at 480 nm.

1-D Electrophoresis, Western Blotting and Image Analysis

Separation of proteins by 1-D electrophoresis was performed on Tris-HCl 10% gels using a Criterion cell (Bio-Rad Laboratories, Milano, Italy) equipped with a Power Pac Bio-Rad 300 at 200 V for approximately 35 min. TGS (25 mM Tris-HCl pH 8.3, 192 mM glycine and 0.1% SDS) was used as running buffer. Gels were stained with Bio-Safe Coomassie blue (Bio-Rad Laboratories, Milano, Italy). Transfer of proteins from gels to nitrocellulose membranes was performed using a Trans-Blot Turbo Transfer System (Bio-Rad) according to the manufacturer's instructions. The quality of blotting was determined by checking the transfer of precision pre-stained molecular standards (Bio-Rad). After blotting, membranes were

blocked overnight at 4 °C in 5% Blocking Agent (Bio-Rad) in TBS (20 mM Tris pH 7.5, 150 mM NaCl) plus 0.1% Tween-20. After washing with TBS, membranes were incubated with the primary antibody for 1 h at room temperature. For immunodetection of actin, we used the mouse monoclonal antibody clone 10-B3 diluted 1:3000 (Sigma Aldrich, Merck Life Science S.r.l., Milano, Italy), for immunodetection of RubisCO we used the rabbit polyclonal antibody clone AS03-037 diluted 1:3500 (Agrisera, Vännäs, SWEDEN), for immunodetection of Susy the rabbit polyclonal antibody clone AS15-2830 diluted 1:5000 (Agrisera), and for immunodetection of Hsp70 we used the rabbit polyclonal antibody clone AS08-371 diluted 1:5000 (Agrisera). Subsequently, membranes were washed several times with TBS and then incubated for 1 h with peroxidase-conjugated secondary antibodies. Specifically, we used a goat anti-mouse IgG (Bio-Rad) and a goat anti-rabbit IgG (Bio-Rad) both diluted 1:3000. After additional washes in TBS, the “Clarity” (Bio-Rad) mixture was used for enzymatic reaction. Images of gels and blots were acquired using a Fluor-S apparatus (Bio-Rad), while analysis of gels and blots was performed with the Quantity One software (Bio-Rad, version 4.6.7). All blots were developed using identical conditions, from substrate incubation to exposure time. All images were processed correspondingly using the Autoscale command (to improve the quality of gels and blots) and the Background Subtraction command (to remove the background noise). The relative intensity of single bands was calculated with the Volume tool of Quantity One software (Bio-Rad, version 4.6.7). Results were exported and graphed with Microsoft Excel.

2-D Electrophoresis, Western Blotting and Image Analysis

Separation of proteins by 2-D electrophoresis was performed on an IPG Strip (Ready Strip IPG Bio-Rad), 11 cm long. Since the isoelectric point of RubisCO is between 6 and 7, strips with a pH range of 5–8 were chosen. Strips were hydrated (overnight) in a solution containing the rehydration/solubilization buffer to which 18 mM DTT and 20 µL / ml IPG Buffer (pH 3–10) were added. Samples to be analyzed were also included in the rehydration/solubilization buffer. Rehydration took place in a special container (GE Immobiline Dry Strip Reswelling Tray) after strips were covered with Mineral Oil (Bio-Rad). Following rehydration, the first electrophoretic run was performed using the Protean IEF (Bio-Rad) system, with the following protocol:

1. From 0 to 500 V in 1 h
2. 500 V constant for 1 h

3. From 500 V to 4000 V in 2 h
4. 4000 V for 2 h
5. From 4000V to 8000V in 2 h
6. 8000 V constant up to 15000 V / hour
7. From 8000 V up to 500 V in 30 min
8. 500 V until the strips are taken.

At the end, strips were taken and immediately processed for separation of proteins in the second dimension. Strips were first equilibrated in 50 mM Tris-HCl pH 8.8, 6 M urea, 30% glycerol, 2% SDS, trace amounts of Bromophenol Blue, and 10 mg/mL DTT. We used Criterion XT PreCast 10% gels (Bio-Rad). The electrophoretic run was performed with the Criterion Cell (Bio-Rad) at 200 V constant for 1 h using the XT-MOPS (Bio-Rad) buffer. Subsequently, gels were processed and transferred to a nitrocellulose membrane for immunoblotting as described above. Membranes were blocked overnight at 4 °C in 5% ECL Blocking Agent (Bio-Rad) in TBS (20 mM Tris pH 7.5, 150 mM NaCl) plus 0.1% Tween-20. Membranes were incubated for 1 h at room temperature with a primary anti-RubisCO antibody, diluted 1: 10,000 (Agrisera code AS03037). After washings, membranes were incubated for 1 h with a secondary anti-rabbit antibody, diluted 1: 3000 conjugated to peroxidase. Images of gels and blots were acquired using a Bio-Rad Fluor-S Multi-Imager, controlled by Quantity One (Bio-Rad) software. For the comparison of immunoblots, the PDQuest software (Bio-Rad) was used, allowing for the alignment and relative quantification of spots. Immunoblots were analyzed according to the olive cultivar by comparing the three time points (T0, T4 and T8); the PDQuest software creates a reference image (“master blot”) by which the various spots can be aligned. Spot quantitation data were exported and graphed with Microsoft Excel. Blot analysis was repeated at least three times in samples from different experiments.

Microscopy analysis

We analyzed olive leaves of both cultivars taken at 3 selected time points (T0, T4, and T8). The protocol is detailed in Behr et al. (2019). For transmission electron microscopy (TEM), samples were fixed in 3% glutaraldehyde in the cacodylate buffer (0.066 M, pH 7.2), for 1 h at room temperature. After fixation, samples were rinsed with a cacodylate buffer and post-fixed with osmium tetroxide 1% in cacodylate buffer for 1 h. Then, samples were rinsed with water and dehydrated gradually in increasing concentrations of ethanol (from 10% to 100%). Samples

were embedded in Spurr's resin (Spurr 1969), polymerized for 8 h at 70 °C, and then cut into 600-Å sections using an LKB Nova ultramicrotome provided with a diamond knife. Sections were stained with uranyl acetate and lead citrate for 10 min, respectively, and finally observed with a Philips Morgagni 268D transmission electron microscope operating at 80KV and equipped with a MegaView II CCD camera (Philips electronics). Three different sets of experiments were subjected to TEM analysis.

Statistical analysis

Statistical analysis was performed by the Systat 11 statistical package (Systat Software Inc., Richmond, CA, USA). Data were checked for normality distribution by the Shapiro–Wilk test before repeated measures of ANOVA analysis. ANOVA tested the significance of each of the three variables: time, treatment and cultivar, as well as their interaction. When the *p* values of the ANOVA were \leq to 0.01 or 0.05, Tukey's pairwise mean comparison within each variable was performed.

Results

Microscopy analysis

In the present study, observations by transmission electron microscopy (TEM) were performed on leaf samples (from control and stressed plants) of both cultivars at T0, T4, and T8. The aim was to examine whether any alterations in photosynthetic parameters (such as the amount and composition of RubisCO) could have a correlation with ultrastructural changes (figure 20). At T0, it was readily possible to detect fundamental differences in chloroplast structure between the two cultivars. In particular, Giarraffa showed a higher relative compactness of thylakoids (figure 20a), so that it was not even easy to distinguish individual grana. Such compactness was not present in Olivastra Seggianese (figure 20b), where the single thylakoids were clearly distinct (black arrows). Olivastra Seggianese showed the presence of some lipid bodies (white arrow), rarely observed in Giarraffa. At T4, the compactness of thylakoids in Giarraffa was maintained (figure 20c); the presence of some small lipid bodies could be observed (white arrow). In Olivastra Seggianese at T4 (figure 20d), individual thylakoids were still clearly discernible and well-aligned with each other (black arrows). At T8, Giarraffa chloroplasts were still characterized by a remarkable compactness of thylakoids (figure 20e) and by the presence of sporadic lipid bodies (white arrow); in Olivastra Seggianese thylakoids and grana were still

easily distinguished (black arrow). In any case, no particular ultrastructural damage was observed.

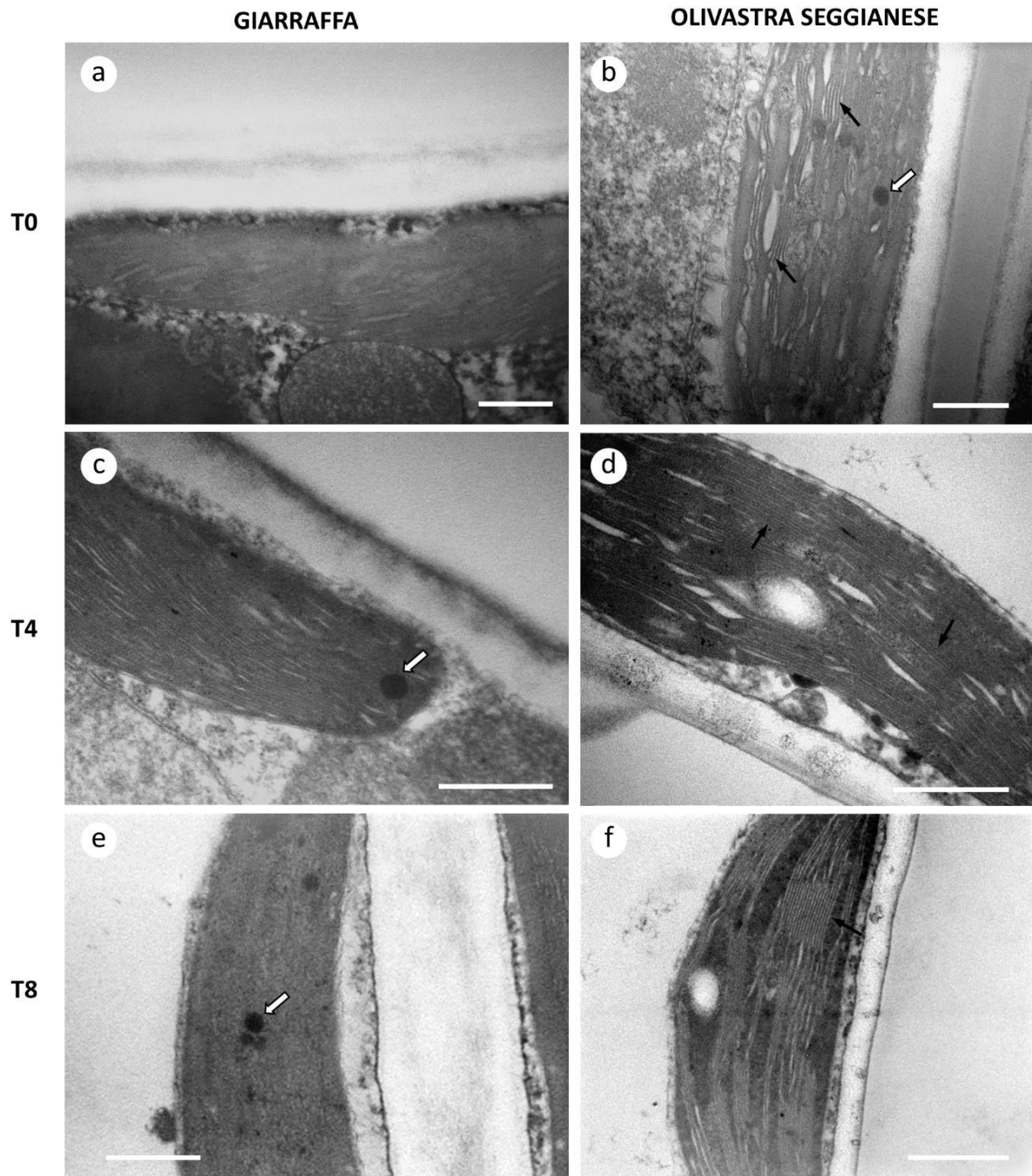


Figure 20. Ultrastructural analysis of chloroplasts of Giarraffa and Olivastra Seggianese leaves. (a) Chloroplast in Giarraffa leaves at T0; note the relative compactness of thylakoids. (b) Chloroplast in Olivastra Seggianese leaves at T0; thylakoids are more spaced and less compact. (c) Chloroplast of Giarraffa at T4, still characterized by a high compactness of thylakoids. (d) Chloroplast of Olivastra Seggianese at T4, characterized by a lower compactness of thylakoids. (e) Two chloroplasts of Giarraffa at T8, where it is still difficult to distinguish individual thylakoids. (f) Ultrastructure of chloroplast of Olivastra Seggianese at T8, with easily distinguishable thylakoids and grana. Black arrows indicate thylakoids, while white arrows indicate lipid bodies. Bars: 500 nm.

Antioxidant enzymes analysis

The ANOVA test showed a significant effect of UV-B stress on olive cultivar, treatment, and of their interaction on RubisCO and Gpox content ($p \leq 0.001$), while MDA and SOD activities showed significant effect of treatment and treatment x cultivar ($p \leq 0.001$). Finally, CAT activity was affected only by the specific cultivar ($p \leq 0.001$) and by the interaction treatment x cultivar ($p \leq 0.005$).

- *Superoxide dismutase (SOD)*

The enzymatic activity assay of superoxide dismutase (SOD) (figure 21) revealed the absence of significant differences between control and stressed plants of both cultivars at T2 ($p > 0.05$). The same finding was also observed at T0 and has been omitted in this graph. After four weeks of stress (T4), a significant increase ($p \leq 0.01$) in SOD enzymatic activity was observed in stressed Olivastra Seggianese plants compared to control plants. In contrast, Giarraffa did not exhibit any change as the stressed plants were characterized by similar SOD values to the control plants. After additional two weeks of stress (T6), the difference previously observed for Olivastra Seggianese was not present and all plants (control and stressed) of both cultivars showed very similar SOD values. At the end of experiment (T8), Olivastra Seggianese again showed a significant ($p \leq 0.01$) increase in SOD enzyme activity in treated plants compared to control plants. Giarraffa, on the other hand, did not exhibit any variation between stressed and control plants.

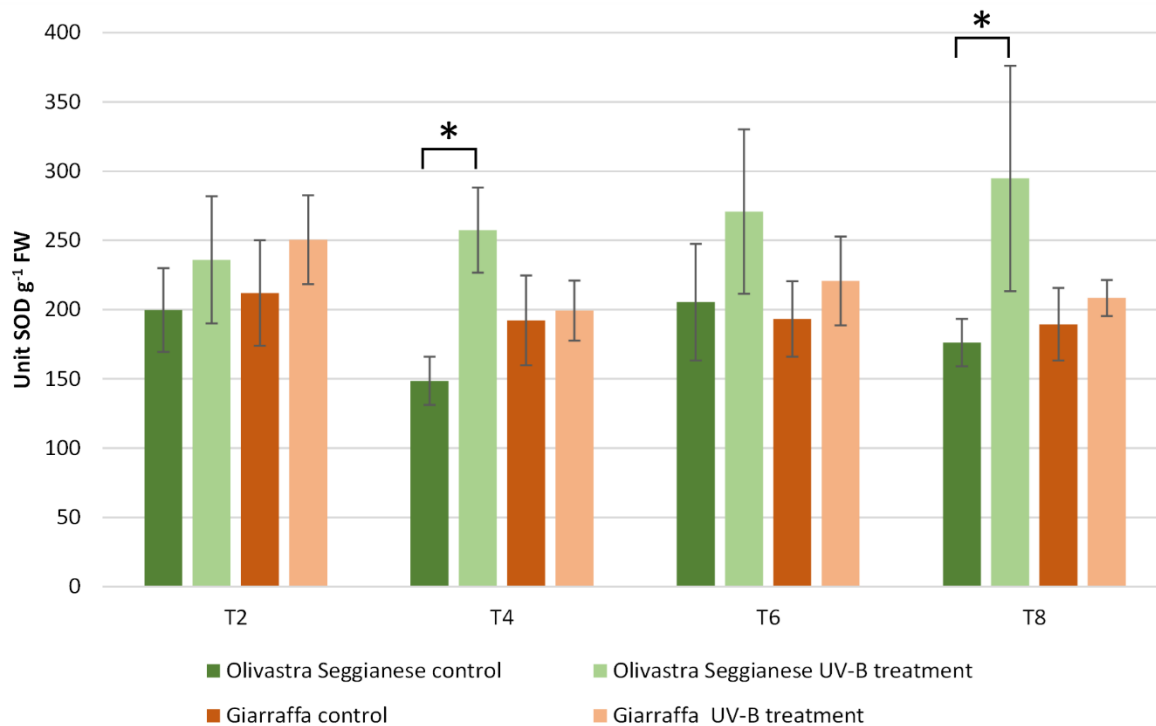


Figure 21. Superoxide dismutase activity in Giarraffa and Olivastra Seggianese leaves under control conditions and after exposure to UV-B treatment. The x-axis reports the treatment times. The asterisks (*) indicate statistically significant differences between control and stressed samples within each cultivar. Values are mean \pm standard ($n = 6$).

- *Catalase (CAT)*

Enzymatic activity assay of catalase (CAT) (figure 22) exhibited a significant difference in control plants of the two cultivars ($p \leq 0.01$) as they progressed from initial (T2) to final (T8) treatment. Basal differences in CAT enzyme activity between control plants of Olivastra Seggianese and Giarraffa were already evident at T0 (data not shown). Indeed, control plants (but also stressed plants) of Olivastra Seggianese cultivar showed significantly higher levels of CAT enzyme activity than plants of Giarraffa cultivar, with a very important increase at T8. The Giarraffa cultivar did not exhibit statistically significant differences ($p > 0.05$) in CAT activity between control and stressed plants throughout the experiment (from T2 to T8) with the sole exception of control plants at T4. In contrast, statistically significant differences ($p \leq 0.01$) in CAT enzyme activity were observed between control and stressed plants of Olivastra Seggianese cultivar at both T2 and T4. In fact, while T2 was characterized by an increase in CAT activity in control plants, T4 conversely showed a significant increase of CAT activity in stressed plants compared to controls.

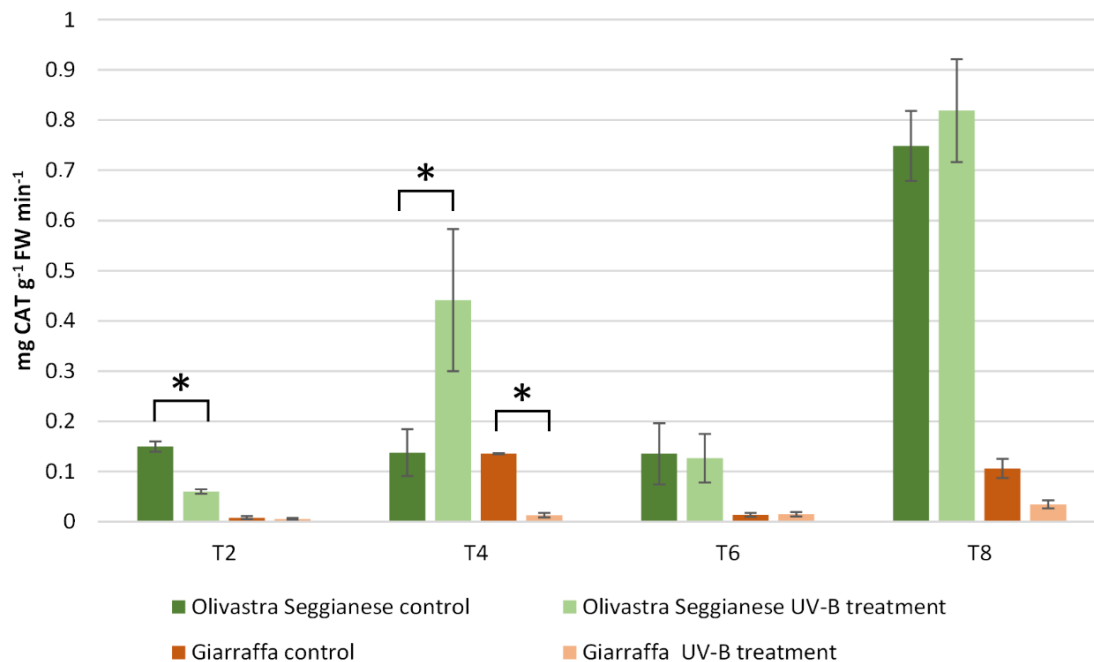


Figure 22. Catalase activity in Giarraffa and Olivastra Seggianese leaves under control conditions and after exposure to UV-B treatment. The x-axis indicates the treatment times. The asterisks (*) indicate statistically significant differences between control and stressed samples within each cultivar. The two cultivars differ by ANOVA test for $p \leq 0.01$. Values are mean \pm standard ($n = 6$).

- *Glutathione peroxidase (GPox)*

The enzymatic activity assay of glutathione peroxidase (GPox) (figure 23) showed a statistically significant difference ($p \leq 0.01$) in control plants of the two cultivars from T2 to T8, as well as at T0 (data not shown). This difference was higher in the Olivastra Seggianese control plants than in the Giarraffa controls. For the Olivastra Seggianese cultivar, a significant ($p \leq 0.01$) and stable decrease in GPox activity was observed in treated plants compared to control plants from T2 to T6. On the contrary, the Giarraffa cultivar showed a significant ($p \leq 0.01$) and progressive increase in GPox enzymatic activity from T2 to T8 in stressed plants compared to control plants. Ultimately, Olivastra Seggianese plants showed a decrease in enzymatic activity after UV-B stress (except at T8) while, on the contrary, stressed Giarraffa plants showed a significant increase in GPox activity from T2 onwards.

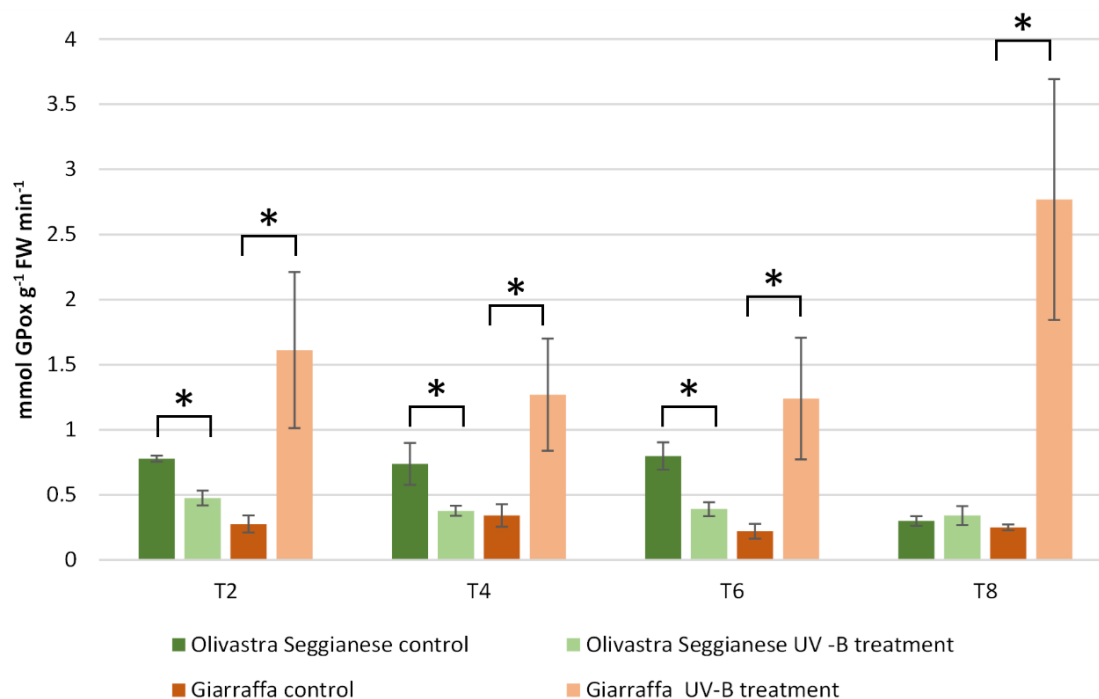


Figure 23. Glutathione peroxidase activity in Giarraffa and Olivastra Seggianese leaves under control conditions and after exposure to UV-B treatment. The x-axis indicates the treatment times. Asterisks (*) indicate statistically significant differences between control and stressed samples within each cultivar. The two cultivars differ by ANOVA test for $p \leq 0.01$. Values are mean \pm standard ($n = 6$).

Lipid peroxidation analysis (Malondialdehyde)

Analysis of lipid peroxidation (figure 24), as measured by malondialdehyde (MDA) production, showed a statistically significant difference ($p \leq 0.01$) in MDA production between control plants of the two cultivars from T2 to T8 (values at T0 were very similar to T2). This difference was more prominent in Giarraffa control plants than in Olivastra Seggianese controls. In addition, when examining the enzyme profile of the Giarraffa cultivar, no statistically significant differences ($p > 0.05$) in MDA production were shown between control and stressed plants, from T2 to T8. In contrast, statistically significant differences ($p \leq 0.01$) were observed between control and stressed plants of the Olivastra Seggianese cultivar. In particular, a significant ($p \leq 0.01$) and progressive increase in MDA production was observed in stressed plants compared with control plants from T4 to T8.

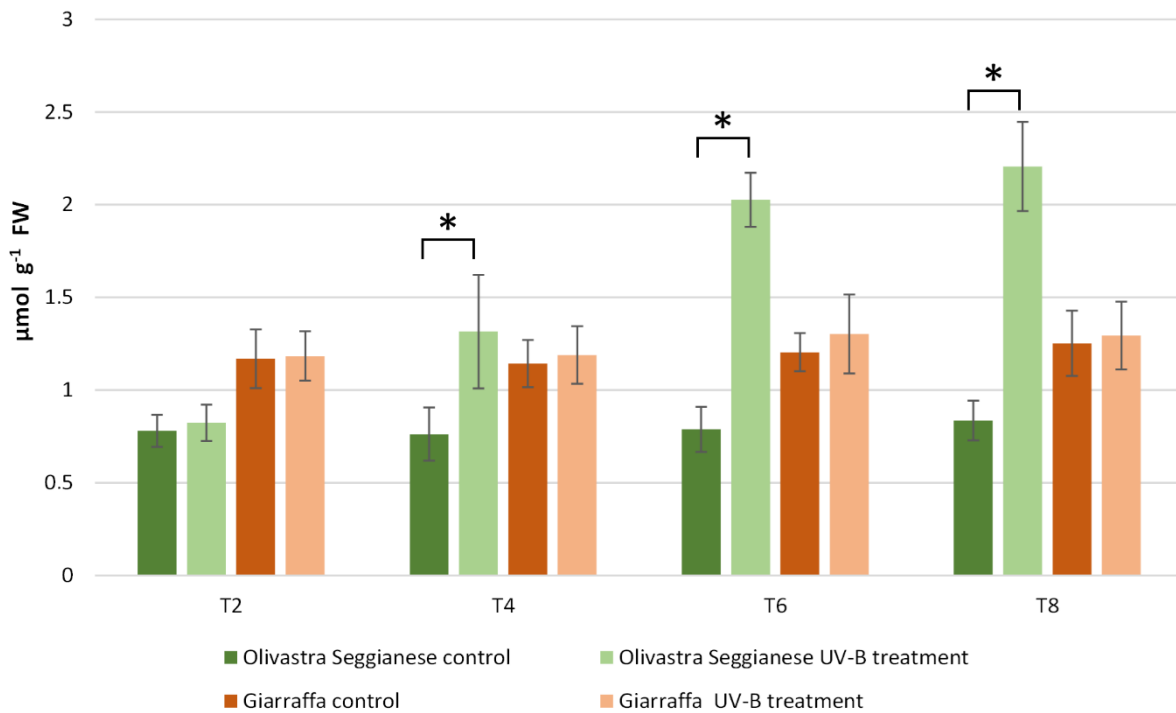


Figure 24. MDA (malondialdehyde) content in Giarraffa and Olivastra Seggianese leaves under control conditions and after exposure to UV-B treatment. Treatment times are indicated in the x-axis. The asterisks (*) indicate statistically significant differences between control and stressed samples within each cultivar. The two cultivars differ by ANOVA test for $p \leq 0.01$. Values are mean \pm standard ($n = 6$).

Ribulose-1,5-Bisphosphate Carboxylase/Oxygenase (RubisCO) Activity

The assay of RubisCO enzymatic activity (figure 25) showed that a statistically significant difference ($p \leq 0.01$) already occurred at T0 between the two cultivars. Indeed, plants of the Giarraffa cultivar showed a higher RubisCO activity than plants of the Olivastra Seggianese cultivar. Data after the UV-B treatment indicated that radiation stress determined a significant change ($p \leq 0.01$) in the enzymatic activity of both cultivars. In particular, a significant decrease in RubisCO enzyme activity was observed at T4 in UV-B stressed plants of both cultivars compared to control plants. The decrease was significantly pronounced (more than 50%) when comparing the stressed and control plants of Giarraffa to the corresponding ones of Olivastra Seggianese. At T8, stressed plants of Olivastra Seggianese were characterized by a further significant decrease in RubisCO activity compared to control plants. On the other hand, stressed plants of the Giarraffa cultivar exhibited a significant increase in RubisCO activity compared to T4, although with values significantly lower ($p \leq 0.01$) than those observed in control plants at T8.

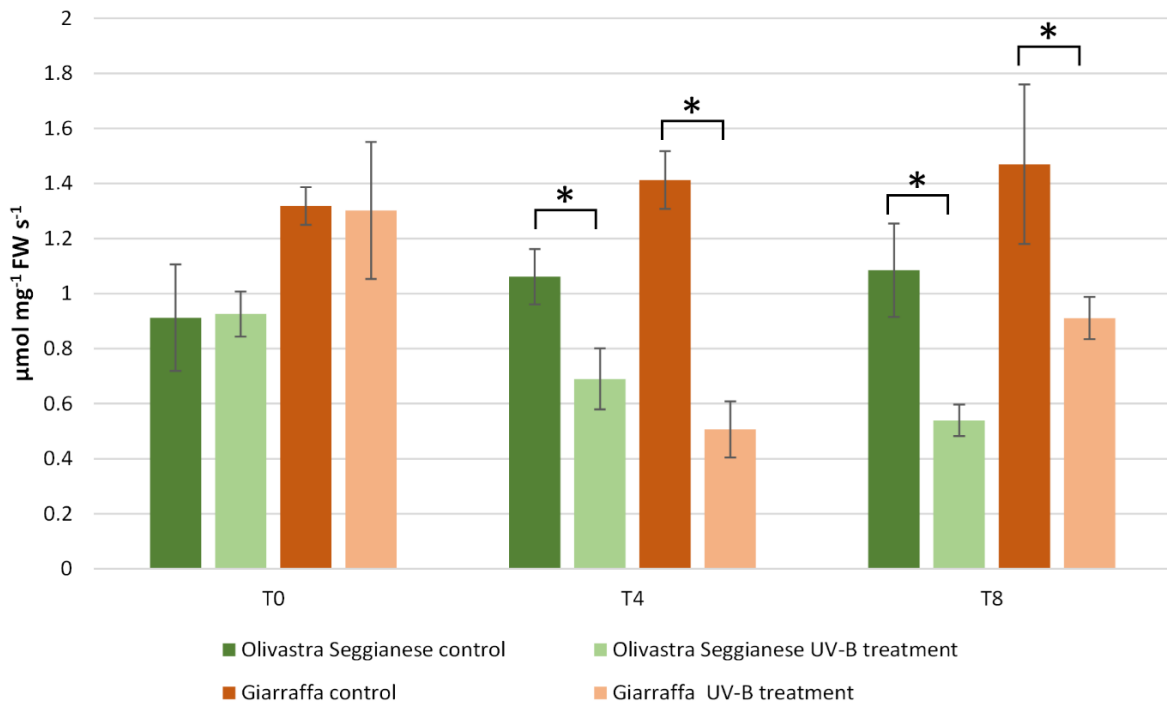


Figure 25. RubisCO activity in Giarraffa and Olivastra Seggiane leaves under control conditions and after exposure to UV-B treatment. The x-axis indicates the treatment times. The asterisks (*) indicate statistically significant differences between control and stressed samples within each cultivar. The two cultivars differ by ANOVA test for $p \leq 0.01$. Values are mean \pm standard ($n = 3$).

Proteomic analysis

1-D Analysis

Protein samples extracted from control and stressed plants of both olive cultivars were analyzed by one-dimensional electrophoresis to detect protein changes after UV-B stress. One-dimensional electrophoretic analysis showed no particular differences between individual cultivars and between the various stages of treatment. Immunoblotting analysis was therefore performed to detect changes in the levels of specific protein such as Hsp70, RubisCO and sucrose synthase. The three proteins have been analyzed using antibodies already extensively tested in our laboratory not only on the olive tree but also on other plant species. The accumulation of the three proteins was studied in leaf samples of olive trees at T0, T4 and T8. As a preliminary remark, it should be specified that unstressed plants behaved very consistently during the UV-B treatment period, at least with regard to the levels of proteins under study. For this reason, the blots show only the comparison with the sample at T0.

- *Hsp70*

The results obtained from the immunoblotting analysis of Hsp70 (figure 26) shows an increase of protein levels in both cultivars at T4 compared to the control at T0. The increase is more evident in the stressed samples of Giarraffa. Subsequently, as stress progresses, I found a decrease in protein content at T8 for both cultivars as compared to values recorded at T4. The decrease is more marked in stressed samples of Giarraffa than in Olivastra Seggianese. The graph in figure 26B shows the relative intensity of immunoblotting against Hsp70 compared to the intensity of actin, the latter considered as a reference protein. It can be observed that the two cultivars under consideration have distinct levels of Hsp70 at T0. However, both cultivars react to stressful conditions by increasing Hsp70 levels at T4. The Giarraffa cultivar almost doubles the levels of Hsp70. At T8, both cultivars show levels of Hsp70 comparable to control values. This means that, after an intermediate stage of protein accumulation because of UV-B stress, plants do not need higher levels of Hsp70 at later stages of stress.

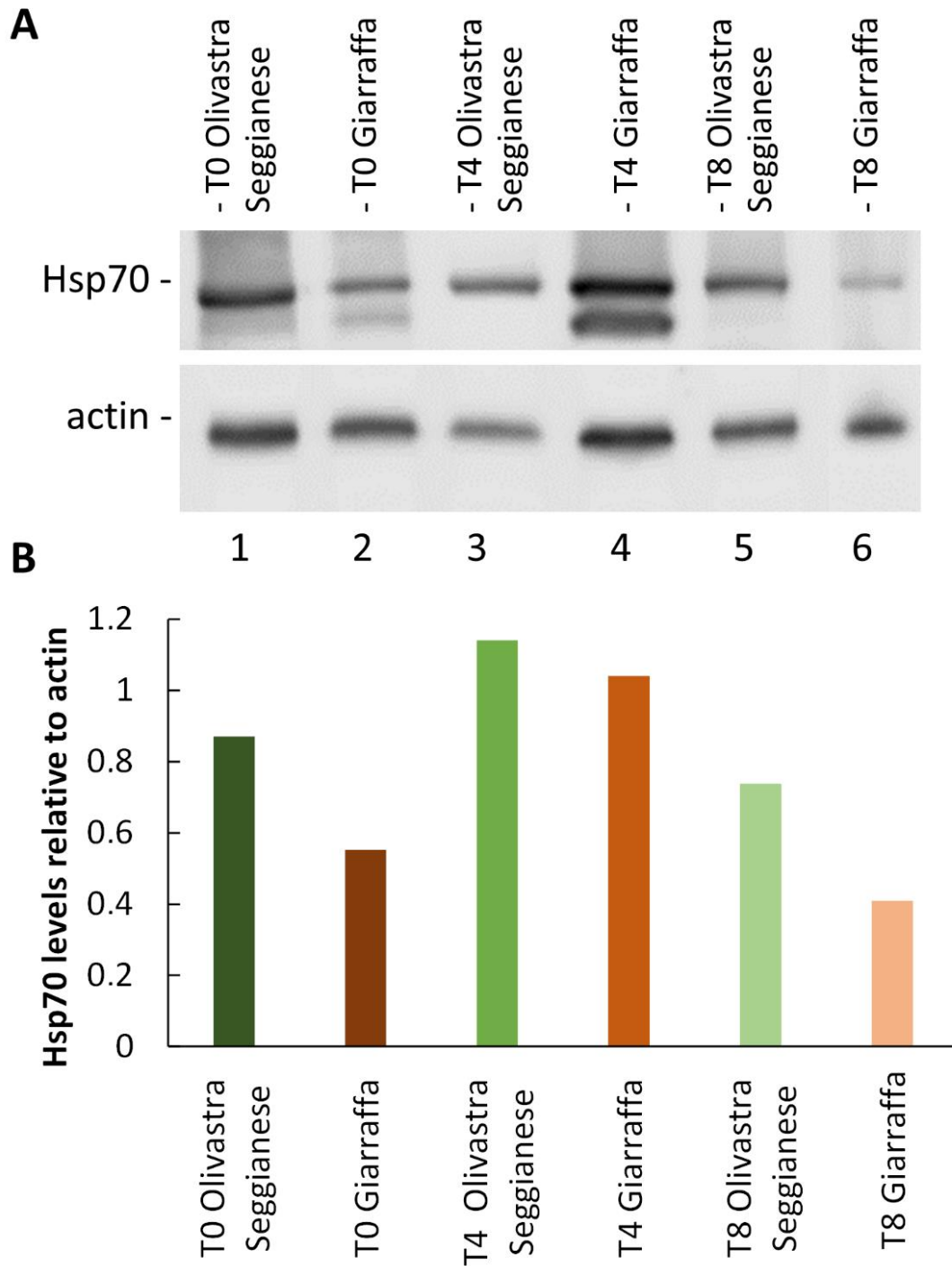


Figure 26. Analysis of Hsp70 content. **(A)** Electrophoresis and immunoblotting with anti-Hsp70 and anti-actin antibodies on proteins extracted from Giarraffa and Olivastra Seggianese plants, subjected to UV-B stress and collected at three selected time points (T0, T4, and T8). Lane 1: Olivastra Seggianese at T0. Lane 2: Giarraffa at T0. Lane 3: Olivastra Seggianese at T4. Lane 4: Giarraffa at T4. Lane 5: Olivastra Seggianese at T8. Lane 6: Giarraffa at T8. The same protein quantities were loaded in each lane. **(B)** Graph of the relative quantification of immunoblot intensities for Hsp70 relative to the actin content.

- *1-D Analysis of Ribulose-1,5-Bisphosphate Carboxylase/Oxygenase (RubisCO)*

The results obtained from RubisCO immunoblotting analysis are shown in figure 27A. The graph in figure 27B was obtained by correlating the intensity of RubisCO immunoblotting against the actin blot (taken as reference protein). Both cultivars have the highest RubisCO values at T0 and are characterized by a decrease in RubisCO content as UV-B treatment progresses. The decrement is very linear, and the two cultivars do not differ in this parameter. It therefore appears that the RubisCO enzyme is equally sensitive to UV-B in the two cultivars considered.

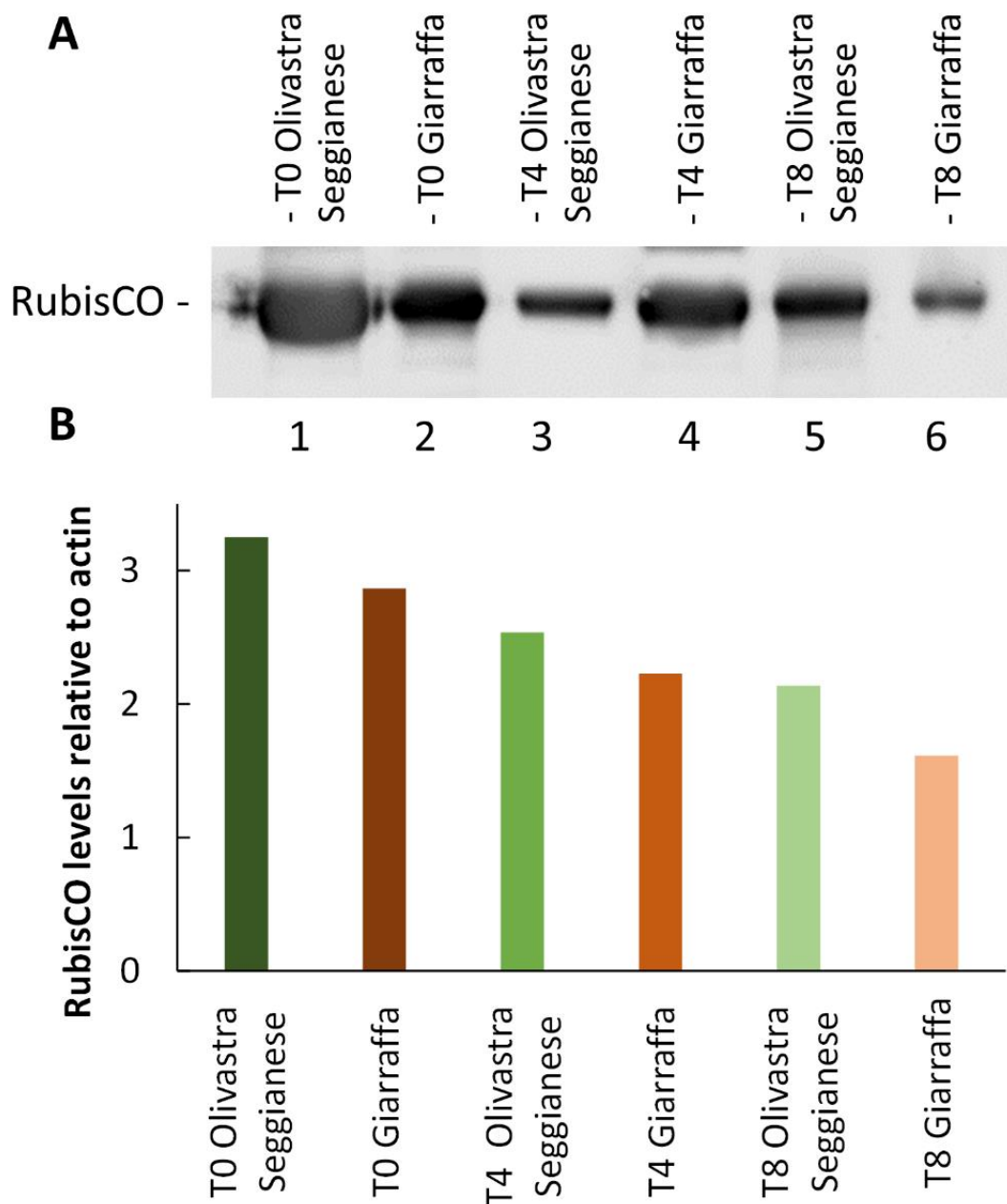


Figure 27. Analysis of RubisCO content. (A) Electrophoresis and immunoblotting with anti-RubisCO antibody on proteins extracted from Giarraffa and Olivastra Seggianese plants, subjected to UV-B stress and collected at T0, T4, and T8. Lane 1: Olivastra Seggianese at T0. Lane 2: Giarraffa at T0. Lane 3: Olivastra Seggianese at T4. Lane 4: Giarraffa at T4. Lane 5: Olivastra Seggianese at T8. Lane 6: Giarraffa at T8. (B) Graph of the relative quantification of immunoblot intensities for RubisCO relative to the actin content.

- *Sucrose Synthase*

The results obtained from sucrose synthase immunoblotting analysis are shown in figure 28A. The graph in figure 28B was obtained by correlating the intensity of sucrose synthase blot against actin blot (taken as reference protein). The graph shows a completely opposite trend in sucrose synthase accumulation for the two cultivars. In fact, the Olivastra Seggianese cultivar shows a significant decrease in the accumulation of sucrose synthase from T0 to T4; from T4 to T8, the enzyme content increases again, almost reaching the level of controls. In contrast, the Giarraffa cultivar showed a moderate increase in sucrose synthase from T0 to T4, whereas the enzyme content decreased from T4 to T8. The most striking result is the different amount of sucrose synthase at T0 between the two cultivars, with Olivastra Seggianese exhibiting about twice as much sucrose synthase content as Giarraffa. The second striking result concerns the last time of analysis, T8, in which Olivastra Seggianese is able to recover the content of sucrose synthase to values comparable to controls; conversely, in Giarraffa, the quantity of sucrose synthase decreases significantly, almost to half compared to T0.

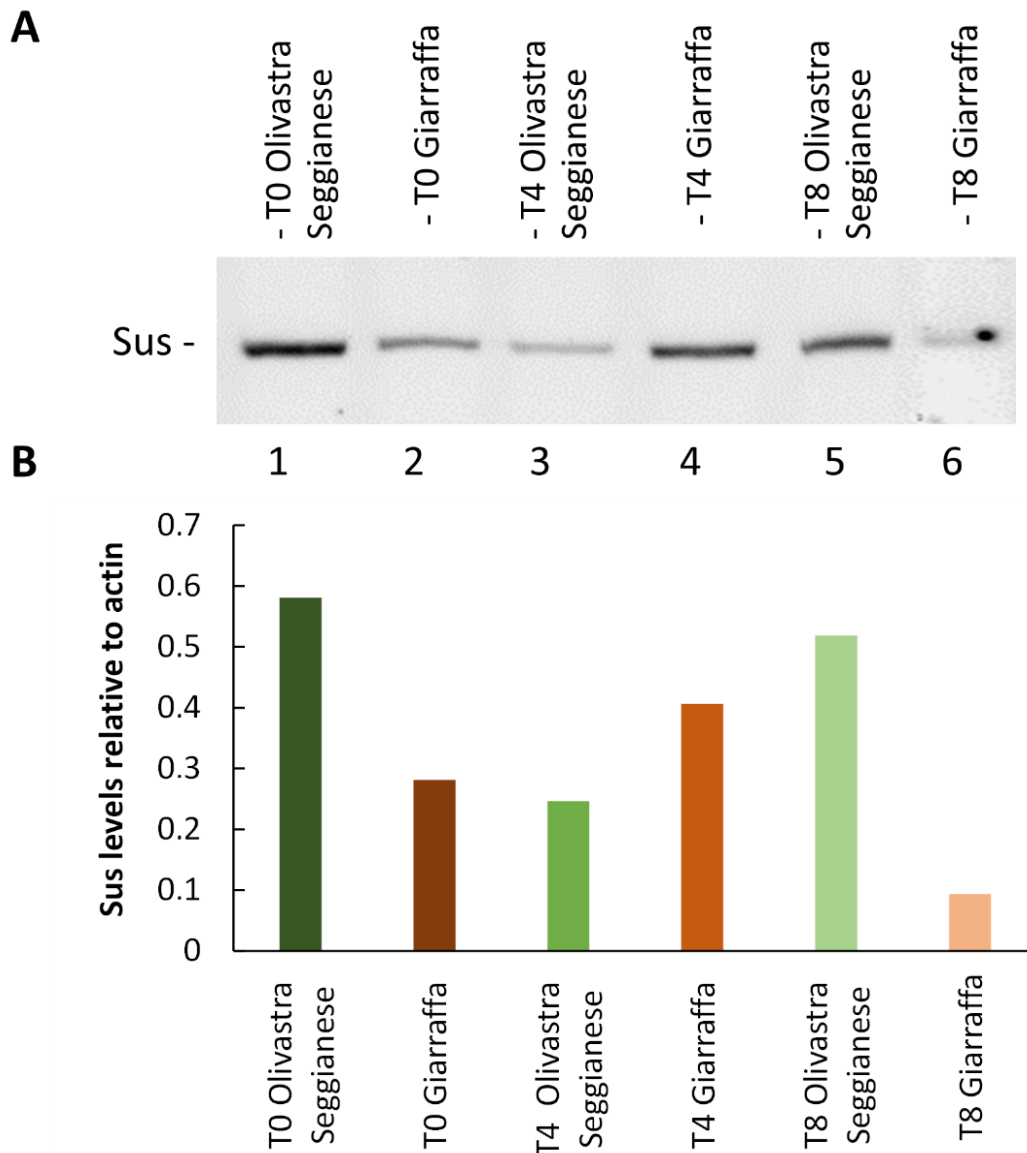


Figure 28. Analysis of sucrose synthase content. (A) Electrophoresis and immunoblotting with anti-sucrose synthase antibody on proteins extracted from Giarraffa and Olivastra Seggianese plants, subjected to UV-B stress and collected at T0, T4, and T8. Lane 1: Olivastra Seggianese at T0. Lane 2: Giarraffa at T0. Lane 3: Olivastra Seggianese at T4. Lane 4: Giarraffa at T4. Lane 5: Olivastra Seggianese at T8. Lane 6: Giarraffa at T8. (B) Graph of the relative quantification of immunoblot intensities for sucrose synthase relative to the actin content.

2-D analysis of Ribulose-1,5-Bisphosphate Carboxylase/Oxygenase (RubisCO)

One-dimensional electrophoretic analysis had previously shown a steady decrease in RubisCO content in both cultivars. Since it is reported in the literature that RubisCO can exist in different isoforms, I analyzed whether the variation in the total RubisCO content was due to some specific isoform. For both olive cultivars, two-dimensional electrophoresis and

immunoblotting analysis of RubisCO were carried out at T0, T4, and T8. For both cultivars, data obtained at each time point were used to construct a “master blot” containing all the RubisCO spots. The intensity of spots was then plotted for Giarraffa (figure 29A,B) and for Olivastra Seggianese (figure 30A,B). Starting from the master blot, the QuantityOne software associated an identification code to each of the spots identified at T0, T4 and T8. Each single spot was then compared as a percentage to the intensity of the same spot as detected in the other analysis times. This made it easier to visualize the relative intensity of each individual RubisCO isoform.

The Giarraffa cultivar presents clear and easily identifiable variations (figure 29). Twelve spots could be detected at T0, but only four spots were found at T4 and six spots were identified at T8. Therefore, I noticed a consistent decrease in the number of spots because most of them were lost at T4. The RubisCO spots detected at T8 were less intense than the corresponding spots at T0. Still, at T8, the remaining isoforms were more focused in the basic region of blots, except for isoform 7901, which was present only at T0.

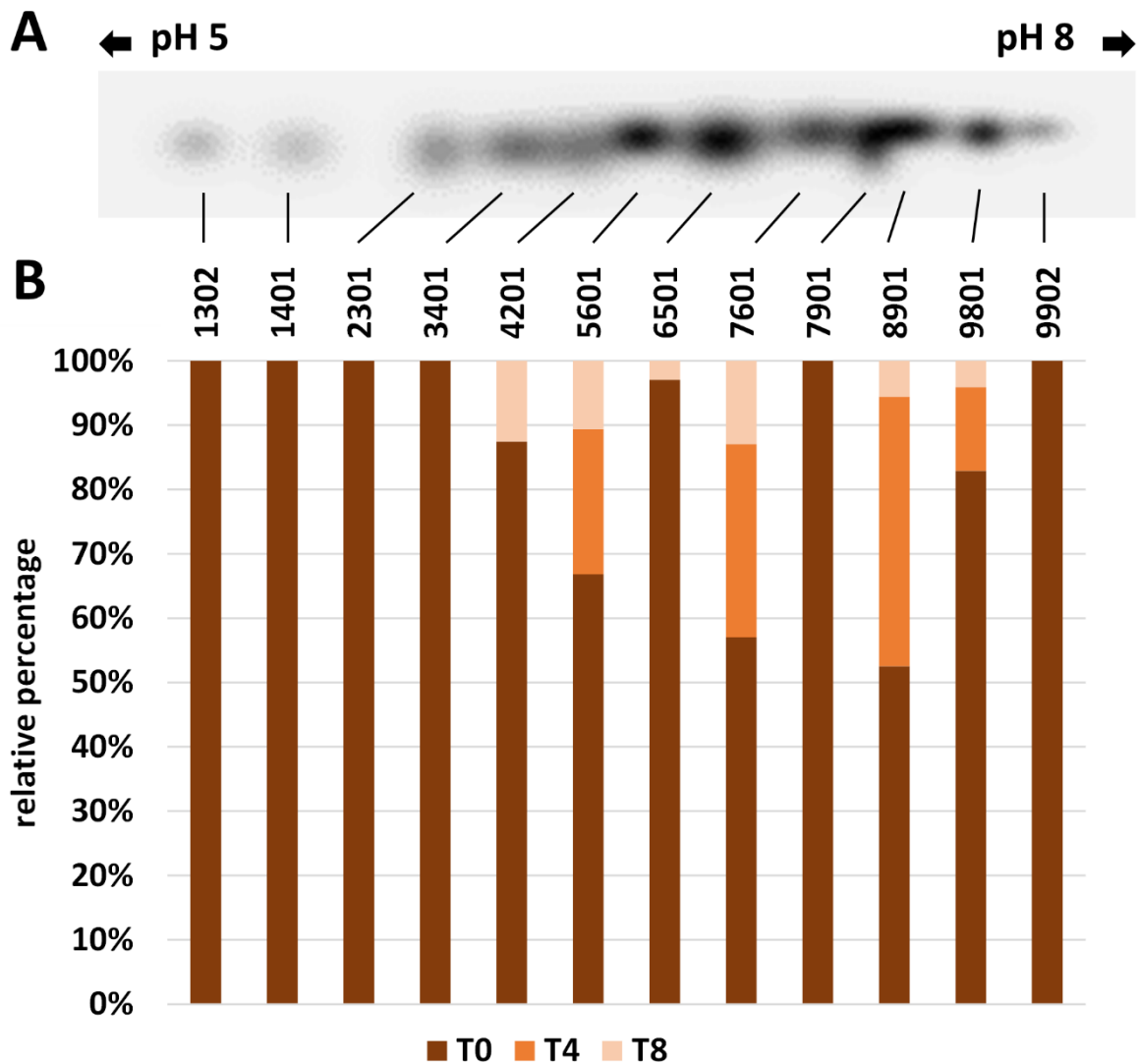


Figure 29. 2-D analysis of RubisCO in Giarraffa plants. (A) Master blot of RubisCO isoforms at T0, T4 and T8 of UV-B stressed plants of Giarraffa. Each spot is identified with a numerical code. (B) Graph of the relative quantification of immunoblot intensities for each spot. Each spot is indicated in percentage relative to each individual analysis time.

The Olivastra Seggianese cultivar, on the other hand, showed isoform variations of more complex interpretation (figure 30). The master blot contained 10 spots at T0, 14 spots at T4 and 11 spots at T8. Of the 10 spots found at T0, only three of them (4801, 6601 and 7701) had a consistent intensity, with the others present in lesser quantities. After four weeks of treatment, the largest number of isoforms was found; however, the isoforms in the central blot area are poorly represented as compared to the more acidic and more basic spots. At the end of experiment (T8), I found that some isoforms disappeared (1801, 9401, 9601), while others

showed a higher intensity than the corresponding spots detected at T4. While Giarraffa seems to focus particularly on some RubisCO isoforms during treatment from T0 to T8, Olivastra Seggianese seems to experience as many isoforms as possible without a specific selection.

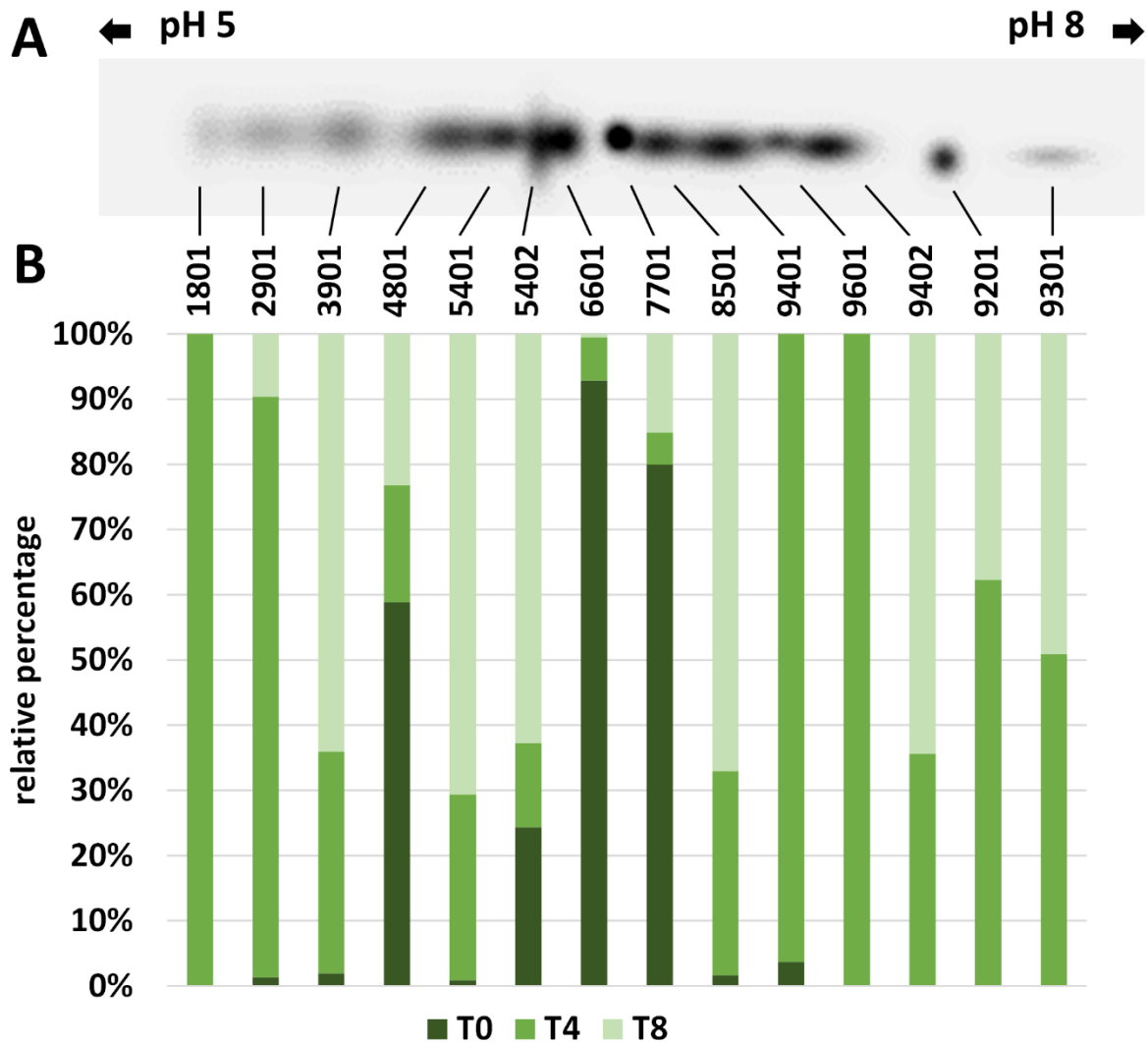


Figure 30. 2-D analysis of RubisCO in Olivastra Seggianese plants. (A) Master blot of RubisCO isoforms at T0, T4 and T8 of UV-B stressed plants of Olivastra Seggianese. Each spot is identified with a numerical code. (B) Graph of the relative quantification of immunoblot intensities for each spot. Each spot is indicated in percentage relative to each individual analysis time.

Discussion

In this chapter I have analyzed the effects of UV-B radiation on the enzymatic activity and isoform composition of RubisCO, together with the effects of UV-B on the enzyme-based antioxidant system and on the activity of sucrose synthase, one of the key enzymes in sucrose metabolism. The data obtained suggest that the two olive cultivars (Olivastra Seggianese and

Giarraffa) exhibit different behaviors both in terms of antioxidant response and differential use of RubisCO.

As a general parameter of stress, differential accumulation of Hsp70, one of the most abundant families of chaperonins involved in the stress response, was also analyzed (Bierkens 2000). The Hsp70 family comprises several isoforms, some of which are constitutively expressed under normal conditions as involved in cell homeostasis (Mayer and Bukau 2005). Results indicate an increase in Hsp70 in both cultivars at T4, most evident in Giarraffa. Progression of stress results in a decrease in protein content at T8 for both cultivars, most evident in Giarraffa. The increase in Hsp70 at T4 in both cultivars indicates that plants suffer a stress condition after four weeks of UV-B radiation. This is not surprising because literature reports that Hsp70 are the proteins par excellence most representative of stress conditions (Sørensen et al. 2003). In organisms under stressful treatments, Hsp70s are subjected to positive regulation and consequently overexpressed proportionally to stress intensity (Bierkens 2000). As clear proof of this, several works report that Hsp70 increases in response to abiotic stresses, such as in *Arabidopsis* where heat shock proteins and heat shock factors are upregulated in response to pathogen infection and abiotic stress, including UV (Swindell et al. 2007). Likewise, in soybean, Hsp70 is upregulated under high temperature stress (Ahsan et al. 2010), as well as in response to UV-B stress (Yoon et al. 2016). The evidence that the increase in Hsp70 coincides with the intermediate time of UV-B stress suggests that the two cultivars subsequently adapt to stress conditions, especially Giarraffa, in which the content of Hsp70 decreases significantly.

Excessive UV-B radiation may increase the levels of ROS in plant cells, causing oxidative stress (Mariz-Ponte et al. 2018). Targets of ROS are essential cellular components and structural elements, and accumulation of ROS is associated with lipid peroxidation, making cell membranes particularly susceptible to oxidative damage (Mittler et al. 2011). In the present study, observations by transmission electron microscopy were performed on leaf samples (control and stressed) of both cultivars. At T0, I found fundamental differences in chloroplast structure between the two cultivars, with Giarraffa showing a higher relative compactness of thylakoids, which was maintained at T4 and T8. Such compactness, instead, was not present in *Olivastra Seggianese*, at T0, T4 and T8. Thylakoid membranes are particularly sensitive to ROS. Therefore, damages on thylakoid membranes can result in reduced photosynthetic activity. A decrease in photosynthetic efficiency in olive trees subjected to UV-B stress has already been observed in the previous chapter (Piccini et al. 2020); reduction of photosynthetic

activity was found in both cultivars but with important differences. In fact, the Giarraffa cultivar was not able to immediately preserve the photosynthetic efficiency but an adaptation-triggered stress protective mechanism allowed the UV-B stressed plants to re-establish photosynthetic performance. The Olivastra Seggianese, on the other hand, responded earlier but was not able to maintain this capacity over time. In the present study I analyzed MDA as a parameter of ROS induced oxidation in macromolecules (namely lipids). Giarraffa showed no statistically significant differences in MDA production. In contrast, differences were observed in Olivastra Seggianese, specifically an increase in MDA production from T2 to T8. The absence of significant changes in MDA production in stressed plants of Giarraffa agrees with previous results of photosynthetic efficiency (Piccini et al. 2020), and suggests that the Giarraffa cultivar shows tolerance to UV-B conditions. These results are in line with what was shown for the “Galega Vulgar” cultivar (Dias et al. 2018), where the UV-B treatment did not increase lipid peroxidation. It should be noted, however, that plants of the Galega Vulgar cultivar were exposed to a lower amount of UV-B radiation and for a shorter exposure time. This suggests again that plants of the Giarraffa cultivar, in contrast to the Olivastra Seggianese cultivar, better tolerate the UV-B stress. The mechanism underlying the improved tolerance could involve the increase in Hsp. As mentioned above, the Hsp family acts as the first defense line against heat stress in olive plants (Assab et al. 2011; McLoughlin et al. 2016; Araújo et al. 2018), as well as against other abiotic stresses such as UV (Swindell et al. 2007; Yoon et al. 2016). My hypothesis is that the increase of Hsp70 levels at T4 in stressed plants of Giarraffa may justify the absence of lipid peroxidation in stressed Giarraffa plants.

To cope with UV-B exposure, as well as to help maintain ROS levels and avoid oxidative damage, plants can activate additional mechanisms. The main defense mechanism against ROS and oxidative stress is the antioxidant defense system. Antioxidants include enzymes like superoxide dismutase (SOD), catalase (CAT) and glutathione peroxidase (GPox), as well as non-enzymatic molecules like ascorbate, tocopherols, carotenoids, albumin, bilirubin, chelating agents and phenolics (Zlatev et al. 2012; Rácz et al. 2018; Dias et al. 2020). In the previous chapter, the changes in phenolic content, especially polyphenols and flavonoids were analyzed. The profile of total polyphenols showed considerable difference already at T0 between the two olive cultivars. Giarraffa responded after just the first week to UV-B radiation by increasing the pool of polyphenols. On the other hand, plants of Olivastra Seggianese responded later to UV-B by triggering an increase of polyphenols only at T2. In addition, the analysis of flavonoids indicated that Giarraffa still responded earlier to UV-B stress (during the

first week), and total flavonoid levels decreased over time. On the contrary, Olivastra Seggianese responded later (after the second week) and maintained high levels of these compounds until the end of treatment. These distinct profiles of UV-B triggered-antioxidant response support the hypothesis that Giarraffa activates defense mechanisms already after the first week of UV-B stress, thereby performing better than Olivastra Seggianese in the long term. This improved defense capacity of Giarraffa is also supported by the slight decrease of antioxidants over the second week, which may result from its efficient neutralization of ROS, leading to an enhanced protection of olive plants from oxidative damage (Piccini et al. 2020; Dias et al. 2020). To complement the previous results, in this chapter have been analyzed antioxidant enzymes such as SOD, CAT, and GPox. In brief, SOD enzyme activity in Giarraffa showed no variation between stressed and control plants; in contrast, stressed Olivastra Seggianese plants showed a significant increase at T4. Giarraffa showed no statistically significant differences in CAT activity while differences in CAT activity were observed in Olivastra Seggianese at T2 and T4. In addition, Olivastra Seggianese plants showed a decrease in GPox activity while stressed Giarraffa plants showed a significant increase in GPox activity from T2 onward. This suggests that the response of stressed Olivastra Seggianese plants was based on stimulation of SOD activity to convert increased $O_2^{\cdot-}$ in H_2O_2 , which is immediately scavenged by the stimulated CAT activity, in particular at T4. On the contrary, stressed plants of Giarraffa invest in the GPox pathway, as they show a constant and progressive increase in enzyme activity for the duration of stress. Supporting these results, other authors demonstrated that SOD, CAT and GPox activities increased in responses to UV-B stress (Araújo et al. 2016; Dias et al. 2020); Rácz et al. (2018) highlighted the importance of GPox in acclimation to enhanced UV-B radiation. *Deschampsia antarctica*, an Antarctic species well acclimated to high UV-B radiation, also showed low indications of oxidative damages and a homeostatic control of ROS due to an increase of SOD, APX, CAT and GPox activities, and of total phenolic content (Köhler et al. 2017). Profiles of antioxidant response (both enzymatic and non-enzymatic) to UV-B stress may support the hypothesis that Giarraffa appears better suited to prolonged UV-B stress, possibly because of a more efficient and quick activation of antioxidant metabolites (such as flavonoids) and of the GPox activity.

Like other proteins, RubisCO can be damaged by UV-B exposure (Panagopoulos et al. 1990; Foyer et al. 1994; Mahdavian et al. 2008). In the present study, the activity of RubisCO was analyzed, and results showed a significant decrease in RubisCO activity at T4 in UV-B stressed plants of both cultivars compared to the control. The decrease was significantly more

pronounced when comparing stressed/control plants of Giarraffa with corresponding plants of Olivastra Seggianese. At T8, Olivastra Seggianese stressed plants showed a significant decrease in RubisCO activity. On the other hand, Giarraffa stressed plants showed an increase in RubisCO activity compared with T4. These results are in line with data in the literature showing that UV-B stress leads to a reduction in the enzymatic activity of RubisCO in various plant species (Allen et al. 1997; Savitch et al. 2001; Dias et al. 2018). However, these results do not fully correlate with those obtained by immunoblotting analysis of RubisCO. In that case, both cultivars are characterized by a decrease in RubisCO content as UV-B treatment progresses. The reduction is extremely linear, and the two cultivars do not differ in this parameter. These results indicate that RubisCO is equally sensitive to UV-B in the two cultivars. Fedina et al. (2010) also demonstrated that UV-B radiation induced quantitative damage to the RubisCO protein. Treatment with UV-B radiation on three different rice cultivars increased the activity of antioxidant enzymes, along with reduction of RubisCO subunits. Therefore, the quantity of RubisCO decreases comparably in the stressed plants of both cultivars; however, in stressed plants of Giarraffa, the gradual decrease in protein quantity does not correspond to the gradual decrease in enzymatic activity. This suggests that stressed plants of Giarraffa implement a defense mechanism to allow plants to gradually regain the RubisCO; this could allow the Giarraffa plants to recover photosynthesis better than stressed plants of Olivastra Seggianese, which conversely show a gradual decrease in the activity and quantity of RubisCO in the course of stress. RubisCO is characterized by many potential co-/post-translational modification sites (Houtz et al. 2008); therefore, it is assumed that, following UV-B stress, modifications can generate RubisCO isoforms more suitable for coping with a stressful situation. As support for this hypothesis, two-dimensional electrophoresis and immunoblotting were performed at T0, T4, and T8 on stressed and control plants of both olive cultivars. Spot analysis in Giarraffa suggested a decrease in the number and intensity of RubisCO isoforms after UV-B treatment and that only undamaged isoforms or those able to effectively function despite the stressful situation persist. This would allow stressed plants of Giarraffa to recover the enzymatic activity of RubisCO. The Olivastra Seggianese cultivar, on the other hand, shows variations in isoforms of more complex interpretation. Basically, only three isoforms remained constant, presumably being the most functional isoforms in the absence of stress. After four weeks of treatment, the number of isoforms increased, while at the end, some isoforms disappeared and others increased in intensity. This could suggest that Olivastra Seggianese takes longer than Giarraffa to discover more functional isoforms to be used during stress or that the best response consists of a mix of different isoforms, which are

nevertheless assembled in a longer time. Therefore, I assume that stressed plants of Giarraffa react better than Olivastra Seggianese to UV-B stress by post-translationally modifying RubisCO so as to produce more effective isoforms (Piccini et al. 2020).

Like all other plants, olive trees must produce sugars (such as sucrose) for growth. Previously the changes in photosynthetic sugars under UV-B stress have been analyzed (Piccini et al. 2020). Results from chapter 2 showed that no significant differences were found in sucrose content between control and UV-B stressed plants of both cultivars. Instead, glucose and fructose were the most responsive to UV-B treatment. UV-B stressed plants of Olivastra Seggianese accumulated less glucose, particularly after the second week, possibly due to a reduction of photosynthesis and to a higher use of glucose to maintain cellular respiration or even to increase the levels of polyols (e.g., mannitol, that increases at T2) (Stoop et al. 1996; Rosa et al. 2009; Vanlerberghe 2013). On the other hand, UV-B seemed to promote fructose accumulation (except at T6) more significantly in Olivastra Seggianese. Increase of fructose can result from sucrose degradation as a stress response or can provide substrates for the synthesis of secondary metabolites (Rosa et al. 2009). Dias et al. (2018) reported that olive plants treated with a lower UV-B dose ($12 \text{ kJm}^{-2} \text{ d}^{-1}$) produced less sucrose and starch but maintained the content of glucose and sorbitol. Given the key role of sucrose (Farrar et al. 2000; Salerno 2003; Roitsch and González 2004), it has been assumed that plants under UV-B stress implemented mechanisms to preserve both the content of sucrose and related metabolic processes. In light of this, the changes in the amount of sucrose synthase (SuSy) by immunoblotting has been analyzed. The results obtained showed a completely opposite profile of Susy accumulation for the two cultivars. Olivastra Seggianese shows an initial decrease in SuSy accumulation, while thereafter the enzyme content increases again. In contrast, Giarraffa shows an initial moderate increase in SuSy content, while the enzyme content subsequently decreases. It is striking that the initial amount of SuSy differs between the two cultivars, as well as the recovery of SuSy by Olivastra Seggianese at T8, while in Giarraffa the amount of SuSy decreases significantly. SuSy reversibly catalyzes the production of fructose and UDP-glucose from sucrose (Koch 2004), preserving a large part of the energy available in sucrose. Given that plants of Giarraffa increase the quantity of SuSy at T4 (when plants are more under stress), this suggests that Giarraffa plants counteract the stressful conditions by storing energy in UDP-glucose and that they do not need to use all the energy contained in the sucrose molecule. After T4, the quantity of SuSy decreases considerably up to T8, which corresponds to the time when plants of Giarraffa, unlike Olivastra Seggianese, have resumed their metabolic

processes. On the contrary, plants of Olivastra Seggianese show a remarkable increase in the content of SuSy at T8 compared to T4, probably because at T8 they are still suffering a severe stress and thus require all the energy available from sucrose breakdown (likely by invertase). This is also confirmed by results from the previous chapter, for which plants need to continue splitting sucrose into glucose and fructose to counteract stress conditions.

Conclusions

In conclusion, the results obtained indicate that the cultivars Giarraffa and Olivastra Seggianese differ significantly in the use of specific antioxidant defense systems, as well as in the activity and isoform composition of RubisCO. Combined with a different use of sucrose synthase, the overall picture shows significant biochemical differences between the two olive cultivars. In particular, Giarraffa optimized the use of GPox, opted for a targeted choice of RubisCO isoforms and managed the content of SuSy, saving energy during the critical stress point. This highlights once again how the two cultivars were able to adapt to different environmental conditions. The two regions in which the cultivars have developed (Tuscany and Sicily) are indeed characterized by different climatic parameters (higher temperatures and drought in Sicily), as well as by probably different UV-B radiation. We therefore hypothesize that biochemical adaptations are part of the global mechanism by which the two cultivars respond independently to UV-B treatment. Although preliminarily, the Giarraffa cultivar is better equipped to tolerate UV-B radiation.

List of contributors to this chapter:

- **Claudio Cantini** (Institute for BioEconomy, National Research Council of Italy, 58022 Follonica, Italy)
- **Giampiero Cai** (Department of Life Sciences, University of Siena, via Mattioli 4, 53100 Siena, Italy)
- **Maria Celeste Dias** (Department of Life Sciences, Centre for Functional Ecology, University of Coimbra, Calçada Martim de Freitas, 3000-456 Coimbra, Portugal)
- **Márcia Araújo** (Department of Life Sciences, Centre for Functional Ecology, University of Coimbra, Calçada Martim de Freitas, 3000-456 Coimbra, Portugal; Department of Biology, Faculty of Sciences, University of Porto, Rua Campo Alegre,

4169-007 Porto, Portugal 5 and CITAB, University of Trás-os-Montes and Alto Douro, 5001-801 Vila Real, Portugal)

- **Sara Parri** (Department of Life Sciences, University of Siena, via Mattioli 4, 53100 Siena, Italy)
- **Marco Romi** (Department of Life Sciences, University of Siena, via Mattioli 4, 53100 Siena, Italy)
- **Claudia Faleri** (Department of Life Sciences, University of Siena, via Mattioli 4, 53100 Siena, Italy)

Chapter 4: Metabolomics of UV-B responses

Introduction

There is currently a lack of comprehensive knowledge about the metabolic factors involved in the tolerance strategies of olive trees to UV-B stress. It remains unclear how UV-B radiation can modulate the metabolome and which metabolic changes enhance plant tolerance (Dias et al., 2018). Functional changes that occur during stress are closely linked to metabolites and to metabolic network adaptations that, with the emergence of metabolomic approaches, are beginning to be unraveled (Schwachtje et al. 2019; Bueno and Lopes 2020). Indeed, the study of metabolomics has helped to identify the most sensitive networks related to physiological adaptations in different species, and to find key stress metabolites (Rodziewicz et al. 2014). In addition to studies on the model species *Arabidopsis* (Kusano et al. 2011), few crops have been studied for metabolome changes in response to UV-B, such as *Zea mays* (Casati et al. 2011) and *Lactuca sativa* (Wargent et al. 2015). In recent years, several studies have employed a metabolomic approach, allowing the identification of lipophilic metabolites involved in the abiotic stress response, such as epicuticular wax components (alkanes, terpenes, and fatty acids), membrane fatty acids, and terpenes commonly known as ROS scavengers (Lytovchenko et al. 2009; Gil et al. 2012; Wenzel et al. 2015; Mihailova et al. 2015; Dias et al. 2018, 2019, 2020). Other studies have investigated the impact of UV-B radiation on the most representative phenolic compounds in olive leaves (Dias et al. 2019). However, much remains to be studied in order to have a complete understanding of the mechanisms of plant response to increased UV radiation and to figure out its impact on other metabolic pathways (Dias et al. 2020).

Metabolomic studies in olive plants are scarce and mostly focused on changes in phenolic compounds (e.g. secoiridoids, flavonoids, and hydroxycinnamic acid derivatives) and lipophilic metabolites related to cuticle wax (e.g., long-chain alkanes and terpenes), ROS scavenger action (e.g., thymol glycosides), maintenance of membrane integrity (e.g., fatty acids and steroids), and carbohydrate pools (Liakopoulos et al. 2006; Dias et al. 2018, 2019, 2020). Previous chapters of this thesis analyzed the physiological and biochemical responses of olive trees subjected to UV-B stress; in this chapter, the integration of metabolomic analysis with physiological and biochemical studies allows a deeper understanding of metabolite dynamics and their connection in a more extensive network of pathways involved in stress response. Thus, in this chapter, I hypothesized that UV-B radiation promotes changes in metabolic pathways, particularly in protective lipophilic and phenolic metabolites that may play an

important role in protection against UV-B stress. Considering that many of these groups of compounds are closely related to photosynthetic reactions and redox balance, I also hypothesized that some metabolite dynamics are associated with photosynthesis and oxidative stress imbalances (analyzed in previous chapters). Therefore, gas chromatography-mass spectrometry (GC-MS) and ultra-high performance liquid chromatography (UHPLC-MS) analyses were undertaken in *O. europaea* plants (Giarrappa and Olivastra Seggianese cultivars) exposed to chronic UV-B stress (14 h per day for eight weeks).

Material and Methods

Plant growth conditions and application of UV-B treatment

Olive plants were grown and stressed by UV-B radiation exactly as described in the materials and methods of chapter 2.

Preparation of leaf extracts

Frozen olive leaves were macerated and mixed with *n*-hexane (5g of leaves for 50 ml of extraction solvent) at room temperature with magnetic stirring for 48h. The *n*-hexane was removed, and a new extraction cycle of 24h was performed with the addition of new *n*-hexane in the same volume. The *n*-hexane from the two extraction cycles was put in a glass balloon, and the *n*-hexane was evaporated to dryness at low pressure in a rotatory evaporator. The extracts obtained were left to dry for one week. The pellet obtained was also left to dry and then mixed with 50 ml of methanol to extract phenolic compounds. After a first extraction cycle of 48h at room temperature with magnetic stirring, the methanol was removed, and new methanol was added for a second extraction cycle. This last cycle lasted 24h. The methanol obtained from both extraction cycles was put together in a glass balloon, evaporated to dryness at low pressure in a rotatory evaporator. The extract was left to dry for two weeks.

Gas chromatography–mass spectrometry

The extracts obtained from the *n*-hexane extraction were weighted and prepared for silylation. In a glass tube, 200 μL of the extract were mixed with 200 μL of tetracosane 0.5 mg mL^{-1} , 250 μL of pyridine, 250 μL of N,O-bis(trimethylsilyl) trifluoroacetamide, and 50 μL of trimethylsilyl chloride and incubated at $70 \text{ }^\circ\text{C}$ for 40 min. A sample (1 μL) of the silylated was injected into the gas chromatography–mass spectrometry (GC–MS) (QP2010 Ultra Shimadzu). The chromatography conditions were performed as described in Dias et al. (2019). For the

identification of the lipophilic compounds, the peaks obtained in the chromatograms were compared with the library entries of the mass spectra database (NIST14 Mass spectral and WILEY RegistryTM of Mass Spectra Data) or compared with mass spectra and the retention times of pure compounds analysed and prepared similarly to the samples. Calibration curves were prepared for quantification with pure compounds representing the main families presented in the extracts (maltose, palmitic acid, octadecane, and cholesterol).

Ultra-high performance liquid chromatography–mass spectrometry

The dry methanolic extract was weighted, and 50 mg were collected and dissolved in 1 mL of methanol. Samples with a concentration of 10mg ml⁻¹ were filtered through a 0.2 mL nylon membrane (Whatman) and injected in the ultra-high-performance liquid chromatography–mass spectrometry (UHPLC-MS) from Thermo Scientific Ultimate 3000RSLC Dionex. The chromatography analysis was performed according to the described by Dias et al. (2019). The UHPLC-MS equipment contained a Dionex UltiMate 3000 RS diode array detector coupled to a mass spectrometer, and a thermostatic hypersil gold column (1000 mm x 2.1 mm) with a particle size of 1.9 µm and a temperature adjusted to 30 °C. The mobile phase was composed of a degassed and filtered acetonitrile and 0.1% formic acid (v/v) with a flow rate of 0.2 mL min⁻¹. During the first 14 min the gradient of the solvent was 5% of acetonitrile, followed by 40% of formic acid for 2 min, 100% over 7 min, and 5% over the last 10 min. One microliter of the sample was injected into the UHPLC-MS. UV-Vis spectral data were collected between 250 to 500 nm wavelengths, and the chromatograms were recorded at 280 nm. The equipment contained a mass spectrometer (LTQ XL linear ion trap 2D) with an orthogonal electrospray ion source (ESI) that operated in a negative-ion mode with electrospray ionization source of 5.00 kV (ESI capillarity temperature of 275 °C). It covered a mass range from 50.00 to 2000.00 *m/z*, and collision-induced dissociation MS/MS and MSⁿ experiments were obtained for precursor ions. The retention times, UV-Vis spectra, and spectra data were compared with those of standard compounds to identify the phenolic compounds. Semi-quantification was performed by peak integration through the standard external method, using the closest standard compound. The detection and quantification limits (LOD and LOQ, respectively) were determined using calibration curves prepared with standard compounds (quercetin, luteolin, and caffeic acid).

Statistical analysis

Statistical analysis was performed by the Systat 11 statistical package (Systat Software Inc., Richmond, CA, USA). Data were checked for normality distribution by the Shapiro–Wilk test before repeated measures of ANOVA analysis. ANOVA tested the significance of each of the three variables: time, treatment and cultivar, as well as their interaction. When the p values of the ANOVA were \leq to 0.01 or 0.05, Tukey’s pairwise mean comparison within each variable was performed.

Results

Phenolic profile

The phenolic profile was evaluated in olive leaves (Giarraffa and Olivastra Seggianese cultivars) of control plants and subjected to UV-B stress, sampled at the 2nd, 4th, 6th and 8th week after the onset of stress. In the Giarraffa cultivar (Table 2), a total of sixteen compounds were quantified: thirteen flavonoids, one secoiridoid, and two hydroxycinnamic acid derivatives. In the Olivastra Seggianese cultivar (table 3), a total of twelve compounds were quantified: eleven flavonoids and one secoiridoid.

An interaction between the factors treatment and cultivar was observed for apigenin 6,8-di-C-glucoside, apigenin, apigenin-7-*O*-rutinoside, luteolin-7-*O*-rutinoside is. 1 and 2, luteolin-4'-methyl ether, luteolin-7-*O*-glucoside, luteolin, quercetin-3-*O*-glucoside, diosmetin is. 1 and 2; the stressed plants of both cultivars present the highest ($p \leq 0.01$) levels of these compounds (except luteolin-7-*O*-rutinoside is. 1 and luteolin-7-*O*-glucoside not detected in stressed plants of the Giarraffa). In particular, the stressed plants of the Giarraffa cultivar show an increase in these compounds (except luteolin-7-*O*-rutinoside is. 1 and luteolin-7-*O*-glucoside) higher than the stressed plants of the Seggianese cultivar. In addition, as regards dihydroquercetin, diosmetin is. 3 and the two derivatives of hydroxycinnamic acids, these compounds were detected only in plants of the Giarraffa cultivar, and they present the highest ($p \leq 0.01$) levels in stressed plants. Concerning caffeoyl-6'-secologanoside, it was detected only in plants of the Olivastra Seggianese cultivar and stressed plants present the highest ($p \leq 0.01$) levels.

Figure 31 shows the fold changes in phenolic metabolites of the Giarraffa (A) and Olivastra Seggianese (B) after UV-B treatment in the different sampling times (T2, T4, T6 and T8). In general, for Olivastra Seggianese cultivar (figure 31B) the profiles of response of phenolic compounds progressively increase as stress progresses (except for the diosmetin is. 1, luteolin and luteolin 7-*O*-glucoside). While in the Giarraffa cultivar (figure 31A), a more heterogenic

profile of response was observed, with a progressive increase of some metabolites with the progress of stress such as: apigenin 6,8-di-C-glucoside, quercetin-3-O-glucoside, diosmetin isomers and apigenin. In other phenolic metabolites, such as luteolin 7-O-rutinoside is. 2, luteolin-4'-methyl ether and β -hydroxy-verbascoside isomers, the response was more intense in the T6 and T8.

Lipophilic profile

The lipophilic profile was evaluated in olive leaves (Giarraffa and Olivastra Seggianese cultivars) of control and UV-B stressed plants, sampled at the 2nd, 4th, 6th and 8th week after the onset of stress (Table 4 and 5). In the Giarraffa cultivar (Table 4), a total of seventeen compounds were quantified: five terpenes, three carbohydrates, four fatty acids, and five alkanes. In the Olivastra Seggianese cultivar (table 5), a total of eighteen compounds were quantified: five terpenes, three carbohydrates, four fatty acids, five alkanes and one sterol.

An interaction between the factors treatment and cultivar was observed for the lupeol derivative, with the plants of the Giarraffa cultivar under control and UV-B stress presenting the highest levels of this terpene, followed by the Olivastra Seggianese UV-B stressed plants. For the other lipophilic compounds (except the oleic acid derivative) an effect of the factor treatment (control *vs* UV-B stress) was observed, and the olive plants exposed to UV-B stress shown a level of these compounds significantly ($p \leq 0.05$) higher than controls. In addition, also an effect of the factor cultivar (Olivastra Seggianese *vs* Giarraffa) was observed for the compounds neophytadiene, palmitic acid, α -linolenic acid, long chain alkanes 1, 2, 3 and 4, β -amyryn and oleic acid derivative. Regarding the neophytadiene, Olivastra Seggianese has a significantly ($p \leq 0.05$) higher content of this compound than Giarraffa. For the other compounds Giarraffa has a significantly ($p \leq 0.05$) higher content than Olivastra Seggianese.

Figure 32 shows the rate of change in lipophilic metabolites of Giarraffa (A) and Olivastra Seggianese (B) after UV-B treatment at different sampling times (T2, T4, T6, and T8). In the Olivastra Seggianese cultivar (Figure 32B), the response profiles of some lipophilic metabolites progressively increased as stress progressed: phytol, ursolic acid, α -D-mannopyranose, D-sorbitol, α -D-(+)-thalopyranose, α -linolenic acid, and long-chain alkane 4. Other metabolites, however, do not show a progressive increase but have peaks at T4 or T6 or both time points as in the case of neophytadiene, β -amyryn, lupeol derivative, long-chain alkanes 1, 2, and 3, and stigmast-5-ene. Others, such as palmitic and oleic acids, have peaks at

T4 and T8. In addition, stearic acid response intensity decreases progressively from T2 to T6 and then increases again slightly at T8, whereas long-chain alkane-5 response intensity decreases with progressing stress from T2 to T8. In the Giarraffa cultivar (Figure 32A), the response profiles of some lipophilic metabolites increase progressively with stress: α -D-mannopyranose, α -D-(+)-thalopyranose, and D-sorbitol. Other metabolites, however, do not show a progressive increase but have peaks at T4 and T8 such as: phytol, β -amyrin, ursolic acid, palmitic acid, β -linolenic acid, stearic acid, and long-chain alkanes 1, 2, 3, 4, and 5. For some lipophilic metabolites, such as the case of lupeol derivative and oleic acid derivative, a steady decrease, albeit with fluctuations, is observed in stressed samples compared to controls.

Table 2. Phenolic profile (mg kg⁻¹ DW) of *Olea europaea* leaves (Giarraffa cultivar) under control (C) and UV-B conditions in the different sampling times. Values are mean ± standard deviation (n=3–4). Rt - Retention time; Nd - not detected; is - isomer.

Rt (min)	Compound	[M- H] ⁻ (m/z)	MS ² (m/z) fragments	T2		T4		T6		T8	
				C	UV-B	C	UV-B	C	UV-B	C	UV-B
Flavonoids											
9.8	Apigenin 6,8-di-C-glucoside	593	353/383/503/575	169.9±15.3	297.6±31.6	174.3±8.49	329.4±10.3	179.6±7.2	443.8±15.0	175.9±4.6	493.4±9.8
11.9	Luteolin-7- <i>O</i> -rutinoside is. 1	593	285/447	175.1±15.5	Nd	183.0±9.65	Nd	57.3±10.1	Nd	87.1±11.6	Nd
12.2	Dihydroquercetin	303	125/177/285	181.2±18.8	309.1±31.5	196.5±12.1	335.6±10.8	201.9±18.3	445.9±15.6	351.0±36.7	503.9±23.7
12.5	Quercetin-3- <i>O</i> -glucoside	463	301	170.3±15.0	337.7±39.3	174.5±8.41	346.2±10.9	180.1±7.3	Nd	180.5±4.9	519.9±48.8
12.9	Apigenin-7- <i>O</i> -rutinoside	577	269	185.4±17.8	392.2±43.3	189.2±10.5	379.6±11.3	225.7±35.6	473.7±27.1	269.6±24.0	531.4±61.5
13.1	Luteolin 7- <i>O</i> -rutinoside is. 2	593	285/447	179.6±18.2	342.8±36.6	184.4±9.71	347.7±10.9	64.9±18.2	450.6±17.0	81.0±16.9	523.1±50.1
13.5	Luteolin-4'-methyl ether	607	284/299	188.1±18.2	331.1±35.2	194.8±11.5	343.2±10.8	74.3±24.3	453.6±19.1	130.8±19.2	535.0±67.6
13.6	Luteolin-7- <i>O</i> -glucoside	447	289	173.8±15.9	Nd	180.0±9.13	Nd	51.8±7.1	Nd	70.0±6.6	Nd
15.9	Luteolin	285	285	211.6±21.4	563.4±66.2	227.0±19.0	522.7±14.6	165.4±75.7	514.8±46.5	253.1±36.8	606.9±171.6
16.7	Diosmetin is. 1	299	284/299	171.3±15.5	318.4±34.4	174.9±8.52	335.2±10.9	183.2±7.2	445.6±15.8	174.9±4.7	501.1±18.4
17.6	Apigenin	269	149/269	176.3±16.4	432.8±39.7	179.2±9.15	391.3±11.2	196.5±14.7	463.3±23.2	202.4±6.9	541.9±77.2
17.9	Diosmetin is. 2	299	284	182.7±15.2	368.1±38.6	187.7±10.4	373.5±11.0	224.7±33.8	465.8±24.6	237.9±17.9	575.5±124.9
20.1	Diosmetin is. 3	299	284	169.7±15.2	349.1±35.5	174.1±8.38	350.0±10.8	179.9±7.2	449.0±17.1	178.2±4.8	533.8±66.6
Secoiridoid											
11.3	Decarboxymethyl oleuropein aglycone	319	183	175.2±16.0	Nd	181.6±9.58	Nd	96.5±40.1	Nd	52.8±6.0	Nd
Hydroxycinnamic Acid Derivatives											
10.6	β-hydroxy-verbascoside is. 1	639	529/621	177.0±16.5	295.3±31.7	195.2±11.8	327.4±9.6	72.2±5.5	447.0±16.1	104.7±7.3	490.6±7.6
10.7	β-hydroxy-verbascoside is. 2	639	529/621	181.7±17.4	296.5±31.9	204.5±13.9	328.7±10.1	76.7±9.6	448.3±16.8	119.9±10.4	492.0±8.9

Table 3. Phenolic profile (mg kg⁻¹ DW) of *Olea europaea* leaves (Olivastra Seggianese cultivar) under control (C) and UV-B conditions in the different sampling times. Values are mean ± standard deviation (n=3–4). Rt - Retention time; is - isomer.

Rt (min)	Compound	[M-H] ⁻ (m/z)	MS ² (m/z) fragments	T2		T4		T6		T8		
				C	UV-B	C	UV-B	C	UV-B	C	UV-B	
Flavonoids												
9.8	Apigenin 6,8-di-C-glucoside	593	353/383/503/575	217.0±13.0	225.6±7.6	207.5±18.4	245.3±3.6	203.1±1.4	271.4±15.4	215.5±6.2	357.0±1.2	
11.6	Quercetin-3- <i>O</i> -rutinoside	609	301	216.1±12.5	222.4±7.	213.0±12.9	244.6±3.3	199.2±1.1	269.7±14.8	210.9±6.9	360.2±1.1	
11.9	Luteolin-7- <i>O</i> -rutinoside is. 1	593	285	224.1±16.8	225.1±8.3	238.4±4.0	248.4±4.4	217.8±5.5	279.1±16.5	236.3±10.8	380.5±4.3	
12.1	Luteolin-7- <i>O</i> -rutinoside is. 2	593	285/447	229.6±20.6	226.1±7.9	251.4±8.0	257.7±5.2	246.7±19.4	292.7±19.7	277.0±22.2	460.9±19.5	
12.8	Apigenin-7- <i>O</i> -rutinoside	577	269	229.3±20.4	252.9±13.7	248.7±10.8	297.1±10.8	256.0±7.7	356.5±35.1	288.6±19.1	427.3±13.3	
13.1	Luteolin-4'-methyl ether	607	299/284	225.5±17.8	239.5±11.2	230.4±6.1	274.3±14.1	225.8±3.0	339.6±46.8	247.9±8.5	414.6±14.4	
13.4	Luteolin-7- <i>O</i> -glucoside	447	285	246.8±33.5	250.7±15.5	282.4±16.1	278.0±4.6	315.6±22.0	321.0±27.9	353.3±30.2	501.1±29.2	
15.8	Luteolin	285	285	342.0±112.1	299.7±29.5	489.8±96.0	449.7±22.7	543.1±104.2	493.9±77.3	471.4±51.2	702.8±47.9	
17.5	Apigenin	269	225/149/201	228.0±19.7	258.3±15.7	234.8±5.9	304.8±14.9	228.5±7.4	340.4±31.2	243.5±9.2	410.8±9.2	
17.8	Diosmetin is. 1	299	284	270.0±52.5	294.7±24.8	317.2±33.6	319.3±18.7	359.4±34.9	383.5±37.4	389.1±28.5	519.9±27.1	
20.1	Diosmetin is. 2	299	284/299	221.4±15.7	251.2±14.6	226.9±7.7	292.0±13.8	224.9±2.2	306.4±24.6	241.7±11.3	399.1±12.5	
Secoiridoid												
12.5	Caffeoyl-6'-secologanoside	551	507/341/389/281	220.3±14.5	232.2±8.6	223.0±8.5	260.8±5.6	215.1±1.7	315.4±24.7	234.4±10.6	388.3±5.7	

Table 4. Lipophilic profile (g kg⁻¹ DW) of *Olea europaea* leaves (Giarraffa cultivar) under control (C) and UV-B conditions in the different sampling times. Values are mean ± standard deviation (n=3). Rt - Retention time.

Rt (min)	Compound	T2		T4		T6		T8	
		C	UV-B	C	UV-B	C	UV-B	C	UV-B
Terpenes									
34.1	Neophytadiene	0.463±0.013	0.340±0.000	0.451±0.004	0.554±0.002	0.421±0.006	0.546±0.003	0.500±0.021	0.623±0.002
42.1	Phytol	0.361±0.001	0.324±0.000	0.358±0.001	0.459±0.001	0.323±0.000	0.397±0.000	0.396±0.001	0.493±0.001
67.9	β-Amyrin	0.633±0.003	0.594±0.003	0.630±0.004	0.862±0.005	0.570±0.005	0.719±0.007	0.697±0.010	0.959±0.012
71.7	Lupeol derivative	1.777±0.004	1.084±0.005	1.763±0.024	1.888±0.036	1.604±0.034	2.202±0.029	1.936±0.033	1.826±0.014
73.3	Ursolic Acid	1.167±0.009	1.194±0.003	1.163±0.010	1.564±0.015	1.072±0.049	1.366±0.013	1.284±0.018	2.005±0.002
Carbohydrates									
35.4	α-D-Mannopyranose	0.103±0.003	0.092±0.000	0.101±0.002	0.122±0.003	0.090±0.000	0.118±0.000	0.113±0.004	0.280±0.008
36.3	D-Sorbitol	0.130±0.000	0.109±0.001	0.129±0.001	0.135±0.001	0.117±0.000	0.152±0.001	0.143±0.000	0.572±0.001
37.7	α-D-(+)-Talopyranose	0.111±0.000	0.099±0.001	0.110±0.000	0.123±0.001	0.100±0.000	0.132±0.000	0.122±0.000	0.348±0.003
Fatty acids									
39.2	Palmitic Acid	3.017±0.008	2.978±0.006	2.992±0.008	4.439±0.008	2.731±0.001	3.406±0.003	3.347±0.010	4.742±0.008
43.0	β-Linolenic Acid	3.284±0.002	3.151±0.005	3.252±0.008	4.815±0.014	2.946±0.002	3.669±0.008	3.618±0.005	5.042±0.023
43.7	Stearic Acid	2.664±0.002	2.792±0.002	2.640±0.001	4.046±0.002	2.423±0.001	2.968±0.000	2.977±0.002	4.255±0.004
72.7	Oleic acid derivative	1.490±0.213	0.829±0.036	1.593±0.226	1.335±0.014	1.578±0.042	2.232±0.034	1.771±0.248	1.014±0.019
Alkanes									
57.9	Long Chain alkane 1	1.341±0.003	1.075±0.007	1.331±0.003	1.780±0.006	1.217±0.008	1.326±0.004	1.491±0.012	2.418±0.021
62.4	Long Chain alkane 2	1.888±0.001	1.534±0.014	1.879±0.010	2.683±0.018	1.717±0.025	2.117±0.009	2.106±0.018	3.644±0.040
67.6	Long Chain alkane 3	2.694±0.007	2.001±0.008	2.676±0.013	3.540±0.031	2.418±0.028	2.965±0.012	2.970±0.032	4.623±0.034
70.2	Long Chain alkane 4	0.741±0.011	0.685±0.006	0.750±0.041	1.059±0.006	0.692±0.014	0.894±0.005	0.838±0.003	1.266±0.009
72.8	Long Chain alkane 5	0.566±0.004	1.008±0.059	0.568±0.004	1.742±0.030	0.526±0.021	0.704±0.017	0.632±0.006	2.468±0.064

Table 5. Lipophilic profile (g kg⁻¹ DW) of *Olea europaea* leaves (Olivastra Seggiane cultivar) under control (C) and UV-B conditions in the different sampling times. Values are mean ± standard deviation (n=3). Rt - Retention time.

Rt (min)	Compound	T2		T4		T6		T8	
		C	UV-B	C	UV-B	C	UV-B	C	UV-B
Terpene									
34.1	Neophytadiene	0.533±0.002	0.487±0.006	0.530±0.003	0.586±0.006	0.578±0.008	0.700±0.003	0.483±0.008	0.534±0.007
42.1	Phytol	0.344±0.001	0.361±0.001	0.333±0.001	0.395±0.000	0.355±0.002	0.424±0.002	0.336±0.002	0.444±0.001
67.9	β -Amyrin	0.357±0.001	0.492±0.001	0.363±0.008	0.621±0.006	0.385±0.015	0.629±0.004	0.353±0.001	0.551±0.005
71.7	Lupeol derivative	1.290±0.012	1.591±0.046	1.281±0.007	1.873±0.009	1.378±0.021	1.794±0.017	1.143±0.003	1.490±0.026
73.3	Ursolic Acid	1.007±0.010	1.297±0.064	1.083±0.006	0.586±0.015	0.578±0.0008	1.647±0.028	0.975±0.006	1.626±0.036
Carbohydrates									
35.5	α-D-Mannopyranose	0.120±0.001	0.111±0.000	0.117±0.004	0.131±0.001	0.121±0.000	0.157±0.001	0.116±0.000	0.191±0.004
36.3	D-Sorbitol	0.127±0.000	0.119±0.000	0.126±0.000	0.159±0.001	0.135±0.000	0.209±0.002	0.124±0.000	0.209±0.004
37.7	α-D-(+)-Talopyranose	0.134±0.001	0.119±0.000	0.133±0.000	0.153±0.001	0.141±0.001	0.192±0.001	0.131±0.001	0.219±0.002
Fatty acids									
39.2	Palmitic Acid	2.777±0.010	3.411±0.003	2.766±0.005	3.433±0.009	2.946±0.004	3.551±0.015	2.961±0.004	3.868±0.013
43.0	β-Linolenic Acid	2.870±0.014	3.463±0.003	2.834±0.006	3.556±0.004	3.024±0.005	3.819±0.005	2.949±0.005	3.980±0.015
43.7	Stearic Acid	2.530±0.005	3.202±0.001	2.529±0.001	3.144±0.001	2.695±0.002	3.145±0.002	2.782±0.002	3.592±0.003
72.6	Oleic acid derivative	1.253±0.004	1.167±0.009	1.252±0.003	1.380±0.247	1.059±0.024	1.114±0.041	0.883±0.006	1.046±0.031
Alkanes									
52.9	Long Chain alkane 1	0.478±0.001	0.621±0.001	0.471±0.001	0.681±0.002	0.503±0.001	0.709±0.001	0.492±0.001	0.681±0.001
57.5	Long Chain alkane 2	0.689±0.005	1.125±0.007	0.684±0.002	1.310±0.003	0.732±0.002	1.409±0.009	0.670±0.001	0.967±0.006
62.4	Long Chain alkane 3	1.034±0.009	1.632±0.007	1.041±0.008	1.890±0.008	1.117±0.010	1.983±0.019	0.992±0.008	1.407±0.020
70.2	Long Chain alkane 4	0.607±0.001	0.770±0.001	0.607±0.003	0.850±0.002	0.647±0.002	0.913±0.007	0.622±0.001	0.899±0.004
72.8	Long Chain alkane 5	0.530±0.002	1.146±0.058	0.531±0.010	1.067±0.0322	0.905±0.049	1.645±0.038	0.894±0.008	1.402±0.005
Sterol									
67.6	<i>Stigmast-5-ene</i>	1.192±0.008	2.344±0.039	1.198±0.008	2.725±0.004	2.030±0.039	3.188±0.014	1.761±0.009	1.686±0.038

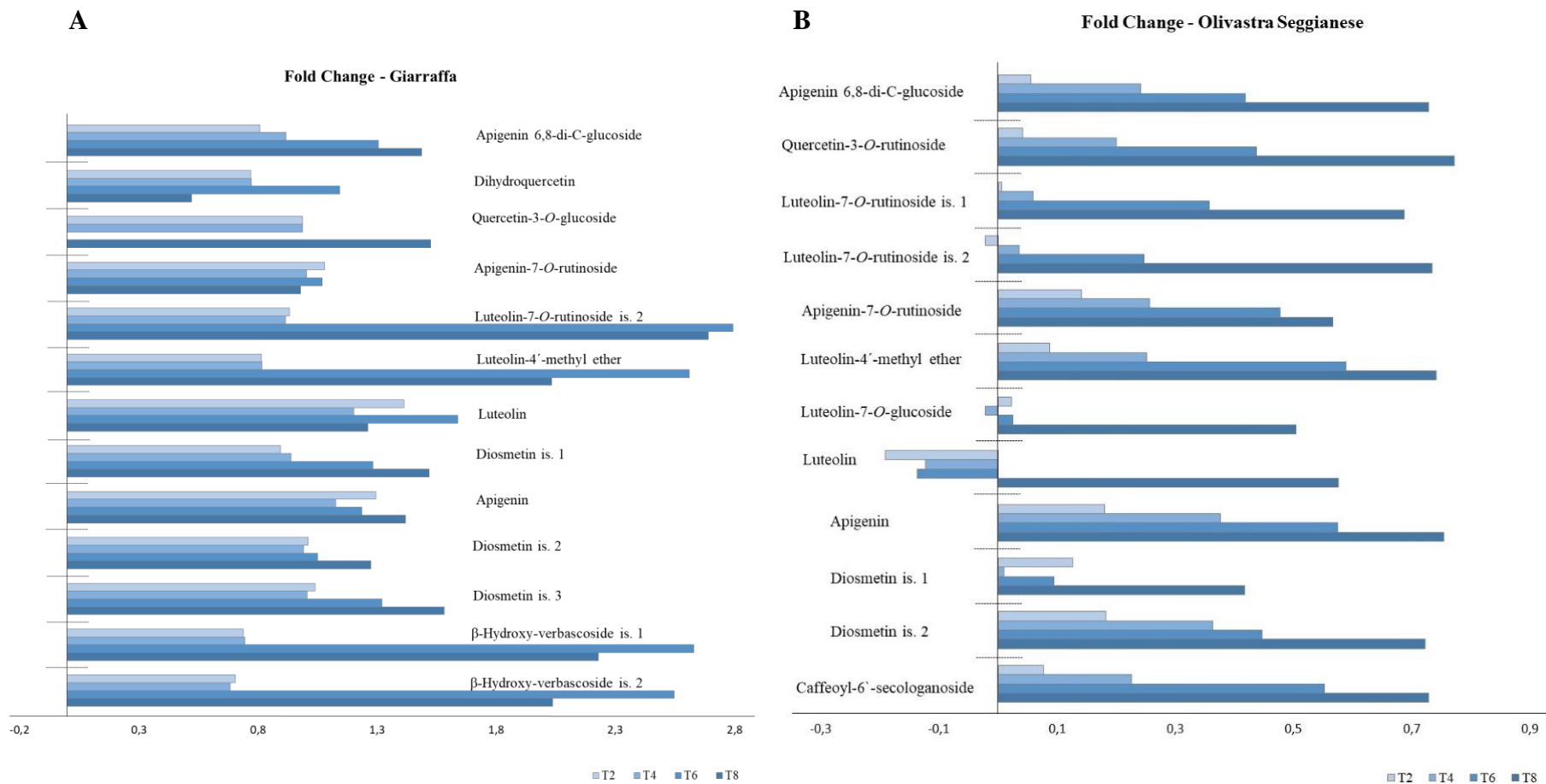


Figure 31. Fold changes (Log_2 (UV-B/Control)) in phenolic metabolites of the Giarraffa (A) and Olivastra Seggianese (B) cultivars after UV-B treatment in the different sampling times.

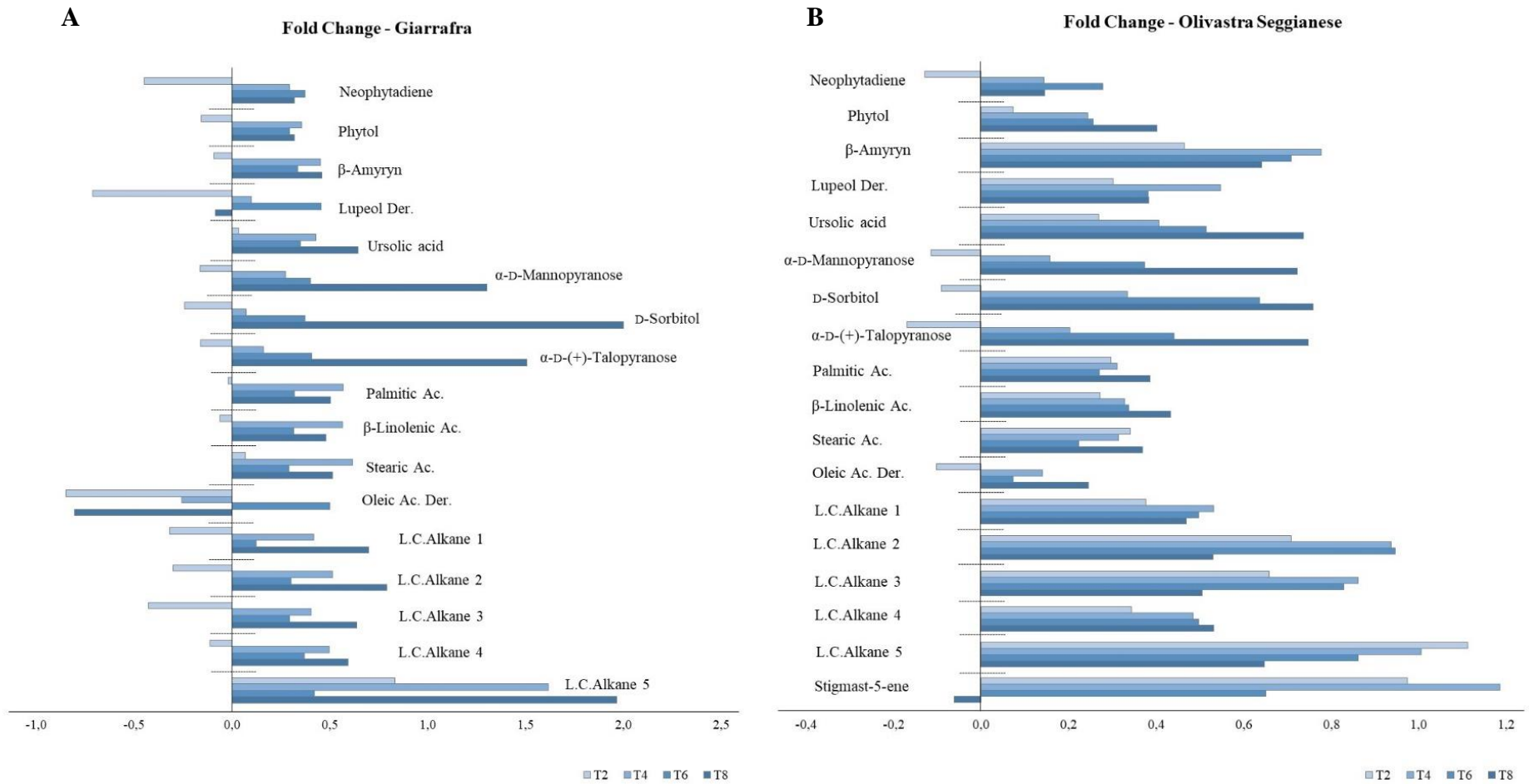


Figure 32. Fold changes ($\text{Log}_2(\text{UV-B}/\text{Control})$) in lipophilic metabolites of the Giarraffa (A) and Olivastra Seggianese (B) cultivars after UV-B treatment in the different sampling times.

Discussion

Olive plant UHPLC–MS metabolite profile

The metabolomic approach provided information on how the content of phenolic metabolites changes in response to UV-B stress and identified specific compounds that appear to be relevant in the plant response. Concerning the profile, some qualitative differences between the two cultivars are detected. However, the flavonoids, secoiridoids and hydroxycinnamic acids identified are already similar to the described for other olive cultivars (Talhaoui et al. 2015).

In Olivastra Seggianese and Giarraffa cultivars, the flavonoids are the main phenolic compounds present in leaves. The flavonoids-family is a vast group of compounds with different structures and roles (Agati et al. 2012). Flavonoids are the principal phenols that significantly contribute to the overall leaf antioxidant potency through the scavenging of ROS (Luengo Escobar et al. 2017). Some studies suggest that *o*-dihydroxy B-ring-substituted flavonoids have a greater antioxidant capacity (Brunetti et al. 2013). The ROS scavenging properties of these compounds rely on the hydroxyl group of the B-ring structure that donate a hydrogen and an electron to a radical, stabilizing them and generating a relative stable flavonoid phenoxyl radical (Mierziak et al. 2014). The formed molecule may react with another radical forming a stable quinone structure (Sarian et al. 2017). Some reports pinpoint that *o*-dihydroxy B-ring-substituted flavonoids can be found in several cell compartments near the centres of ROS generation, or be transported from their sites of biosynthesis to these compartments, such as mesophyll chloroplast (where they have a role as scavengers $^1\text{O}_2$), nucleus (where may inhibit ROS-generation making complexes with Fe and Cu ions), and vacuoles (where they serve as co-substrates for peroxidases to reduce H_2O_2 escape from the chloroplast) (Agati et al. 2012; Brunetti et al. 2013). Moreover, flavonoids can also prevent oxygen radical formation by inhibiting the activity of the enzymes involved in their generation (Mierziak et al. 2014). In Giarraffa cultivar, with the exception of the luteolin-7-*O*-rutinoside is. 1, luteolin-7-*O*- glucoside and the oleuropein derivative that are not detected in UV-B stresses leaves, all the other flavonoids increased in response to the UV-B stressed and these levels where, in general, higher than those found in Olivastra Seggianese stressed plants. In turn, the Olivastra Seggianese cultivar, showed a more heterogenic response to UV-B, but with a progressive increase of the majority of the flavonoids (from T2 to T8). The flavonoids, luteolin 7-*O*-rutinoside is. 2, luteolin 7-*O*-glucosideo and luteolin in this cultivar, despite some

fluctuations during the stress, at the end of the UV-B treatment achieved positive values (higher than the respective control). These data suggest that both cultivars respond to stress increasing flavonoids pools, which represent a high capacity to deal with the stress, particularly in the cultivar Giarraffa. In the literature it is reported that *O. europaea* leaves are rich in luteolin-7-*O*-glucoside, an *o*-dihydroxy B-ring-substituted flavonoid, which could be related to this species' high tolerance to stress (Dias et al. 2019). However, in other plants the luteolin methylated forms (e.g. 4'-methoxy luteolin and 4' or 3'-methoxy luteolin glucoside) seems more responsive to stress, particularly the UV-B stress, decreasing their levels possibly due to their use in the neutralization of ROS (Agati et al. 2011), or due to the inactivation of the enzymes involved in the conversion of luteolin in their methylated forms (e.g. flavone-*O*-methyltransferase catalyse the reaction of luteolin into 4'-methoxy luteolin) (Grignon-Dubois and Rezzonico 2012). Oxidative reactions derived from these flavonoid radicals may interact with other antioxidant pathways (e.g. GSH cycle) increasing the antioxidant response (Petrucci et al. 2013). In the present study, luteolin methylated forms were also found in both cultivars, but their levels were always higher than the controls. The profile of response of flavonoids to UV-B obtained here is in line with those obtained in chapter 2 from the analysis of the total flavonoid content, where, in general, UV-B plants showed a level of these compounds higher than the controls (Piccini et al. 2020).

Another class of phenolic compounds identified are the secoiridoids. This family of polyphenols plays, together with flavonoids, a crucial defensive role against different stressful conditions in species of major importance in the Mediterranean landscape like *O. europaea* (Rodrigues et al. 2015). In the literature, it is reported that secoiridoids play a crucial protective role against drought, salt (Petridis et al. 2012a, b) and UV-B stress (Dias et al. 2020) suggesting some involvement in plant stress defense mechanisms. Contrarily to other studies with other olive cultivars, only two secoiridoids are identified (Dias et al. 2020, 2021; Araújo et al. 2021). The decarboxymethyl oleuropein aglycone was identified in the Giarraffa cultivar but only in control plants while it was not detected in samples of stressed plants. This compound is a derivative of the oleuropein, which is one of the main phenolic compounds present in olive leaves (Dias et al. 2019). Some studies reported the important role of oleuropein in plant stress response, including UV-B (Talhaoui et al. 2015; Dias et al. 2020). The secoiridoid caffeoyl-6-scologanoside was identified in Olivastra Seggianese, stressed plants showed a significant and progressive increase of this metabolite compared to controls. An increase in caffeoyl-6-

secologanoside was also found in Cordovil de Castelo Branco olives in response to combined drought and heat stress (Valente et al. 2020).

The last class of phenolic compounds identified are the hydroxycinnamic acids derivatives (HCADs). Some studies suggest that hydroxycinnamic acids are predominantly involved in UV-B screening, hydroxycinnamic acids accumulated mainly in the leaf epidermal cells, screening UV-B radiation that can reach photosynthetic leaf tissues (Neugart et al. 2014; Luengo Escobar et al. 2017). These and other secondary metabolites can also act as antioxidants through the scavenging of ROS, such as $O_2^{\cdot-}$, OH^{\cdot} and 1O_2 (Luengo Escobar et al. 2017). In the present study HCADs were detected only in the leaves of the Giarraffa cultivar. In particular, the presence of β -hydroxy-verbascoside was detected, which increase in stressed plants compared to control plants. The HCAD β -hydroxy-verbascoside was identified in olive leaves from several cultivars (Michel et al. 2015). In the study conducted by Dias et al. (2020) a significant increase in β -hydroxy-verbascoside is observed after UV-B treatments, putatively providing an extra UV-B shield protection. In fact, HCADs are considered more effective UV-sunscreens compared with some others flavonoids (Burchard et al. 2000; Agati et al. 2012). Therefore, these results allow to hypothesize that, the high levels of these HCADs, particularly in stressed plants, allows the Giarraffa cultivar to cope better with UV-B stress when compared with the Olivastra Seggianese.

Olive plant GC–MS metabolite profile

How UV-B modulates crops' metabolic pathways is a matter of current debate (Luengo Escobar et al. 2017; Dias et al. 2018, 2020). By using a GC–MS approach, I analyzed the olive leaf (Giarraffa and Olivastra Seggianese cultivars) lipophilic metabolome under UV-B stress, which may allow better understanding of the physiological responses of this species to environmental challenges. In the literature, it is reported that one defense mechanism put in place by plants in response to adverse environmental conditions, such as infections by pathogens and herbivore attacks and abiotic stresses (such as drought, heat, cold, lack of nutrients, excess of toxic salts or metals in the soil) (Gondor et al. 2014) and stress induced by UV-B radiation (Kramer et al. 1991; Choudhary and Agrawal 2016; Takshak and Agrawal 2019), is the modulation of the lipophilic profile (Bowsher et al. 2008; Upchurch 2008; Hou et al. 2016). In recent studies, the variation of the lipophilic profile in olive trees and fruits has been observed in response to abiotic stress (Hernández et al. 2019) and in particular following UV radiation (Dias et al. 2018, 2019, 2020; Rogowska and Szakiel 2020; Valente et al. 2020).

The lipophilic compounds in Olivastra Seggianese and Giarraffa leaves have a very similar qualitative profile. In Olivastra Seggianese leaves the sterol stigmast-5-ene is also present in relative high amounts, but it is not detected in Giarraffa. Moreover, in other cultivars similar groups of compounds were found and the fatty acids and long chain alkanes are the most representative compounds found in leaves (Araújo et al. 2021; Dias et al. 2018, 2019).

Regarding fatty acids, UV-B stress stimulates the production of palmitic acid, α -linolenic acid and stearic acid in both cultivars. In agreement with what reported in the literature (Upchurch 2008), the profile of response allows to hypothesize that plants subjected to abiotic stress accomplish defense mechanisms to perform normal physiological functions, in particular modulating the lipid profile. For example, Tripathi et al.(2019) observed a change in the concentrations of fatty acids in *Helianthus annuus* L. in response to stress by UV-B and tropospheric ozone (O₃). In addition, the work of Baux et al. (2008) reported that low temperatures affects the concentration of fatty acids in rapeseed oil. In Kramer et al. (1991) a change in the ratio was observed between saturated/unsaturated fatty acids in the lipidic membranes of cucumbers (*Cucumis serious*) following UV-B radiation; the same effect was also observed in wheat (*Triticum aestivum* L.) following multiple stresses such as UV-B, heavy metals (Cd) and drought (Gondor et al. 2014). Following water stress, a change in the lipidic content is also reported in *Cynodon dactylon* (Zhong et al. 2011). Furthermore, stressed plants of Giarraffa show more palmitic acid, α -linolenic acid, and stearic acid than the stressed plants of Olivastra Seggianese. Therefore, the UV-B stress response is weaker in Olivastra Seggianese. This allows to hypothesize that the Tuscan cultivar is unable to achieve the same defense mechanisms based on variations of fatty acids. These results are in line with what obtained in chapter 3 by analysis of lipid peroxidation as measured by malondialdehyde (MDA) production. Giarraffa showed no variations in MDA levels between control and stressed plants; in contrast, Olivastra Seggianese shows an increase in MDA production from T2 to T8 in stressed plants compared to controls (Piccini et al. 2021). The absence of variations in MDA production in stressed Giarraffa plants could be affected by higher palmitic acid, α -linolenic acid and stearic acid content found in these plants. Indeed, fatty acids are described as constitutive elements of complex lipids, but recent studies also suggest their direct involvement in abiotic and biotic responses to stress in plants (Tumlinson and Engelberth 2008; Upchurch 2008). Complex lipids in turn play an essential role in the structure and functions of cells by maintaining the integrity of cells and of organelles (Spector and Yorek 1985).

Mannitol is the main polyol usually found in olive leaves (Conde et al. 2011); together with the isomer sorbitol, it was identified in both cultivars we analyzed. In general, in both Giarrappa and Olivastra Seggianese cultivars, the UV-B stress induces the accumulation of this polyol. The profile of response is in line with the data described in chapter 2. Indeed, the concentration of mannitol increases significantly in both olive cultivars we analyzed. However, UV-B Giarrappa plants maintained high mannitol concentrations throughout the treatment, unlike UV-B Seggianese plants which resumed the control values after the peak at T2 (Piccini et al. 2020). Mannitol concentration may increase in response to UV-B stress because of an osmoprotective and antagonistic function against free radicals (Piccini et al. 2020). Olive trees are well adapted to regions with high irradiances (in particular UV), and the maintenance of high levels of polyols may be essential to cope with this stress because these compounds provide a more efficient use of carbon, can act as osmolytes and in the defense against photo-oxidative damage (Conde et al. 2011). Since Giarrappa has a higher concentration of mannitol throughout the treatment, it probably developed this response mechanism to adapt to the more intense radiation in its area of origin (Sicily). Beside mannitol, UV-B stress also induces a significantly increase of the carbohydrates α -D-mannopyranose and α -D-(+)-talopyranose up to T4 in stressed plants of both cultivars. Carbohydrates are reported to be involved in several stress protective mechanism, and their increase following stress is a typical response of olive trees, particularly under drought (Araújo et al. 2021). An increase in the sugar pool can be interpreted as an increased availability of carbon and energy to cope with stressful conditions or as a slowing of their use in growth processes (Araújo et al. 2019).

UV-B treatment also induces adjustments in the levels of triterpenes (neophytadiene, phytol, β -amyrin, lupeol derivative and ursolic acid) and long-chain alkanes in both cultivars. Considering that the main components of olive leaf cuticular wax are triterpenes (e.g. ursolic acid, α - and β -amyrin), long-chain alkanes, alcohols, aldehydes and fatty acids (Bianchi et al. 1992; Mihailova et al. 2015; Lv et al. 2016), I hypothesize that plants invested in these compounds to strengthen the cuticle structure. Leaf cuticular waxes provide a protective barrier against UV radiation, and account for 20–60% of cuticle mass, thereby increasing light reflectance, decreasing penetration of UV radiation into the mesophyll and reducing membrane damages (Le Provost et al. 2013; Choudhary and Agrawal 2016; Dias et al. 2018). These data are in line with the morpho-anatomical studies performed in olive leaves showing an increase of cuticle thickness in response to a long period of UV-B exposure (Liakoura et al. 1999). Furthermore, Giarrappa stressed plants have more β -amyrin, lupeol derivative and long-chain

alkanes 1, 2, 3 and 4 than Olivastra Seggiane stressed plants. In particular, long-chain alkanes in Giarrappa stressed plants show values about twice as high as those found in Olivastra Seggiane stressed plants. The higher content of terpenes and long chain alkanes could allow Giarrappa stressed plants to better resist UV-B radiation than Olivastra Seggiane stressed plants.

Conclusions

In this chapter, the levels of the most representative phenolic and lipophilic compounds of Giarrappa and Olivastra Seggiane were characterized and has been proved how these levels are modulated by UV-B stress. Giarrappa cultivar seems better suited to prolonged UV-B stress, possible due to the higher availability of flavonoids that neutralize ROS and radicals, and to the accumulation of HCAs that provide an extra UV-B shield protection. Beside phenolic compounds, this also stands out due to the high levels of fatty acids (e.g. palmitic, α -linolenic, and stearic acids) that can help to maintain membrane integrity, accumulation of mannitol that may have osmoprotective and antagonistic function against free radicals, and increase in some terpenes and long-chain alkanes that can provide a better protection from UV-B radiation.

List of contributors to this chapter:

- **Claudio Cantini** (Institute for BioEconomy, National Research Council of Italy, 58022 Follonica, Italy)
- **Giampiero Cai** (Department of Life Sciences, University of Siena, via Mattioli 4, 53100 Siena, Italy)
- **Maria Celeste Dias** (Department of Life Sciences, Centre for Functional Ecology, University of Coimbra, Calçada Martim de Freitas, 3000-456 Coimbra, Portugal)
- **Diana C. G. A. Pinto** (LAQV-REQUIMTE, Department of Chemistry, University of Aveiro, 3810-193 Aveiro, Portugal)
- **Artur M. S. Silva** (LAQV-REQUIMTE, Department of Chemistry, University of Aveiro, 3810-193 Aveiro, Portugal)
- **Marco Romi** (Department of Life Sciences, University of Siena, via Mattioli 4, 53100 Siena, Italy)

Chapter 5: Conclusions and perspectives

Given the extreme importance of the olive tree in our country from an economic, territorial, social and landscape point of view, it is important to study its responses to stress agents such as excessive UV-B radiation to understand the defense mechanisms and the cultivars that put them in place to cope with it. In the literature there are few studies concerning the relationship between olive tree and UV-B radiation; therefore, it is not precisely known the extent of possible damage that this stress could cause and, above all, the actions that the plant can take to counteract it and develop resistance. Both cultivars considered (Giarrappa and Olivastra Seggianese), while proving to be resistant to the treatment to which they were subjected, have shown clear effects even if in different ways and times. The photosynthetic mechanism as a whole is the target of UV-B stress. In fact, under optimal conditions the light radiation reaches the pigments and then the photosystems, producing ATP and NADPH necessary for the functioning of the Calvin cycle. This cycle of reactions, mainly powered by the enzyme Rubisco, generates glyceraldehyde-3-phosphate from which all the sugars needed by plants are subsequently produced. Under conditions of excess UV radiation, a number of alterations can occur at the level of this mechanism. The data collected in this thesis show that the fluorescence value of chlorophyll does not undergo significant changes but the yield index of the photosynthetic apparatus significantly decreases. This suggests to me that the pigments are probably preserved but that the damage occurs in the photosystems. Therefore, when the energy dissipation mechanisms are not sufficient to dispose of the excess UV radiation, the plant undergoes photo-oxidative stress and ROS production that cause severe DNA and protein damage. Among the latter, RubisCO is one of the most important. In the present study, RubisCO was analyzed in terms of quantity, isoform variation, and enzymatic activity. The results obtained show that RubisCO is equally sensitive to UV-B in the two cultivars. Therefore, the amount of RubisCO decreases comparably in stressed plants of both cultivars as UV-B treatment progresses; however, in Giarrappa stressed plants the gradual decrease in the amount of protein does not correspond to the gradual decrease in enzymatic activity. This suggests that Giarrappa-stressed plants implement a defense mechanism that allows the plants to gradually recover RubisCO activity. This would allow Giarrappa plants to recover photosynthesis better than stressed Olivastra Seggianese plants. In addition, the results obtained by two-dimensional electrophoresis and immunoblotting show that Giarrappa plants react better than Olivastra Seggianese to UV-B stress by post-translationally modifying RubisCO to produce isoforms more effective in performing their functions and also more resistant to

degradation by UV stress; in this way, they balance the damage suffered by the photosynthetic apparatus. Like all other plants, the purpose of the olive tree is to ensure the production of sugars essential for growth, such as sucrose, from which fructose and glucose are obtained by splitting. The results obtained showed no significant differences in sucrose content between control plants and UV-B stressed plants of both cultivars. Given the key role of sucrose, I assume that plants under UV-B stress implement mechanisms to maintain constant sucrose levels and related metabolic processes. In contrast, glucose and fructose were the most responsive to UV-B treatment. UV-B-stressed Olivastra Seggianese plants accumulated less glucose, probably due to reduced photosynthesis and increased utilization of glucose to maintain cellular respiration or to increase polyol levels. On the other hand, UV-B promotes fructose accumulation more significantly in Olivastra Seggianese. The increase in fructose may result from sucrose degradation; therefore, Olivastra Seggianese plants must continue to break down sucrose into glucose and fructose to counteract stress conditions. However, the two cultivars attempt to maintain the sugar pool at a sufficient level; this allows the plants to activate alternative metabolic response pathways, for example the production of mannitol, a protective sugar-alcohol. The concentration of mannitol increases significantly in both olive cultivars. In Giarraffa, mannitol concentration increases at T2 in plants subjected to UV-B compared to the control, and mannitol content remains high throughout the treatment compared to Seggianese. The concentration of mannitol may increase in response to UV-B stress for an osmoprotective and antagonistic function against free radicals. Because Giarraffa responds better than Seggianese to UV-B stress and has a higher concentration of mannitol, it likely developed this response mechanism to adapt to the more intense radiation in its home area. Given the key role of sucrose, changes in the amount of sucrose synthase (SuSy) were analyzed by immunoblotting. The results obtained showed a completely opposite profile of Susy accumulation for the two cultivars. Olivastra Seggianese shows an initial decrease of SuSy accumulation, while afterwards the content of the enzyme increases again. Probably this occurs because at T8 the plants are still under stress and therefore require the available energy from the breakdown of sucrose (probably by invertase). In contrast, Giarraffa shows an initial moderate increase in SuSy content, while the enzyme content decreases at the end of the experiment (T8), corresponding to the time when Giarraffa plants have resumed their metabolic processes. High UV-B radiation can trigger an increase in reactive oxygen species (ROS) at the cellular level, which causes oxidation of proteins, lipids and other biomolecules. To deal with the damage caused by ROS, living organisms have developed a complex defense system composed of enzymatic and non-enzymatic antioxidants. The profile of total polyphenols

showed a significant difference already at T0 between the two olive cultivars. Giarraffa responds after the first week to UV-B radiation by increasing the polyphenol pool. On the other hand, Olivastra Seggianese plants respond later to UV-B triggering an increase in polyphenols only at T2. Furthermore, flavonoid analysis indicates that Giarraffa responds first to UV-B stress (in the first week), and that total flavonoid levels decrease over time. In contrast, Olivastra Seggianese responds later (after the second week) and maintains high levels of these compounds until the end of treatment. These distinct profiles of UV-B triggered-antioxidant response support the hypothesis that Giarraffa activates defense mechanisms after the first week of UV-B stress, thus behaving better than Olivastra Seggianese in the long run. Regarding enzyme complexes, SOD enzyme activity in Giarraffa showed no variation between stressed and control plants; in contrast, stressed Olivastra Seggianese plants showed a significant increase at T4. Giarraffa showed no statistically significant differences in CAT activity, whereas differences in CAT activity were observed in Olivastra Seggianese at T2 and T4. In addition, Olivastra Seggianese plants show a decrease in GPox activity while stressed Giarraffa plants show a significant increase in GPox activity from T2 onward. This suggests that the response of stressed Olivastra Seggianese plants was based on stimulation of SOD activity to convert increased $O_2^{\bullet-}$ in H_2O_2 , which is immediately scavenged by the stimulated CAT activity, in particular at T4. In contrast, stressed Giarraffa plants invest in the GPox pathway, as they show a steady and progressive increase in enzyme activity throughout the stress. When the antioxidant complex fails to dispose of excess ROS, they can cause damage to essential cellular components. Accumulation of ROS is associated with lipid peroxidation, which makes cell membranes particularly susceptible to oxidative damage. In the present study, I analyzed MDA as a parameter of ROS-induced oxidation in macromolecules (i.e., lipids). Giarraffa showed no statistically significant differences in MDA production. In contrast, a significant increase in MDA production was observed in Olivastra Seggianese. The absence of significant changes in MDA production in Giarraffa stressed plants suggests that plants of this cultivar, in contrast to Olivastra Seggianese, better tolerate UV-B stress. The mechanism underlying the improved tolerance may involve the increase in Hsp. In fact, the Hsp family acts as the first line of defense against heat stress in olive plants as well as against other abiotic stresses such as UV. My hypothesis is that the increase of Hsp70 found in stressed plants of Giarraffa may justify the absence of lipid peroxidation in these plants. Thus, the metabolomics analysis confirmed that Giarraffa cultivar seems better suited to prolonged UV-B stress, possible due to the higher availability of flavonoids that neutralize ROS and radicals, and because of the

increased presence of HCAdS, as well as for the presence of palmitic acid, α -linolenic acid, and stearic acid and for the higher content of terpenes and long-chain alkanes.

In conclusion, the analyses carried out in this study show that UV-B radiation is a dangerous source of stress for the olive tree, especially in the current increasingly changing environmental conditions. Considering the results for both cultivars, it is possible to note the critical points where the most evident changes occur, i.e. after the first two weeks of stress (T2) and during the last two weeks (T6-T8). The Giarrappa cultivar seems to respond and resist to UV-B stress better than the Olivastra Seggianese cultivar. The data obtained suggest some possible mechanisms by which Giarrappa becomes more resistant to UV-B stress, including the ability to maintain photosynthetic efficiency, a more efficient and rapid activation of the antioxidant response, the higher availability of flavonoids that neutralize ROS and radicals, an increase of HCAdS (providing additional UV-B protection), optimization of GPox use as well as a relatively high content of mannitol and Hsp70 levels. Moreover, Giarrappa opted for a targeted choice of RubisCO isoforms and managed SuSy content, saving energy during the critical stress point. In addition, the Giarrappa cultivar seems better adapted to prolonged UV-B stress due to a higher presence of palmitic acid, α -linolenic acid, and stearic acid, as well as some terpenes and long-chain alkanes. Therefore, in my opinion, Giarrappa could be a cultivar to be further analyzed and used to obtain plants with metabolic characteristics suitable to challenge environmental stresses caused by climate change.

References

- Abbasi SA, Abbasi T (2017) Impacts of Ozone Hole. pp 51–99
- Abebe T, Guenzi AC, Martin B, Cushman JC (2003) Tolerance of Mannitol-Accumulating Transgenic Wheat to Water Stress and Salinity. *Plant Physiol* 131:1748–1755.
<https://doi.org/10.1104/pp.102.003616>
- Abozed SS, El-Kalyoubi M, Abdelrashid A, Salama MF (2014) Total phenolic contents and antioxidant activities of various solvent extracts from whole wheat and bran. *Ann Agric Sci* 59:63–67
- Agarwal S, Sairam RK, Srivastava GC, Meena RC (2005) Changes in antioxidant enzymes activity and oxidative stress by abscisic acid and salicylic acid in wheat genotypes. *Biol Plant* 49:541–550. <https://doi.org/10.1007/s10535-005-0048-z>
- Agati G, Azzarello E, Pollastri S, Tattini M (2012) Flavonoids as antioxidants in plants: Location and functional significance. *Plant Sci* 196:67–76.
<https://doi.org/10.1016/j.plantsci.2012.07.014>
- Agati G, Biricolti S, Guidi L, et al (2011) The biosynthesis of flavonoids is enhanced similarly by UV radiation and root zone salinity in *L. vulgare* leaves. *J Plant Physiol* 168:204–212. <https://doi.org/10.1016/j.jplph.2010.07.016>
- Ahmad P, Jaleel CA, Salem MA, et al (2010) Roles of enzymatic and nonenzymatic antioxidants in plants during abiotic stress. *Crit Rev Biotechnol* 30:161–175
- Ahsan N, Donnart T, Nouri M-Z, Komatsu S (2010) Tissue-Specific Defense and Thermo-Adaptive Mechanisms of Soybean Seedlings under Heat Stress Revealed by Proteomic Approach. *J Proteome Res* 9:4189–4204. <https://doi.org/10.1021/pr100504j>
- Ainsworth EA, Gillespie KM (2007) Estimation of total phenolic content and other oxidation substrates in plant tissues using Folin–Ciocalteu reagent. *Nat Protoc* 2:875–877
- Albert KR, Mikkelsen TN, Ro-Poulsen H, et al (2011) Ambient UV-B radiation reduces PSII performance and net photosynthesis in high Arctic *Salix arctica*. *Environ Exp Bot* 73:10–18. <https://doi.org/10.1016/j.envexpbot.2011.08.003>

- Allen DJ, Mckee IF, Farage PK, Baker NR (1997) Analysis of limitations to CO₂ assimilation on exposure of leaves of two *Brassica napus* cultivars to UV-B. *Plant, Cell Environ* 20:633–640. <https://doi.org/10.1111/j.1365-3040.1997.00093.x>
- Amouretti M-C, Comet G (1985) *Le livre de l'olivier*
- Antolovich M, Prenzler PD, Patsalides E, et al (2002) Methods for testing antioxidant activity. *Analyst* 127:183–198. <https://doi.org/10.1039/b009171p>
- Araújo M, Ferreira de Oliveira JMP, Santos C, et al (2019) Responses of olive plants exposed to different irrigation treatments in combination with heat shock: physiological and molecular mechanisms during exposure and recovery. *Planta* 249:1583–1598. <https://doi.org/10.1007/s00425-019-03109-2>
- Araújo M, Prada J, Mariz-Ponte N, et al (2021) Antioxidant Adjustments of Olive Trees (*Olea Europaea*) under Field Stress Conditions. *Plants* 10:684. <https://doi.org/10.3390/plants10040684>
- Araújo M, Santos C, Costa M, et al (2016) Plasticity of young *Moringa oleifera* L. plants to face water deficit and UVB radiation challenges. *J Photochem Photobiol B Biol* 162:278–285. <https://doi.org/10.1016/j.jphotobiol.2016.06.048>
- Araújo M, Santos C, Dias MC (2018) Can young olive plants overcome heat shock? In: *Climate Change Management*
- Assab E, Rampino P, Mita G, Perrotta C (2011) Heat shock response in olive (*olea europaea* L.) twigs: Identification and analysis of a cDNA coding a class I small heat shock protein. *Plant Biosyst.* <https://doi.org/10.1080/11263504.2011.558711>
- Baird C, Cann M (2012) The pollution and purification of water. *Environ Chem* 601–660
- Ballaré CL (2014) Light regulation of plant defense. *Annu Rev Plant Biol* 65:335–363
- Barnes PW, Williamson CE, Lucas RM, et al (2019) Ozone depletion, ultraviolet radiation, climate change and prospects for a sustainable future. *Nat Sustain* 2:569–579. <https://doi.org/10.1038/s41893-019-0314-2>
- Baroja-Fernandez E, Munoz FJ, Li J, et al (2012) Sucrose synthase activity in the

- sus1/sus2/sus3/sus4 Arabidopsis mutant is sufficient to support normal cellulose and starch production. *Proc Natl Acad Sci* 109:321–326.
<https://doi.org/10.1073/pnas.1117099109>
- Baux A, Hebeisen T, Pellet D (2008) Effects of minimal temperatures on low-linolenic rapeseed oil fatty-acid composition. *Eur J Agron* 29:102–107
- Beers RF, Sizer IW (1952) A spectrophotometric method for measuring the breakdown of hydrogen peroxide by catalase. *J Biol Chem* 195:133–140.
[https://doi.org/10.1016/s0021-9258\(19\)50881-x](https://doi.org/10.1016/s0021-9258(19)50881-x)
- Beggs CJ, Wellmann E (1985) Analysis of light-controlled anthocyanin formation in coleoptiles of *Zea mays* L.: the role of UV-B, blue, red and far-red light. *Photochem Photobiol* 41:481–486
- Behr M, Faleri C, Hausman JF, et al (2019) Distribution of cell-wall polysaccharides and proteins during growth of the hemp hypocotyl. *Planta*. <https://doi.org/10.1007/s00425-019-03245-9>
- Benzie IFF, Strain JJ (1996) The ferric reducing ability of plasma (FRAP) as a measure of “antioxidant power”: the FRAP assay. *Anal Biochem* 239:70–76
- Besnard G, Khadari B, Baradat P, Bervillé A (2002) *Olea europaea* (Oleaceae) phylogeography based on chloroplast DNA polymorphism. *Theor Appl Genet* 104:1353–1361. <https://doi.org/10.1007/s00122-001-0832-x>
- Bianchi G, Murelli C, Vlahov G (1992) Surface waxes from olive fruits. *Phytochemistry* 31:3503–3506. [https://doi.org/10.1016/0031-9422\(92\)83716-C](https://doi.org/10.1016/0031-9422(92)83716-C)
- Bierkens JGEA (2000) Applications and pitfalls of stress-proteins in biomonitoring. *Toxicology*. [https://doi.org/10.1016/S0300-483X\(00\)00304-8](https://doi.org/10.1016/S0300-483X(00)00304-8)
- Bilger W, Veit M, Schreiber L, Schreiber U (1997) Measurement of leaf epidermal transmittance of UV radiation by chlorophyll fluorescence. *Physiol Plant* 101:754–763.
<https://doi.org/10.1034/j.1399-3054.1997.1010411.x>
- Bischof K, Hanelt D, Wiencke C (2000) Effects of ultraviolet radiation on photosynthesis and related enzyme reactions of marine macroalgae. *Planta*.

<https://doi.org/10.1007/s004250000313>

Bornman JF, Vogelmann TC (1991) Effect of UV-B radiation on leaf optical properties measured with fibre optics. *J Exp Bot* 42:547–554. <https://doi.org/10.1093/jxb/42.4.547>

Bowsher C, Steer M, Tobin A (2008) *Plant biochemistry*. Garland Science

Brestic M, Zivcak M (2013) PSII Fluorescence Techniques for Measurement of Drought and High Temperature Stress Signal in Crop Plants: Protocols and Applications. In: *Molecular Stress Physiology of Plants*. Springer India, India, pp 87–131

Breton C, Terral J-F, Pinatel C, et al (2009) The origins of the domestication of the olive tree. *C R Biol* 332:1059–1064

Brito, Dinis, Moutinho-Pereira, Correia (2019) Drought Stress Effects and Olive Tree Acclimation under a Changing Climate. *Plants* 8:232. <https://doi.org/10.3390/plants8070232>

Britt AB (1996) DNA damage and repair in plants. *Annu Rev Plant Physiol Plant Mol Biol* 47:75–100. <https://doi.org/10.1146/annurev.arplant.47.1.75>

Brun J-P, Amouretti M-C (1993) *La production du vin et de l'huile en Méditerranée*. École française d'Athènes

Brunetti C, Di Ferdinando M, Fini A, et al (2013) Flavonoids as Antioxidants and Developmental Regulators: Relative Significance in Plants and Humans. *Int J Mol Sci* 14:3540–3555. <https://doi.org/10.3390/ijms14023540>

Bueno PCP, Lopes NP (2020) Metabolomics to Characterize Adaptive and Signaling Responses in Legume Crops under Abiotic Stresses. *ACS Omega* 5:1752–1763. <https://doi.org/10.1021/acsomega.9b03668>

Burchard P, Bilger W, Weissenböck G (2000) Contribution of hydroxycinnamates and flavonoids to epidermal shielding of UV-A and UV-B radiation in developing rye primary leaves as assessed by ultraviolet-induced chlorophyll fluorescence measurements. *Plant Cell Environ* 23:1373–1380

Caldwell MM (1979) *Plant Life and Ultraviolet Radiation: Some Perspective in the History*

- of the Earth's UV Climate. *Bioscience* 29:520–525. <https://doi.org/10.2307/1307719>
- Caldwell MM, Robberecht R, Flint SD (1983) Internal filters: prospects for UV-acclimation in higher plants. *Physiol Plant* 58:445–450
- Carmo-Silva AE, Gore MA, Andrade-Sanchez P, et al (2012) Decreased CO₂ availability and inactivation of Rubisco limit photosynthesis in cotton plants under heat and drought stress in the field. *Environ Exp Bot* 83:1–11.
<https://doi.org/10.1016/j.envexpbot.2012.04.001>
- Casati P, Campi M, Morrow DJ, et al (2011) Transcriptomic, proteomic and metabolomic analysis of UV-B signaling in maize. *BMC Genomics* 12:321.
<https://doi.org/10.1186/1471-2164-12-321>
- Cen Y, Bornman JF (1993) The effect of exposure to enhanced UV-B radiation on the penetration of monochromatic and polychromatic UV-B radiation in leaves of *Brassica napus*. *Physiol Plant* 87:249–255. <https://doi.org/10.1111/j.1399-3054.1993.tb01727.x>
- Chen C, Dickman MB (2005) Proline suppresses apoptosis in the fungal pathogen *Colletotrichum trifolii*. *Proc Natl Acad Sci* 102:3459–3464
- Choudhary KK, Agrawal SB (2016) Assessment of Fatty Acid Profile and Seed Mineral Nutrients of Two Soybean (*Glycine max* L.) Cultivars Under Elevated Ultraviolet-B: Role of ROS, Pigments and Antioxidants. *Photochem Photobiol* 92:134–143
- Ciferri R (1950) Dati e ipotesi sull'origine ed evoluzione dell'olivo
- Conde A, Silva P, Agasse A, et al (2011) Mannitol Transport and Mannitol Dehydrogenase Activities are Coordinated in *Olea europaea* Under Salt and Osmotic Stresses. *Plant Cell Physiol* 52:1766–1775. <https://doi.org/10.1093/pcp/pcr121>
- Conde C, Silva P, Agasse A, et al (2006) Utilization and Transport of Mannitol in *Olea europaea* and Implications for Salt Stress Tolerance. *Plant Cell Physiol* 48:42–53.
<https://doi.org/10.1093/pcp/pcl035>
- Cornu AM (1879) II. Sur la limite ultraviolette du spectre solaire. *Proc R Soc London* 29:47–55. <https://doi.org/10.1098/rspl.1879.0011>

- Correia CM, Coutinho JF, Bacelar EA, et al (2012) Ultraviolet-B Radiation and Nitrogen Affect Nutrient Concentrations and the Amount of Nutrients Acquired by Above-Ground Organs of Maize. *Sci World J* 2012:1–11. <https://doi.org/10.1100/2012/608954>
- Crafts-Brandner SJ, Salvucci ME (2000) Rubisco activase constrains the photosynthetic potential of leaves at high temperature and CO₂. *Proc Natl Acad Sci* 97:13430–13435. <https://doi.org/10.1073/pnas.230451497>
- Dany A-L, Douki T, Triantaphylides C, Cadet J (2001) Repair of the main UV-induced thymine dimeric lesions within *Arabidopsis thaliana* DNA: evidence for the major involvement of photoreactivation pathways. *J Photochem Photobiol B Biol* 65:127–135. [https://doi.org/10.1016/S1011-1344\(01\)00254-8](https://doi.org/10.1016/S1011-1344(01)00254-8)
- de Zafra RL, Jaramillo M, Parrish A, et al (1987) High concentrations of chlorine monoxide at low altitudes in the Antarctic spring stratosphere: diurnal variation. *Nature* 328:408–411. <https://doi.org/10.1038/328408a0>
- Demmig B, Björkman O (1987) Comparison of the effect of excessive light on chlorophyll fluorescence (77K) and photon yield of O₂ evolution in leaves of higher plants. *Planta* 171:171–184
- Dias MC, Figueiredo C, Pinto DCGA, et al (2019) Heat shock and UV-B episodes modulate olive leaves lipophilic and phenolic metabolite profiles. *Ind Crops Prod* 133:269–275. <https://doi.org/10.1016/j.indcrop.2019.03.036>
- Dias MC, Pinto DCGA, Correia C, et al (2018) UV-B radiation modulates physiology and lipophilic metabolite profile in *Olea europaea*. *J Plant Physiol* 222:39–50. <https://doi.org/10.1016/j.jplph.2018.01.004>
- Dias MC, Pinto DCGA, Figueiredo C, et al (2021) Phenolic and lipophilic metabolite adjustments in *Olea europaea* (olive) trees during drought stress and recovery. *Phytochemistry* 185:112695
- Dias MC, Pinto DCGA, Freitas H, et al (2020) The antioxidant system in *Olea europaea* to enhanced UV-B radiation also depends on flavonoids and secoiridoids. *Phytochemistry* 170:112199. <https://doi.org/10.1016/j.phytochem.2019.112199>

- Díaz-Guerra L, Verdaguer D, Gispert M, et al (2018) Effects of UV radiation and rainfall reduction on leaf and soil parameters related to C and N cycles of a Mediterranean shrubland before and after a controlled fire. *Plant Soil* 424:503–524.
<https://doi.org/10.1007/s11104-017-3485-5>
- Dichio B, Xiloyannis C, Angelopoulos K, et al (2003) Drought-induced variations of water relations parameters in *Olea europaea*. *Plant Soil* 257:381–389.
<https://doi.org/10.1023/A:1027392831483>
- Dotto M, Casati P (2017) Developmental reprogramming by UV-B radiation in plants. *Plant Sci* 264:96–101. <https://doi.org/10.1016/j.plantsci.2017.09.006>
- Ennajeh M, Vadel AM, Khemira H (2009) Osmoregulation and osmoprotection in the leaf cells of two olive cultivars subjected to severe water deficit. *Acta Physiol Plant* 31:711–721. <https://doi.org/10.1007/s11738-009-0283-6>
- Everard JD, Cantini C, Grumet R, et al (1997) Molecular Cloning of Mannose-6-Phosphate Reductase and Its Developmental Expression in Celery. *Plant Physiol* 113:1427–1435.
<https://doi.org/10.1104/pp.113.4.1427>
- Farman JC, Gardiner BG, Shanklin JD (1985) Large losses of total ozone in Antarctica reveal seasonal ClO_x/NO_x interaction. *Nature* 315:207–210. <https://doi.org/10.1038/315207a0>
- Farrar J, Pollock C, Gallagher J (2000) Sucrose and the integration of metabolism in vascular plants. *Plant Sci* 154:1–11. [https://doi.org/10.1016/S0168-9452\(99\)00260-5](https://doi.org/10.1016/S0168-9452(99)00260-5)
- Fedina I, Hidema J, Velitchkova M, et al (2010) UV-B induced stress responses in three rice cultivars. *Biol Plant*. <https://doi.org/10.1007/s10535-010-0102-3>
- Feng H, An L, Tan L, et al (2000) Effect of enhanced ultraviolet-B radiation on pollen germination and tube growth of 19 taxa in vitro. *Environ Exp Bot* 43:45–53.
[https://doi.org/10.1016/S0098-8472\(99\)00042-8](https://doi.org/10.1016/S0098-8472(99)00042-8)
- Flora L, Madore M (1993) Stachyose and mannitol transport in olive (*Olea europaea* L.). *Planta* 189:.. <https://doi.org/10.1007/BF00198210>
- Fonini AM, Barufi JB, Schmidt EC, et al (2017) Leaf anatomy and photosynthetic efficiency of *Acrostichum danaeifolium* after UV radiation. *Photosynthetica* 55:401–410.

<https://doi.org/10.1007/s11099-016-0654-3>

Forster PM, Thompson, D.W.J., Baldwin MP, Chipperfield, M.P., Dameris M, et al (2011) Stratospheric changes and climate. Scientific Assessment of Ozone Depletion, Global Ozone Research and Monitoring Project-Report No 52.

Foyer CH, Lelandais M, Kunert KJ (1994) Photooxidative stress in plants. *Physiol. Plant.*

Frohnmeier H, Staiger D (2003) Ultraviolet-B radiation-mediated responses in plants.

Balancing damage and protection. *Plant Physiol* 133:1420–8.

<https://doi.org/10.1104/pp.103.030049>

Gil M, Pontin M, Berli F, et al (2012) Metabolism of terpenes in the response of grape (*Vitis vinifera* L.) leaf tissues to UV-B radiation. *Phytochemistry* 77:89–98.

<https://doi.org/10.1016/j.phytochem.2011.12.011>

Gill SS, Tuteja N (2010) Reactive oxygen species and antioxidant machinery in abiotic stress tolerance in crop plants. *Plant Physiol Biochem* 48:909–930

Gondor OK, Szalai G, Kovács V, et al (2014) Impact of UV-B on drought- or cadmium-induced changes in the fatty acid composition of membrane lipid fractions in wheat. *Ecotoxicol Environ Saf* 108:129–134. <https://doi.org/10.1016/j.ecoenv.2014.07.002>

Gong H, Zhu X, Chen K, et al (2005) Silicon alleviates oxidative damage of wheat plants in pots under drought. *Plant Sci* 169:313–321

Green PS (2002) A revision of *Olea* L.(Oleaceae). *Kew Bull* 91–140

Grignon-Dubois M, Rezzonico B (2012) First Phytochemical Evidence of Chemotypes for the Seagrass *Zostera noltii*. *Plants* 1:27–38. <https://doi.org/10.3390/plants1010027>

Gupta AK, Kaur N (2000) Sugar alcohols as carbohydrate reserves in some higher plants. In: *Carbohydrate Reserves in Plants-Synthesis and Regulation*. p 337

Gwynn-Jones D (2001) Short-term impacts of enhanced UV-B radiation on photo-assimilate allocation and metabolism: a possible interpretation for time-dependent inhibition of growth. In: *Responses of Plants to UV-B Radiation*. Springer, pp 65–73

Hartley WN (1881) XXI.—On the absorption of solar rays by atmospheric ozone. *J Chem*

- Soc, Trans 39:111–128. <https://doi.org/10.1039/CT8813900111>
- He J, Huang L, Chow W, et al (1993) Effects of Supplementary Ultraviolet-B Radiation on Rice and Pea Plants. *Funct Plant Biol* 20:129. <https://doi.org/10.1071/PP9930129>
- Hegglin MI, Fahey DW, McFarland M, et al (2014) 20 Questions and Answers About the Ozone Layer: 2014 Update, Scientific Assessment of Ozone Depletion: 2014. *Sci. Assess. Ozone Deplet.* 2014 88
- Hernández ML, Sicardo MD, Alfonso M, Martínez-Rivas JM (2019) Transcriptional regulation of stearoyl-acyl carrier protein desaturase genes in response to abiotic stresses leads to changes in the unsaturated fatty acids composition of olive mesocarp. *Front Plant Sci* 10:251
- Hideg E, Jansen MAK, Strid A (2013) UV-B exposure, ROS, and stress: inseparable companions or loosely linked associates? *Trends Plant Sci* 18:107–15. <https://doi.org/10.1016/j.tplants.2012.09.003>
- Higuchi Y, Hisamatsu T (2016) Light Acts as a Signal for Regulation of Growth and Development. In: *LED Lighting for Urban Agriculture*. Springer Singapore, Singapore, pp 57–73
- Hodges DM, DeLong JM, Forney CF, Prange RK (1999) Improving the thiobarbituric acid-reactive-substances assay for estimating lipid peroxidation in plant tissues containing anthocyanin and other interfering compounds. *Planta* 207:604–611. <https://doi.org/10.1007/s004250050524>
- Hou Q, Ufer G, Bartels D (2016) Lipid signalling in plant responses to abiotic stress. *Plant Cell Environ* 39:1029–1048
- Houtz RL, Magnani R, Nayak NR, Dirk LMA (2008) Co- and post-translational modifications in Rubisco: unanswered questions. *J Exp Bot* 59:1635–45. <https://doi.org/10.1093/jxb/erm360>
- Hui R, Li X, Chen C, et al (2013) Responses of photosynthetic properties and chloroplast ultrastructure of *Bryum argenteum* from a desert biological soil crust to elevated ultraviolet-B radiation. *Physiol Plant* 147:489–501. <https://doi.org/10.1111/j.1399->

- Impa SM, Nadaradjan S, Jagadish SVK (2012) Drought stress induced reactive oxygen species and anti-oxidants in plants. In: *Abiotic stress responses in plants*. Springer, pp 131–147
- Interdonato R, Rosa M, Nieva CB, et al (2011) Effects of low UV-B doses on the accumulation of UV-B absorbing compounds and total phenolics and carbohydrate metabolism in the peel of harvested lemons. *Environ Exp Bot*.
<https://doi.org/10.1016/j.envexpbot.2010.09.006>
- Jaleel CA, Riadh K, Gopi R, et al (2009) Antioxidant defense responses: physiological plasticity in higher plants under abiotic constraints. *Acta Physiol Plant* 31:427–436
- Jansen MAK, Gaba V, Greenberg BM (1998) Higher plants and UV-B radiation: Balancing damage, repair and acclimation. *Trends Plant Sci*.
- Johnson GN, Young AJ, Scholes JD, Horton P (1993) The dissipation of excess excitation energy in British plant species. *Plant, Cell Environ* 16:673–679.
<https://doi.org/10.1111/j.1365-3040.1993.tb00485.x>
- Kakani V., Reddy K., Zhao D, Sailaja K (2003) Field crop responses to ultraviolet-B radiation: a review. *Agric For Meteorol* 120:191–218.
<https://doi.org/10.1016/j.agrformet.2003.08.015>
- Kaling M, Kanawati B, Ghirardo A, et al (2015) UV-B mediated metabolic rearrangements in poplar revealed by non-targeted metabolomics. *Plant Cell Environ* 38:892–904
- Kampa M, Castanas E (2008) Human health effects of air pollution. *Environ Pollut* 151:362–367. <https://doi.org/10.1016/j.envpol.2007.06.012>
- Kataria S, Guruprasad KN, Ahuja S, Singh B (2013) Enhancement of growth, photosynthetic performance and yield by exclusion of ambient UV components in C3 and C4 plants. *J Photochem Photobiol B Biol* 127:140–152.
<https://doi.org/10.1016/j.jphotobiol.2013.08.013>
- Kendrick RE, Kerckhoffs LHJ, Van Tuinen A, Koornneef M (1997) Photomorphogenic mutants of tomato. *Plant Cell Environ* 20:746–751

- Koch K (2004) Sucrose metabolism: Regulatory mechanisms and pivotal roles in sugar sensing and plant development. *Curr. Opin. Plant Biol.*
- Köhler H, Contreras RA, Pizarro M, et al (2017) Antioxidant responses induced by UVB radiation in *Deschampsia Antarctica* Desv. *Front Plant Sci.*
<https://doi.org/10.3389/fpls.2017.00921>
- Koubouris GC, Kavroulakis N, Metzidakis IT, et al (2015) Ultraviolet-B radiation or heat cause changes in photosynthesis, antioxidant enzyme activities and pollen performance in olive tree. *Photosynthetica* 53:279–287. <https://doi.org/10.1007/s11099-015-0102-9>
- Kramer GF, Norman HA, Krizek DT, Mirecki RM (1991) Influence of UV-B radiation on polyamines, lipid peroxidation and membrane lipids in cucumber. *Phytochemistry* 30:2101–2108
- Kumar HD, Häder D-P (1999) *Global Aquatic and Atmospheric Environment*. Springer Science & Business Media
- Kusano M, Tohge T, Fukushima A, et al (2011) Metabolomics reveals comprehensive reprogramming involving two independent metabolic responses of *Arabidopsis* to UV-B light. *Plant J* 67:354–369. <https://doi.org/10.1111/j.1365-313X.2011.04599.x>
- Kwon Y, Smerdon MJ (2005) DNA repair in a protein–DNA complex: searching for the key to get in. *Mutat Res Mol Mech Mutagen* 577:118–130.
<https://doi.org/10.1016/j.mrfmmm.2005.02.013>
- Kyparissis A, Drilias P, Petropoulou Y, et al (2001) Effects of UV-B radiation and additional irrigation on the Mediterranean evergreen sclerophyll *Ceratonia siliqua* L. under field conditions. *Plant Ecol* 154:187–193
- Law YK, Forties RA, Liu X, et al (2013) Sequence-dependent thymine dimer formation and photoreversal rates in double-stranded DNA. *Photochem Photobiol Sci* 12:1431.
<https://doi.org/10.1039/c3pp50078k>
- Le Provost G, Domergue F, Lalanne C, et al (2013) Soil water stress affects both cuticular wax content and cuticle-related gene expression in young saplings of maritime pine (*Pinus pinaster* Ait). *BMC Plant Biol* 13:1–12

- Li J, Ou-Lee T-M, Raba R, et al (1993) Arabidopsis flavonoid mutants are hypersensitive to UV-B irradiation. *Plant Cell* 5:171–179
- Liakopoulos G, Stavrianakou S, Karabourniotis G (2006) Trichome layers versus dehaired lamina of *Olea europaea* leaves: differences in flavonoid distribution, UV-absorbing capacity, and wax yield. *Environ Exp Bot* 55:294–304
- Liakoura V, Stavrianakou S, Liakopoulos G, et al (1999) Effects of UV-B radiation on *Olea europaea*: comparisons between a greenhouse and a field experiment. *Tree Physiol* 19:905–908. <https://doi.org/10.1093/treephys/19.13.905>
- Lidon FC, Ramalho JC (2011) Impact of UV-B irradiation on photosynthetic performance and chloroplast membrane components in *Oryza sativa* L. *J Photochem Photobiol B Biol* 104:457–466. <https://doi.org/10.1016/j.jphotobiol.2011.05.004>
- Lilley RMC, Walker DA (1974) An improved spectrophotometric assay for ribulosebisphosphate carboxylase. *BBA - Enzymol.* [https://doi.org/10.1016/0005-2744\(74\)90274-5](https://doi.org/10.1016/0005-2744(74)90274-5)
- Loescher W, Everard J, Cantini C, Grumet R (1995) Sugar alcohol metabolism in source leaves
- Loescher WH, Everard JD (2000) Regulation of Sugar Alcohol Biosynthesis. pp 275–299
- Luengo Escobar A, Alberdi M, Acevedo P, et al (2017) Distinct physiological and metabolic reprogramming by highbush blueberry (*Vaccinium corymbosum*) cultivars revealed during long-term UV-B radiation. *Physiol Plant* 160:46–64. <https://doi.org/10.1111/ppl.12536>
- Lv Y, Tahir II, Olsson ME (2016) Factors affecting the content of the ursolic and oleanolic acid in apple peel: influence of cultivars, sun exposure, storage conditions, bruising and *Penicillium expansum* infection. *J Sci Food Agric* 96:2161–2169. <https://doi.org/10.1002/jsfa.7332>
- Lytovchenko A, Beleggia R, Schauer N, et al (2009) Application of GC-MS for the detection of lipophilic compounds in diverse plant tissues. *Plant Methods* 5:4. <https://doi.org/10.1186/1746-4811-5-4>

- Machado F, Dias MC, Pinho PG de, et al (2017) Photosynthetic performance and volatile organic compounds profile in *Eucalyptus globulus* after UVB radiation. *Environ Exp Bot* 140:141–149. <https://doi.org/10.1016/j.envexpbot.2017.05.008>
- Mahdavian K, Ghorbanli M, Kalantari KM (2008) The effects of ultraviolet radiation on the contents of chlorophyll, flavonoid, anthocyanin and proline in *Capsicum annuum* L. *Turk J Botany*
- Manova V, Gruszka D (2015) DNA damage and repair in plants – from models to crops. *Front Plant Sci* 6:885. <https://doi.org/10.3389/fpls.2015.00885>
- Mariz-Ponte N, Mendes RJ, Sario S, et al (2018) Tomato plants use non-enzymatic antioxidant pathways to cope with moderate UV-A/B irradiation: A contribution to the use of UV-A/B in horticulture. *J Plant Physiol.* <https://doi.org/10.1016/j.jplph.2017.11.013>
- Martínez-Lüscher J, Morales F, Delrot S, et al (2015) Characterization of the adaptive response of grapevine (cv. Tempranillo) to UV-B radiation under water deficit conditions. *Plant Sci* 232:13–22. <https://doi.org/10.1016/j.plantsci.2014.12.013>
- Matsumura Y, Ananthaswamy HN (2004) Toxic effects of ultraviolet radiation on the skin. *Toxicol Appl Pharmacol* 195:298–308. <https://doi.org/10.1016/j.taap.2003.08.019>
- Maverakis E, Miyamura Y, Bowen MP, et al (2010) Light, including ultraviolet. *J Autoimmun* 34:J247–J257. <https://doi.org/10.1016/j.jaut.2009.11.011>
- Mayer MP, Bukau B (2005) Hsp70 chaperones: cellular functions and molecular mechanism. *Cell Mol Life Sci* 62:670–84. <https://doi.org/10.1007/s00018-004-4464-6>
- McKenzie R, Bodeker G, Scott G, et al (2006) Geographical differences in erythemally-weighted UV measured at mid-latitude USDA sites. *Photochem Photobiol Sci* 5:343–352
- McLoughlin F, Basha E, Fowler ME, et al (2016) Class I and II small heat shock proteins together with HSP101 protect protein translation factors during heat stress. *Plant Physiol.* <https://doi.org/10.1104/pp.16.00536>
- Michel T, Khelif I, Kanakis P, et al (2015) UHPLC-DAD-FLD and UHPLC-HRMS/MS based

- metabolic profiling and characterization of different *Olea europaea* organs of Koroneiki and Chetoui varieties. *Phytochem Lett* 11:424–439.
<https://doi.org/10.1016/j.phytol.2014.12.020>
- Mierziak J, Kostyn K, Kulma A (2014) Flavonoids as Important Molecules of Plant Interactions with the Environment. *Molecules* 19:16240–16265.
<https://doi.org/10.3390/molecules191016240>
- Mihailova A, Abbado D, Pedentchouk N (2015) Differences in n -alkane profiles between olives and olive leaves as potential indicators for the assessment of olive leaf presence in virgin olive oils. *Eur J Lipid Sci Technol* 117:1480–1485.
<https://doi.org/10.1002/ejlt.201400406>
- Mirecki RM, Teramura AH (1984) Effects of Ultraviolet-B Irradiance on Soybean. *Plant Physiol* 74:475–480. <https://doi.org/10.1104/pp.74.3.475>
- Mittler R, Vanderauwera S, Suzuki N, et al (2011) ROS signaling: The new wave? *Trends Plant Sci*.
- Molina MJ, Rowland FS (1974) Stratospheric sink for chlorofluoromethanes: chlorine atom-catalysed destruction of ozone. *Nature* 249:810–812. <https://doi.org/10.1038/249810a0>
- Morettini A (1972) *Olivicoltura*, 1st edn (REDA, Roma)
- Mosley S (2014) Environmental History of Air Pollution and Protection. In: *The basic environmental history*. Springer, pp 143–169
- Müller-Xing R, Xing Q, Goodrich J (2014) Footprints of the sun: Memory of UV and light stress in plants. *Front Plant Sci* 5:474. <https://doi.org/10.3389/fpls.2014.00474>
- Murchie EH, Lawson T (2013) Chlorophyll fluorescence analysis: a guide to good practice and understanding some new applications. *J Exp Bot* 64:3983–98.
<https://doi.org/10.1093/jxb/ert208>
- Muzzalupo I (2012) *Olive Germplasm: Italian Catalogue of Olive Varieties*. BoD–Books on Demand
- Neugart S, Fiol M, Schreiner M, et al (2014) Interaction of Moderate UV-B Exposure and

- Temperature on the Formation of Structurally Different Flavonol Glycosides and Hydroxycinnamic Acid Derivatives in Kale (*Brassica oleracea* var. *sabellica*). *J Agric Food Chem* 62:4054–4062. <https://doi.org/10.1021/jf4054066>
- Newman PA, Oman LD, Douglass AR, et al (2009) What would have happened to the ozone layer if chlorofluorocarbons (CFCs) had not been regulated? *Atmos Chem Phys* 9:2113–2128. <https://doi.org/10.5194/acp-9-2113-2009>
- Ni Y, Xia R, Li J (2014) Changes of epicuticular wax induced by enhanced UV-B radiation impact on gas exchange in *Brassica napus*. *Acta Physiol Plant* 36:2481–2490
- Nicoli F, Negro C, Vergine M, et al (2019) Evaluation of Phytochemical and Antioxidant Properties of 15 Italian *Olea europaea* L. Cultivar Leaves. *Molecules* 24:1998. <https://doi.org/10.3390/molecules24101998>
- Nogues S, Baker NR (2000) Effects of drought on photosynthesis in Mediterranean plants grown under enhanced UV-B radiation. *J Exp Bot* 51:1309–1317. <https://doi.org/10.1093/jexbot/51.348.1309>
- Pal M, Sengupta UK, Srivastava AC, et al (1999) Changes in growth and photosynthesis of mungbean induced by UV-B radiation. *Indian J Plant Physiol* 4:79–84
- Panagopoulos I, Bornman JF, Björn LO (1990) Effects of ultraviolet radiation and visible light on growth, fluorescence induction, ultraweak luminescence and peroxidase activity in sugar beet plants. *J Photochem Photobiol B Biol.* [https://doi.org/10.1016/1011-1344\(90\)85189-4](https://doi.org/10.1016/1011-1344(90)85189-4)
- Pang Q, Hays JB (1991) UV-B-inducible and temperature-sensitive photoreactivation of cyclobutane pyrimidine dimers in *Arabidopsis thaliana*. *Plant Physiol* 95:536–543
- Parson EA, Greene O (1995) The Complex Chemistry of the International Ozone Agreements. *Environ Sci Policy Sustain Dev* 37:16–35. <https://doi.org/10.1080/00139157.1995.9929219>
- Paul ND, Moore JP, McPherson M, et al (2012) Ecological responses to UV radiation: interactions between the biological effects of UV on plants and on associated organisms. *Physiol Plant* 145:565–581

- Pearson K (1896) VII. Mathematical contributions to the theory of evolution.—III. Regression, heredity, and panmixia. *Philos Trans R Soc London Ser A, Contain Pap a Math or Phys Character* 187:253–318. <https://doi.org/10.1098/rsta.1896.0007>
- Pessoa FM (2012) Algae and aquatic macrophytes responses to cope to ultraviolet radiation – a Review. *Emirates J Food Agric* 24:. <https://doi.org/10.9755/ejfa.v24i6.14672>
- Petridis A, Therios I, Samouris G, et al (2012a) Effect of water deficit on leaf phenolic composition, gas exchange, oxidative damage and antioxidant activity of four Greek olive (*Olea europaea* L.) cultivars. *Plant Physiol Biochem* 60:1–11. <https://doi.org/10.1016/j.plaphy.2012.07.014>
- Petridis A, Therios I, Samouris G, Tananaki C (2012b) Salinity-induced changes in phenolic compounds in leaves and roots of four olive cultivars (*Olea europaea* L.) and their relationship to antioxidant activity. *Environ Exp Bot* 79:37–43. <https://doi.org/10.1016/j.envexpbot.2012.01.007>
- Petrussa E, Braidot E, Zancani M, et al (2013) Plant Flavonoids—Biosynthesis, Transport and Involvement in Stress Responses. *Int J Mol Sci* 14:14950–14973. <https://doi.org/10.3390/ijms140714950>
- Pfeifer GP (1997) Formation and Processing of UV Photoproducts: Effects of DNA Sequence and Chromatin Environment. *Photochem Photobiol* 65:270–283. <https://doi.org/10.1111/j.1751-1097.1997.tb08560.x>
- Pharr DM, Stoop JMH, Williamson JD, et al (1995) The Dual Role of Mannitol as Osmoprotectant and Photoassimilate in Celery. *HortScience* 30:1182–1188. <https://doi.org/10.21273/HORTSCI.30.6.1182>
- Piccini C, Cai G, Dias MC, et al (2020) UV-B radiation affects photosynthesis-related processes of two Italian olea *Europaea* (L.) varieties differently. *Plants*. <https://doi.org/10.3390/plants9121712>
- Piccini C, Cai G, Dias MC, et al (2021) Olive Varieties under UV-B Stress Show Distinct Responses in Terms of Antioxidant Machinery and Isoform/Activity of RubisCO. *Int J Mol Sci* 22:11214. <https://doi.org/10.3390/ijms222011214>

- Pignatti S (1982) Volume terzo. Edagricole, Bologna
- Rácz A, Hideg É, Czégény G (2018) Selective responses of class III plant peroxidase isoforms to environmentally relevant UV-B doses. *J Plant Physiol* 221:101–106. <https://doi.org/10.1016/j.jplph.2017.12.010>
- Ranjbarfordoei A, Samson R, Damme P (2011) Photosynthesis performance in sweet almond [*Prunus dulcis* (Mill) D. Webb] exposed to supplemental UV-B radiation. *Photosynthetica* 49:. <https://doi.org/10.1007/s11099-011-0017-z>
- Reddy AR, Chaitanya KV, Vivekanandan M (2004) Drought-induced responses of photosynthesis and antioxidant metabolism in higher plants. *J Plant Physiol* 161:1189–1202
- Reuber S, Bornman JF, Weissenböck G (1996) A flavonoid mutant of barley (*Hordeum vulgare* L.) exhibits increased sensitivity to UV-B radiation in the primary leaf. *Plant Cell Environ* 19:593–601
- Rinnan R, Nerg AM, Ahtoniemi P, et al (2008) Plant-mediated effects of elevated ultraviolet-B radiation on peat microbial communities of a subarctic mire. *Glob Chang Biol* 14:925–937. <https://doi.org/10.1111/j.1365-2486.2008.01544.x>
- Robson TM, Klem K, Urban O, Jansen MAK (2015) Re-interpreting plant morphological responses to UV-B radiation. *Plant Cell Environ* 38:856–866. <https://doi.org/10.1111/pce.12374>
- Rodrigues F, Pimentel FB, Oliveira MBPP (2015) Olive by-products: Challenge application in cosmetic industry. *Ind Crops Prod* 70:116–124. <https://doi.org/10.1016/j.indcrop.2015.03.027>
- Rodziewicz P, Swarczewicz B, Chmielewska K, et al (2014) Influence of abiotic stresses on plant proteome and metabolome changes. *Acta Physiol Plant* 36:1–19. <https://doi.org/10.1007/s11738-013-1402-y>
- Rogowska A, Szakiel A (2020) The role of sterols in plant response to abiotic stress. *Phytochem Rev* 19:1525–1538
- Roitsch T, González M-C (2004) Function and regulation of plant invertases: sweet

- sensations. *Trends Plant Sci* 9:606–613. <https://doi.org/10.1016/j.tplants.2004.10.009>
- Rosa M, Prado C, Podazza G, et al (2009) Soluble sugars. *Plant Signal Behav* 4:388–393. <https://doi.org/10.4161/psb.4.5.8294>
- Rubio CP, Hernández-Ruiz J, Martínez-Subiela S, et al (2016) Spectrophotometric assays for total antioxidant capacity (TAC) in dog serum: an update. *BMC Vet Res* 12:166. <https://doi.org/10.1186/s12917-016-0792-7>
- Salerno G (2003) Origin of sucrose metabolism in higher plants: when, how and why? *Trends Plant Sci* 8:63–69. [https://doi.org/10.1016/S1360-1385\(02\)00029-8](https://doi.org/10.1016/S1360-1385(02)00029-8)
- Sanchez-Lorenzo A, Enriquez-Alonso A, Calbó J, et al (2017) Fewer clouds in the Mediterranean: consistency of observations and climate simulations. *Sci Rep* 7:41475. <https://doi.org/10.1038/srep41475>
- Sarian MN, Ahmed QU, Mat So'ad SZ, et al (2017) Antioxidant and Antidiabetic Effects of Flavonoids: A Structure-Activity Relationship Based Study. *Biomed Res Int* 2017:1–14. <https://doi.org/10.1155/2017/8386065>
- Savitch L V., Poccock T, Krol M, et al (2001) Effects of growth under UVA radiation on CO₂ assimilation, carbon partitioning, PSII photochemistry and resistance to UVB radiation in *Brassica napus* cv. Topas. *Aust J Plant Physiol*. <https://doi.org/10.1071/pp00116>
- Schuch AP, Moreno NC, Schuch NJ, et al (2017) Sunlight damage to cellular DNA: Focus on oxidatively generated lesions. *Free Radic Biol Med* 107:110–124
- Schwachtje J, Whitcomb SJ, Firmino AAP, et al (2019) Induced, imprinted, and primed responses to changing environments: does metabolism store and process information? *Front Plant Sci* 10:106
- Searles PS, Flint SD, Caldwell MM (2001) A meta-analysis of plant field studies simulating stratospheric ozone depletion. *Oecologia* 127:1–10. <https://doi.org/10.1007/s004420000592>
- Sebastian A, Kumari R, Kiran BR, Prasad MNV (2018) Ultraviolet B induced bioactive changes of enzymatic and non-enzymatic antioxidants and lipids in *Trigonella foenum-graecum* L. (Fenugreek). *EuroBiotech J* 2:64–71. <https://doi.org/10.2478/ebtj-2018-0010>

- Sharma A, Shahzad B, Rehman A, et al (2019) Response of Phenylpropanoid Pathway and the Role of Polyphenols in Plants under Abiotic Stress. *Molecules* 24:2452. <https://doi.org/10.3390/molecules24132452>
- Shen B, Jensen RG, Bohnert HJ (1997) Mannitol Protects against Oxidation by Hydroxyl Radicals. *Plant Physiol* 115:527–532. <https://doi.org/10.1104/pp.115.2.527>
- Shine MB, Guruprasad KN (2012) Oxyradicals and PSII activity in maize leaves in the absence of UV components of solar spectrum. *J Biosci* 37:703–712. <https://doi.org/10.1007/s12038-012-9248-9>
- Siefermann-Harms D (1990) Chlorophyll, carotenoids and the activity of the xanthophyll cycle. *Environ Pollut* 68:293–303. [https://doi.org/10.1016/0269-7491\(90\)90032-8](https://doi.org/10.1016/0269-7491(90)90032-8)
- Siefermann-Harms D (1985) Carotenoids in photosynthesis. I. Location in photosynthetic membranes and light-harvesting function. *Biochim Biophys Acta - Rev Bioenerg* 811:325–355. [https://doi.org/10.1016/0304-4173\(85\)90006-0](https://doi.org/10.1016/0304-4173(85)90006-0)
- Silva S, Santos C, Serodio J, et al (2018) Physiological performance of drought-stressed olive plants when exposed to a combined heat–UV-B shock and after stress relief. *Funct Plant Biol* 45:1233. <https://doi.org/10.1071/FP18026>
- Smirnoff N (1998) Plant resistance to environmental stress. *Curr Opin Biotechnol*. [https://doi.org/10.1016/S0958-1669\(98\)80118-3](https://doi.org/10.1016/S0958-1669(98)80118-3)
- Soheila A-H, John CF, Jordan B, Thomas B (2001) Early signaling components in ultraviolet-B responses: distinct roles for different reactive oxygen species and nitric oxide. *FEBS Lett* 489:237–242
- Solomon KR (2008) Effects of ozone depletion and UV-B radiation on humans and the environment. *Atmosphere-Ocean* 46:185–202. <https://doi.org/10.3137/ao.460109>
- Sørensen JG, Kristensen TN, Loeschcke V (2003) The evolutionary and ecological role of heat shock proteins. *Ecol. Lett*.
- Spector AA, Yorek MA (1985) Membrane lipid composition and cellular function. *J Lipid Res* 26:1015–1035

- Spurr AR (1969) A low-viscosity epoxy resin embedding medium for electron microscopy. *J Ultrastructure Res.* [https://doi.org/10.1016/S0022-5320\(69\)90033-1](https://doi.org/10.1016/S0022-5320(69)90033-1)
- Sriastava v A, Strasser RJ, Govindjee G (1999) Greening of Peas: Parallel Measurements of 77 K Emission Spectra, OJIP Chlorophyll a Fluorescence Transient, Period Four Oscillation of the Initial Fluorescence Level, Delayed Light Emission, and P700. *Photosynthetica* 37:. <https://doi.org/10.1023/A:1007199408689>
- Stirbet A, Lazar D, Kromdijk J, Govindjee G (2018) Chlorophyll a fluorescence induction: Can just a one-second measurement be used to quantify abiotic stress responses? *Photosynthetica* 56:86–104. <https://doi.org/10.1007/s11099-018-0770-3>
- Stoop JMH, Williamson JD, Pharr DM (1996) Mannitol metabolism in plants: A method for coping with stress. *Trends Plant Sci* 1:139–144. [https://doi.org/10.1016/s1360-1385\(96\)80048-3](https://doi.org/10.1016/s1360-1385(96)80048-3)
- Strid Å, Chow WS, Anderson JM (1994) UV-B damage and protection at the molecular level in plants. *Photosynth Res* 39:475–489. <https://doi.org/10.1007/BF00014600>
- Sullivan JH, Gitz DC, Peek MS, McElrone AJ (2003) Response of three eastern tree species to supplemental UV-B radiation: leaf chemistry and gas exchange. *Agric For Meteorol* 120:219–228. <https://doi.org/10.1016/j.agrformet.2003.08.016>
- Sullivan JH, Teramura AH (1990) Field study of the interaction between solar ultraviolet-B radiation and drought on photosynthesis and growth in soybean. *Plant Physiol* 92:141–146
- Suzuki R, Takahashi M, Furuya K, Ishimaru T (1993) Simplified technique for the rapid determination of phytoplankton pigments by reverse-phase high-performance liquid chromatography. *J Oceanogr* 49:571–580. <https://doi.org/10.1007/BF02237463>
- Swindell WR, Huebner M, Weber AP (2007) Transcriptional profiling of Arabidopsis heat shock proteins and transcription factors reveals extensive overlap between heat and non-heat stress response pathways. *BMC Genomics* 8:125. <https://doi.org/10.1186/1471-2164-8-125>
- Takshak S, Agrawal SB (2019) Defense potential of secondary metabolites in medicinal

plants under UV-B stress. *J Photochem Photobiol B Biol* 193:51–88

Talhaoui N, Taamalli A, Gómez-Caravaca AM, et al (2015) Phenolic compounds in olive leaves: Analytical determination, biotic and abiotic influence, and health benefits. *Food Res Int* 77:92–108. <https://doi.org/10.1016/j.foodres.2015.09.011>

Taulavuori E, Bäckman M, Taulavuori K et al, et al (1998) Long-term exposure to enhanced ultraviolet-B radiation in the sub-arctic does not cause oxidative stress in *Vaccinium myrtillus*. *New Phytol* 140:691–697

Tevini M, Braun J, Fieser G (1991) The protective function of the epidermal layer of rye seedlings against ultraviolet-B radiation. *Photochem Photobiol* 53:329–333

Tevini M, Iwanzik W, Thoma U (1981) Some effects of enhanced UV-B irradiation on the growth and composition of plants. *Planta* 153:388–394.
<https://doi.org/10.1007/BF00384258>

Tripathi R, Rai K, Singh S, et al (2019) Role of supplemental UV-B in changing the level of ozone toxicity in two cultivars of sunflower: growth, seed yield and oil quality. *Ecotoxicology* 28:277–293

Tumlinson JH, Engelberth J (2008) Fatty acid-derived signals that induce or regulate plant defenses against herbivory. In: *Induced plant resistance to herbivory*. Springer, pp 389–407

Upchurch RG (2008) Fatty acid unsaturation, mobilization, and regulation in the response of plants to stress. *Biotechnol Lett* 30:967–977

Valente S, Machado B, Pinto DCGA, et al (2020) Modulation of phenolic and lipophilic compounds of olive fruits in response to combined drought and heat. *Food Chem* 329:127191. <https://doi.org/10.1016/j.foodchem.2020.127191>

Vanlerberghe G (2013) Alternative Oxidase: A Mitochondrial Respiratory Pathway to Maintain Metabolic and Signaling Homeostasis during Abiotic and Biotic Stress in Plants. *Int J Mol Sci* 14:6805–6847. <https://doi.org/10.3390/ijms14046805>

Vasques AR, Pinto G, Dias MC, et al (2016) Physiological response to drought in seedlings of *Pistacia lentiscus* (mastic tree). *New For* 47:119–130. <https://doi.org/10.1007/s11056->

- Velders GJM, Andersen SO, Daniel JS, et al (2007) The importance of the Montreal Protocol in protecting climate. *Proc Natl Acad Sci* 104:4814–4819
- Verdaguer D, Llorens L, Bernal M, Badosa J (2012) Photomorphogenic effects of UVB and UVA radiation on leaves of six Mediterranean sclerophyllous woody species subjected to two different watering regimes at the seedling stage. *Environ Exp Bot* 79:66–75.
<https://doi.org/10.1016/j.envexpbot.2012.01.008>
- Verhoeven GJJ, Archaeology V (2017) The reflection of two fields – Electromagnetic radiation and its role in (aerial) imaging. *AARGnews* 55 55:10–18
- Wang W, Vinocur B, Altman A (2003) Plant responses to drought, salinity and extreme temperatures: towards genetic engineering for stress tolerance. *Planta* 218:1–14.
<https://doi.org/10.1007/s00425-003-1105-5>
- Wang X, Fu X, Chen M, et al (2018) Ultraviolet B irradiation influences the fruit quality and sucrose metabolism of peach (*Prunus persica* L.). *Environ Exp Bot*.
<https://doi.org/10.1016/j.envexpbot.2018.04.015>
- Wargent JJ, Nelson BCW, Mcghie TK, Barnes PW (2015) Acclimation to UV-B radiation and visible light in *Lactuca sativa* involves up-regulation of photosynthetic performance and orchestration of metabolome-wide responses. *Plant Cell Environ* 38:929–940.
<https://doi.org/10.1111/pce.12392>
- Watanabe K, Yamada N, Takeuchi Y (2006) Oxidative DNA damage in cucumber cotyledons irradiated with ultraviolet light. *J Plant Res* 119:239–246.
<https://doi.org/10.1007/s10265-006-0266-2>
- Wenzel A, Frank T, Reichenberger G, et al (2015) Impact of induced drought stress on the metabolite profiles of barley grain. *Metabolomics* 11:454–467.
<https://doi.org/10.1007/s11306-014-0708-0>
- Wu X, Xiong E, Wang W, et al (2014) Universal sample preparation method integrating trichloroacetic acid/acetone precipitation with phenol extraction for crop proteomic analysis. *Nat Protoc*. <https://doi.org/10.1038/nprot.2014.022>

- Yao X, Liu Q (2009) The effects of enhanced ultraviolet-B and nitrogen supply on growth, photosynthesis and nutrient status of *Abies faxoniana* seedlings. *Acta Physiol Plant* 31:523–529. <https://doi.org/10.1007/s11738-008-0261-4>
- Yin Y, Li S, Liao W, et al (2010) Photosystem II photochemistry, photoinhibition, and the xanthophyll cycle in heat-stressed rice leaves. *J Plant Physiol* 167:959–966
- Yoon MY, Kim MY, Shim S, et al (2016) Transcriptomic profiling of soybean in response to high-intensity UV-B irradiation reveals stress defense signaling. *Front Plant Sci.* <https://doi.org/10.3389/fpls.2016.01917>
- Yu GH, Li W, Yuan ZY, et al (2013) The effects of enhanced UV-B radiation on photosynthetic and biochemical activities in super-high-yield hybrid rice Liangyoupeijiu at the reproductive stage. *Photosynthetica* 51:33–44. <https://doi.org/10.1007/s11099-012-0081-z>
- Zhong D, Du H, Wang Z, Huang B (2011) Genotypic variation in fatty acid composition and unsaturation levels in bermudagrass associated with leaf dehydration tolerance. *J Am Soc Hortic Sci* 136:35–40
- Zlatev ZS, J. C. Lidon F, Kaimakanova M (2012) Plant physiological responses to UV-B radiation. *Emirates J Food Agric* 24:. <https://doi.org/10.9755/ejfa.v24i6.14669>
- Zohary D, Hopf M (1994) Olive: *Olea europaea*. Domestication of plants in the Old World
- Zuk-Golaszewska K, Upadhyaya MK, Golaszewski J (2003) The effect of UV-B radiation on plant growth and development. *Plant, Soil Environ* 49:135–140. <https://doi.org/10.17221/4103-pse>

Sitography:

Environmental European Agency, <https://www.eea.europa.eu/it/themes/air/intro>
 GreenFacts - Facts on Health and the Environment, <https://www.greenfacts.org>
 Meteo Aeronautica Militare, <http://clima.meteoam.it/>

NASA Ozone Watch, <https://ozonewatch.gsfc.nasa.gov/NH.html>

The Food and Agriculture Organization, <http://www.fao.org/faostat/en/#data/QD#ancor>